

## **INFORMATION TO USERS**

This manuscript has been reproduced from the microfilm master. UMI films the text directly from the original or copy submitted. Thus, some thesis and dissertation copies are in typewriter face, while others may be from any type of computer printer.

**The quality of this reproduction is dependent upon the quality of the copy submitted.** Broken or indistinct print, colored or poor quality illustrations and photographs, print bleedthrough, substandard margins, and improper alignment can adversely affect reproduction.

In the unlikely event that the author did not send UMI a complete manuscript and there are missing pages, these will be noted. Also, if unauthorized copyright material had to be removed, a note will indicate the deletion.

Oversize materials (e.g., maps, drawings, charts) are reproduced by sectioning the original, beginning at the upper left-hand corner and continuing from left to right in equal sections with small overlaps. Each original is also photographed in one exposure and is included in reduced form at the back of the book.

Photographs included in the original manuscript have been reproduced xerographically in this copy. Higher quality 6" x 9" black and white photographic prints are available for any photographs or illustrations appearing in this copy for an additional charge. Contact UMI directly to order.

**UMI<sup>®</sup>**

**Bell & Howell Information and Learning  
300 North Zeeb Road, Ann Arbor, MI 48106-1346 USA  
800-521-0600**



**Efficiency of Biosurfactants Applied  
by Means of Electrokinetics**

Lin Ju

A Thesis

In

the Department

of

Building, Civil and Environmental Engineering

Presented in Partial Fulfillment of the Requirements  
for the Degree of Doctor of Philosophy at  
Concordia University  
Montreal, Quebec, Canada

December 1999

© Lin Ju, 1999



**National Library  
of Canada**

**Acquisitions and  
Bibliographic Services**

395 Wellington Street  
Ottawa ON K1A 0N4  
Canada

**Bibliothèque nationale  
du Canada**

**Acquisitions et  
services bibliographiques**

395, rue Wellington  
Ottawa ON K1A 0N4  
Canada

*Your file* *Votre référence*

*Our file* *Notre référence*

**The author has granted a non-exclusive licence allowing the National Library of Canada to reproduce, loan, distribute or sell copies of this thesis in microform, paper or electronic formats.**

**The author retains ownership of the copyright in this thesis. Neither the thesis nor substantial extracts from it may be printed or otherwise reproduced without the author's permission.**

**L'auteur a accordé une licence non exclusive permettant à la Bibliothèque nationale du Canada de reproduire, prêter, distribuer ou vendre des copies de cette thèse sous la forme de microfiche/film, de reproduction sur papier ou sur format électronique.**

**L'auteur conserve la propriété du droit d'auteur qui protège cette thèse. Ni la thèse ni des extraits substantiels de celle-ci ne doivent être imprimés ou autrement reproduits sans son autorisation.**

0-612-47709-6

**Canada**

## ABSTRACT

### Efficiency of Biosurfactants Applied by Means of Electrokinetics

Lin Ju, Ph.D.  
Concordia University, 1999

An evaluation of the efficiency of rhamnolipids (biosurfactants) used in electrokinetic remediation of soil contaminated with phenanthrene was presented. Bench scale tests were conducted using four experimental series in order to determine the feasibility and mechanisms of biosurfactant-enhanced phenanthrene removal from mica soil.

The bench-scale study showed that bacteria (*Pseudomonas aeruginosa*) could survive to a certain extent when a low voltage DC electric field was applied. In addition, it was found that these bacteria could produce rhamnolipids in the clayey soil under the electric field. Experimental results showed that during the 14-day experimental period, phenanthrene was partially removed. The highest removal was achieved in the cathode area (85% removal). These promising results are an indication that this process can be applied as an *in-situ* enhancement technique for improving the efficiency of electrokinetic soil remediation. It was proved that bio-micelles, formed due to the introduction of *ex-situ* produced biosurfactants, could be transported to the electrode areas due to both electroosmotic and electrophoretic phenomena. It also indicated that the electrokinetic introduction of engineering produced biosurfactants into the contaminated clayey soil was feasible.

The mechanisms involved in the formation of bio-micelles were described in a bench-scale test using Fourier Transform Infrared Spectrometers (FTIR) and Atomic Force Microscopy (AFM). Results permitted to describe that the transformation of bio-

micelles kinetically changed under the electric field. It was found that spherical, bilayer, and multi-lamellar micelles were formed at different phases of the electrokinetic experiment. The presence of clayey particles and the electric field attenuated and deferred the formation of bio-micelles. Knowledge of the kinetics of bio-micelle formation process are paramount to the accurate application of biosurfactants in electrokinetic remediation of PAH contaminated clayey soil.

The effort to desorb and solubilize phenanthrene, by promoting the formation of bilayer bio-micelles, became successful in bench-scale electrokinetic experiments. In addition, the successful *ex-situ* production of biosurfactants can be used on an industrial scale for electrokinetic soil remediation. The above-described developments can be applied as a new *in-situ* remediation technology: bio-electrokinetics.

## **ACKNOWLEDGEMENTS**

Here, I would like to express my sincere gratitude to my thesis supervisor, Dr. Maria Elektorowicz, for her inspiration, encouragement, invaluable suggestion and support in the course of my research. My deep gratitude to her is beyond words and will last a lifetime.

Also thanks gave to Dr. Rosalia Chifrina, Adjunct Professor at Concordia University, for her guiding in using FTIR equipment. In addition, I would like to thank Prof. Wanda Smoragiewicz from Department of Biological Sciences at Université du Québec à Montréal (UQAM) for providing the laboratory facilities, and Mr. Luc Dubé for his technical support. Special thanks to the Digital Instruments Company for providing the access to Atomic Force Microscopy.

I also acknowledge the support of the National Science and Engineering Research Council (NSERC), Concordia Graduate Fellowships from School of Graduate Studies at Concordia University, and Concordia Academic Research Aid from Faculty of Engineering and Computer Science during the course of my study.

Finally, thanks to my parents for raising me up to a responsible and sensitive person and for their encouragement on my educational life. And thanks to my husband, for his patient and continuous support.

## TABLE OF CONTENTS

LIST OF FIGURES . . . . .	ix
LIST OF TABLES . . . . .	xiv
LIST OF SYMBOLS . . . . .	xv
CHAPTER 1 INTRODUCTION . . . . .	1
1.1 Statement of the problem . . . . .	1
1.2 Objectives of thesis . . . . .	4
1.3 Organization of thesis . . . . .	6
1.4 Contributions . . . . .	7
CHAPTER 2 LITERATURE REVIEW . . . . .	9
2.1 Organic contaminants: PAHs . . . . .	9
2.2 Clay materials . . . . .	15
2.2.1 Soil components . . . . .	15
2.2.2 Effect of clay materials on the fate of contaminants . . . . .	23
2.3 Soil remediation and bioremediation . . . . .	25
2.4 Role of surfactants in remediation . . . . .	30
2.5 Biosurfactants . . . . .	33
2.5.1 Characteristics of biosurfactants . . . . .	34
2.5.2 Biosurfactants production . . . . .	38
2.5.3 Biosurfactants application in soil remediation . . . . .	41
CHAPTER 3 PRINCIPLE OF ELECTROKINETICS . . . . .	43
3.1 Introduction . . . . .	43
3.2 Fundamental theory of electrokinetics . . . . .	44
3.2.1 Effect of electroosmosis on electrokinetic remediation . . . . .	45



3.2.2 Effect of electrophoresis on electrokinetic remediation	48
3.2.3 Effect of electromigration on electrokinetic remediation	49
<b>CHAPTER 4 METHODOLOGY AND MATERIALS</b>	<b>52</b>
4.1 Preparation of soil specimens	52
4.2 Preparation of microorganisms	55
4.3 Production, extraction and identification of biosurfactants	56
4.4 Determination of pH, moisture content, and concentration of rhamnolipids and phenanthrene in soil	58
4.5 Electrokinetic cell configuration	59
4.5.1 Test series 1: Behavior of bacteria under the electric field	62
4.5.2 Test series 2: Potential <i>in-situ</i> production of biosurfactants under the electric field	64
4.5.3 Test series 3: Transport of biosurfactants under the electric field	65
4.5.4 Test series 4: Investigation on bio-micelles under the electric field	67
<b>CHAPTER 5 CHARACTERIZATION OF MATERIALS</b>	<b>70</b>
5.1 Characterization of soil	70
5.2 Characterization of materials by means of FTIR	72
<b>CHAPTER 6 RESULTS AND DISCUSSION FOR TEST SERIES 1:     Behavior of bacteria under the electric field</b>	<b>76</b>
6.1 Electrical potential and resistance distribution	77
6.2 Moisture distribution	80
6.3 pH distribution	82
6.4 Bacterial response to electric field	82
<b>CHAPTER 7 RESULTS AND DISCUSSION FOR TEST SERIES 2:     Potential <i>in-situ</i> production of biosurfactants under the electric field</b>	<b>88</b>

7.1 Electrical potential and resistance distribution . . . . .	88
7.2 Moisture distribution . . . . .	92
7.3 pH distribution . . . . .	93
7.4 Bacterial response to electric field . . . . .	95
7.5 Biosurfactants production under the electric field . . . . .	96
7.6 Phenanthrene removal due to <i>in-situ</i> produced biosurfactants . . . . .	98
<b>CHAPTER 8 RESULTS AND DISCUSSION FOR TEST SERIES 3:</b>	
Transport of biosurfactants under the electric field . . . . .	101
8.1 Electrical potential and resistance distribution in cells T3C1 and T3C2	101
8.2 Electrical potential and resistance distribution in cells T3C3 and T3C4	108
8.3 pH distribution in the electrokinetic cells . . . . .	114
8.4 Moisture distribution in the electrokinetic cells . . . . .	116
8.5 Rhamnolipids concentration in the electrokinetic cells . . . . .	118
8.6 Phenanthrene concentration in the electrokinetic cells . . . . .	120
<b>CHAPTER 9 RESULTS AND DISCUSSION FOR TEST SERIES 4:</b>	124
Investigation on bio-micelles formation under the electric field	
9.1 Results from test series 4 . . . . .	124
9.2 Mechanism of phenanthrene removal . . . . .	133
9.2.1 Factors effecting the fate of bio-micelles . . . . .	134
9.2.2 Kinetic approach to the fate of bio-micelles . . . . .	143
<b>CHAPTER 10 CONCLUSIONS AND RECOMMENDATIONS</b> . . . . .	149
10.1 Conclusions . . . . .	149
10.2 Recommendations . . . . .	152
<b>REFERENCES</b> . . . . .	154

## LIST OF FIGURES

Figure 1.1 Scope of research . . . . .	5
Figure 2.1 Natural soil composition, focus on solid phase . . . . .	16
Figure 2.2 Schematic diagrams of clay basic coordination units . . . . .	17
Figure 2.3 Scheme of clay mineral structure . . . . .	19
Figure 2.4 Scheme of clay mineral (muscovite and chlorite) structure . . . . .	20
Figure 2.5 Structure of rhamnolipids . . . . .	37
Figure 4.1 Scope of experiments . . . . .	54
Figure 4.2 Schematic diagram of experimental setup for cells T1C1, T1C2, T2C1, and T2C2 . . . . .	60
Figure 4.3 Schematic diagram of experimental setup for cells T3C1, T3C2, T3C3, and T3C4 . . . . .	60
Figure 4.4 Schematic diagram of experimental setup for cells T4C1, T4C2, and T4C3 . . . . .	61
Figure 4.5 Stainless steel mesh electric plate . . . . .	62
Figure 5.1 Mineralogical analysis of soil specimens . . . . .	70
Figure 5.2 The FTIR spectroscopy spectrum of clay minerals with 50 scans at a resolution of $4\text{ cm}^{-1}$ . . . . .	72
Figure 5.3 The FTIR spectroscopy spectrum of phenanthrene with 50 scans at a resolution of $4\text{ cm}^{-1}$ . . . . .	74
Figure 5.4 The FTIR spectroscopy spectrum of rhamnolipids with 50 scans at a resolution of $4\text{ cm}^{-1}$ . . . . .	75
Figure 6.1 A. Electrical potential distribution in cell T1C1 B. Electrical potential distribution in cell T1C2 . . . . .	78
Figure 6.2 A. Resistance distribution in cell T1C1 B. Resistance distribution in cell T1C2 . . . . .	79

Figure 6.3 Moisture content distribution in cells T1C1 and T1C2 . . . . .	83
Figure 6.4 pH distribution in cells T1C1 and T1C2 . . . . .	83
Figure 6.5 A. pH and bacterial distribution in cell T1C1 B. pH and bacterial distribution in cell T1C2 . . . . .	84
Figure 7.1 Electrical potential distribution in cell T2C1 during two weeks test . . . . .	89
Figure 7.2 Electrical potential distribution in cell T2C2 during two weeks test . . . . .	89
Figure 7.3 Resistance distribution in cell T2C1 during two weeks test . . . . .	91
Figure 7.4 Resistance distribution in cell T2C2 during two weeks test . . . . .	91
Figure 7.5 Moisture content distribution in cells T2C1 and T2C2 . . . . .	93
Figure 7.6 pH distribution in cells T2C1 and T2C2 . . . . .	94
Figure 7.7 Bacteria and pH distribution in cell T2C1 . . . . .	95
Figure 7.8 Bacteria and pH distribution in cell T2C2 . . . . .	96
Figure 7.9 Biosurfactants distribution versus distance in cells T2C1 and T2C2 after the test . . . . .	97
Figure 7.10 Biosurfactants and phenanthrene removal distribution versus distance after the test in T2C2 . . . . .	98
Figure 8.1 Electrical potential distribution in cell T3C1 before daily introduction of biosurfactants . . . . .	102
Figure 8.2 Electrical potential distribution in cell T3C1 after daily introduction of biosurfactants with a concentration of 20 mg/l . . . . .	102
Figure 8.3 Electrical potential distribution in cell T3C2 before daily introduction of biosurfactants . . . . .	103
Figure 8.4 Electrical potential distribution in cell T3C2 after daily introduction of biosurfactants with a concentration of 20 mg/l . . . . .	103
Figure 8.5 Resistance distribution in cell T3C1 before daily introduction of biosurfactants . . . . .	105

Figure 8.6 Resistance distribution in cell T3C1 after daily introduction of biosurfactants with a concentration of 20 mg/l	105
Figure 8.7 Resistance distribution in cell T3C2 before daily introduction of biosurfactants	106
Figure 8.8 Resistance distribution in cell T3C2 after daily introduction of biosurfactants with a concentration of 20 mg/l	106
Figure 8.9 Electrical potential distribution in cell T3C3 before daily introduction of biosurfactants	110
Figure 8.10 Electrical potential distribution in cell T3C3 after daily introduction of biosurfactants with a concentration of 166 mg/l	110
Figure 8.11 Electrical potential distribution in cell T3C4 before daily introduction of biosurfactants	111
Figure 8.12 Electrical potential distribution in cell T3C4 after daily introduction of biosurfactants with a concentration of 166 mg/l	111
Figure 8.13 Resistance distribution in cell T3C3 before daily introduction of biosurfactants	112
Figure 8.14 Resistance distribution in cell T3C3 after daily introduction of biosurfactants with a concentration of 166 mg/l	112
Figure 8.15 Resistance distribution in cell T3C4 before daily introduction of biosurfactants	113
Figure 8.16 Resistance distribution in cell T3C4 after daily introduction of biosurfactants with a concentration of 166 mg/l	113
Figure 8.17 Final average pH value of soil in cells T3C1 and T3C2	115
Figure 8.18 Final average pH value of soil in cells T3C3 and T3C4	115
Figure 8.19 Final average moisture content of soil in cells T3C1 and T3C2	117
Figure 8.20 Final average moisture content of soil in cells T3C3 and T3C4	117
Figure 8.21 Final average biosurfactants distribution in cells T3C1 and T3C2 (the introduced concentration of biosurfactants: 20 mg/l)	119
Figure 8.22 Final average biosurfactants distribution in cells T3C3 and T3C4 (the introduced concentration of biosurfactants: 166 mg/l)	119

Figure 8.23 Average remaining phenanthrene distribution in cells T3C1 and T3C2 (the introduced concentration of biosurfactants: 20 mg/l)	121
Figure 8.24 Average remaining phenanthrene distribution in cells T3C3 and T3C4 (the introduced concentration of biosurfactants: 20 mg/l)	121
Figure 9.1 Biosurfactant profile in different layers during the test in the phenanthrene- water-biosurfactant system (cell T4C1)	125
Figure 9.2 Biosurfactants profile during the first 11 hours testing in the phenanthrene-water- biosurfactant system (cell T4C1)	126
Figure 9.3 Biosurfactants profile from 14 hours to 48 hours testing in the phenanthrene-water-biosurfactant system (cell T4C1)	126
Figure 9.4 Biosurfactants profile for last 120 hours testing in the phenanthrene-water- biosurfactant system (cell T4C1)	126
Figure 9.5 Phenanthrene profile during the test in the phenanthrene-water- biosurfactant system (cell T4C1)	127
Figure 9.6 Ratio of bio-micelles to phenanthrene during the test in the phenanthrene-water- biosurfactant system (cell T4C1)	127
Figure 9.7 Biosurfactant profile during the test in the soil-phenanthrene-water- biosurfactant system (cell T4C2)	128
Figure 9.8 Biosurfactant profile during the first 17 hours test in the soil-phenanthrene-water- biosurfactant system (cell T4C2)	129
Figure 9.9 Biosurfactant profile during last 148 hours test in the soil-phenanthrene-water- biosurfactant system (cell T4C2)	129
Figure 9.10 Soil profile during the test in the soil-phenanthrene-water- biosurfactant system (cell T4C2)	130
Figure 9.11 Phenanthrene profile during the test in the soil-phenanthrene-water- biosurfactant system (cell T4C2)	132
Figure 9.12 Ratio of bio-micelles to phenanthrene during the test in the soil-phenanthrene-water- biosurfactant system (cell T4C2)	132
Figure 9.13 Morphology of biosurfactants (adapted from Vinson et al., 1989)	135
Figure 9.14 Schematic representation of biosurfactant molecule	139

Figure 9.15 Image of vesicular micelles by AFM with scan rate of 1.001 Hz, scan size of 5.00 $\mu\text{m}$ and data scale of 50.00 nm	142
Figure 9.16 Image of bilayer micelles by AFM with scan rate of 1.001 Hz, scan size of 10.00 $\mu\text{m}$ and data scale of 200.00 nm	142
Figure 9.17 Image of clayey soil by AFM with scan rate of 1.001 Hz, scan size of 5.00 $\mu\text{m}$ and data scale of 2.00 $\mu\text{m}$	143
Figure 9.18 Conceptual representation of the process related to the partitioning of phenanthrene and biosurfactants at the cathode region (at pH of 8.0)	145
Figure 9.19 Conceptual representation of the process related to the partitioning of phenanthrene and biosurfactants in the middle of electrokinetic cell (at pH of 7.5)	146
Figure 9.20 Conceptual representation of the process related to the partitioning of phenanthrene and biosurfactants at the anode region (at pH of 5.0)	146

## **LIST OF TABLES**

Table 2.1 Cleanup criteria for contaminated sites by PAHs in Canada (CCME, 1991)	11
Table 2.2 Classification of synthetic surfactants	32
Table 2.3 The properties of biosurfactants and synthetic surfactants	34
Table 2.4 Various biosurfactants produced by microorganisms	36
Table 5.1 Physical and chemical properties of soil specimen	71
Table 8.1 Resistance difference in cells T3C1 and T3C2	107
Table 8.2 Resistance difference in cells T3C3 and T3C4	109



## LIST OF SYMBOLS

A	cross-sectional area (cm <sup>2</sup> )
A <sub>0</sub>	molecular optimal surface area
A <sub>c</sub>	the area per charge
d <sub>l</sub>	the bilayer thickness
d <sub>w</sub>	the separation distance of the two surfaces
H	effective London-Hamaker coefficient
I	current (A)
i <sub>e</sub>	electrical potential gradient (V/cm)
k	Boltzmann Constant
k <sub>e</sub>	coefficient of electroosmotic permeability (cm <sup>2</sup> /V-s)
k <sub>h</sub>	hydraulic conductivity
k <sub>i</sub>	coefficient of water transport efficiency (cm <sup>2</sup> /A-s)
L <sub>c</sub>	the critical chain length
M	number of molecule in one micelle
n	number of carbon in chains
P <sub>H</sub>	repulsive pressure
q <sub>e</sub>	electroosmotic flow rate (cm <sup>3</sup> /s)
R	radius of the micelles
V	hydrocarbon volume
σ	electrical conductivity (S/cm)
ξ	correlation length

# **CHAPTER 1 INTRODUCTION**

## **1.1 Statement of the problem**

With the rapid development of industry and agriculture, there are a considerable amount of contaminated sites around the world. These sites are a result of leaking of pipelines and underground petroleum storage tanks and spilling of manufacturing oil or gas manufacturing production. The major contaminants at these sites are polynuclear aromatic hydrocarbons (PAHs). PAHs are a group of solid phase organic chemicals containing two or more fused benzene rings. Because many PAHs are known as carcinogens and mutagens, and exposure to them may represent a significant health risk to human populations (White, 1986), their fate in nature is of great environmental concern. Therefore, soil contaminated by PAHs has become an important environmental issue. The remediation of PAH contaminated sites is desirable.

PAHs are characterized by low aqueous solubility, high molecular weight and a tendency to sorb strongly to soil, especially soil with high organic matter content (Manilal and Alexander, 1991). After Mihelcic, et al. (1993), PAHs have shown to be only used by bacteria in its dissolved state - in the water phase rather than the sorbed phase and solid phase. This low aqueous solubility affects their transport and degradation in the soil and water (Wiesel, et al. 1993). The recent studies have shown that the addition of surfactants and biosurfactants can increase the bioavailability and biodegradation of PAHs (Oberbremer, et al. 1990; Aronstein and Alexander, 1993; Francy, et al. 1991; Jain, et al. 1992; Abdul et al. 1992; Zhang and Miller, 1994). Surfactants enhance the mobilization of soil-bound PAHs by lowering the interfacial tension. Due to its hydrophobic properties, PAHs have a high affinity with the

hydrophobic micellar core of the surfactants and therefore partition into it. Thus, their aqueous solubility is greatly increased.

There are a lot of remediation methodologies applied for the removal of PAHs from the soil. *Ex-situ* application such as excavation followed by physico-chemical methods (e.g., thermal treatment, incineration or soil washing) are established approaches to soil cleanup. Innovative *in-situ* methods have recently been gaining interest because they alleviate the problems associated with *ex-situ* methods, such as the cost of excavation, and the possibility of exposure to the workers and neighborhoods in the proximity of the contaminated soil, especially in residential area. There are many *in-situ* remediation processes, which could offer cost savings, such as pump & treat, soil vapor extraction and bioremediation. However, in field conditions, clay represents a major challenge due to several characteristics, such as high specific surface area (SSA), low permeability, and high cation exchange capacity (CEC), which retard the transport of contaminants and supplied materials through the soil. Therefore, it may influence the efficiency of soil remediation. Consequently, standard remediation technologies can not be applied directly to clayey soils, because in these conditions, the supply of nutrients and electron acceptors *in-situ* is almost impossible. Therefore, the development of new technologies is required to satisfy *in-situ* remediation requirements in clayey soil. Researchers have found that electrokinetic phenomena applied to *in-situ* soil decontamination promises to be effective. The electrokinetic technique applies electroosmosis, electrophoresis, and electromigration processes in order to enhance the transport of materials (e.g., nutrients, contaminant, bacteria, etc.) into clayey soils (Elektorowicz and Boeva, 1996; DeFlaun and Condee, 1997). Some successful results

have already been reported (Lageman, 1989; Elektorowicz, et al. 1995a, 1995b, 1996; Pamukcu, et al. 1995; Acar, et al. 1994, 1995). With more emphasis now being placed on *in-situ* technologies, the electrokinetic remediation process is emerging as one of the most promising technologies for treating clayey soil contaminated by heavy metals and some slightly soluble organics. In general, the major advantages of electrokinetics are: 1) it is a unique *in-situ* methodology that is effective in low permeability soils (such as clay); 2) the flow direction can be controlled; 3) it is capable of removing a wide range of contaminants; and 4) it has a low electric power consumption.

As mentioned above, due to the low solubility of PAHs, the introduction of biosurfactants can allow for the partitioning of PAHs into bio-micelles (an agglomeration of biosurfactants and PAHs). As a result of a combination of biosurfactant and electrokinetics, it is hypothesized that the increased solubilization, desorption, and mobilization of organic contaminants can increase the efficiency of PAH removal from clayey soil. Due to the nature of biosurfactants produced from microorganisms, such as non-toxic and biodegradable, removal of PAHs enhanced by the application of biosurfactants under the electric field is envisioned to be environmentally acceptable, feasible and cost-efficient. In this research work, phenanthrene, which belongs to the group of PAHs, is used as a model to investigate the effect of biosurfactants on the solubilization of PAHs under the electric field. Derived from previous work on synthetic surfactants (Elektorowicz, 1995), research on the electrokinetic transport of surfactants applied to phenanthrene contaminated clayey soil seems to be feasible. The efficiency of using biosurfactants under an electric field requires a scientific investigation. The results

can be applied to a new hybrid method called *bio-electrokinetics*, which promises to be successful *in situ* as well as *ex situ*.

## **1.2 Objectives of thesis**

In order to tackle the problem, the major objective of the research is to evaluate the efficiency of a new soil remediation method, bio-electrokinetics, based on the enhancement of phenanthrene removal from clayey soil using biosurfactants (rhamnolipids) under the electric field. The overall aims of the research is:

- 1) to investigate behavior of producing biosurfactants bacteria under the electric field;
- 2) to assess potential *in-situ* production of biosurfactants in clay materials under the electric field;
- 3) to study the efficiency of enhanced electrokinetics remediation by introduction of *ex-situ* produced biosurfactants as engineering approach to remove PAHs from clay materials;
- 4) to describe the kinetics of bio-micelles formation in the presence of clayey materials under the electric field, as a part of the mechanisms in electrokinetic remediation enhanced by biosurfactants for hydrophobic organic compounds.

The scope of research to achieve the above-mentioned objectives is presented in Figure 1.1.

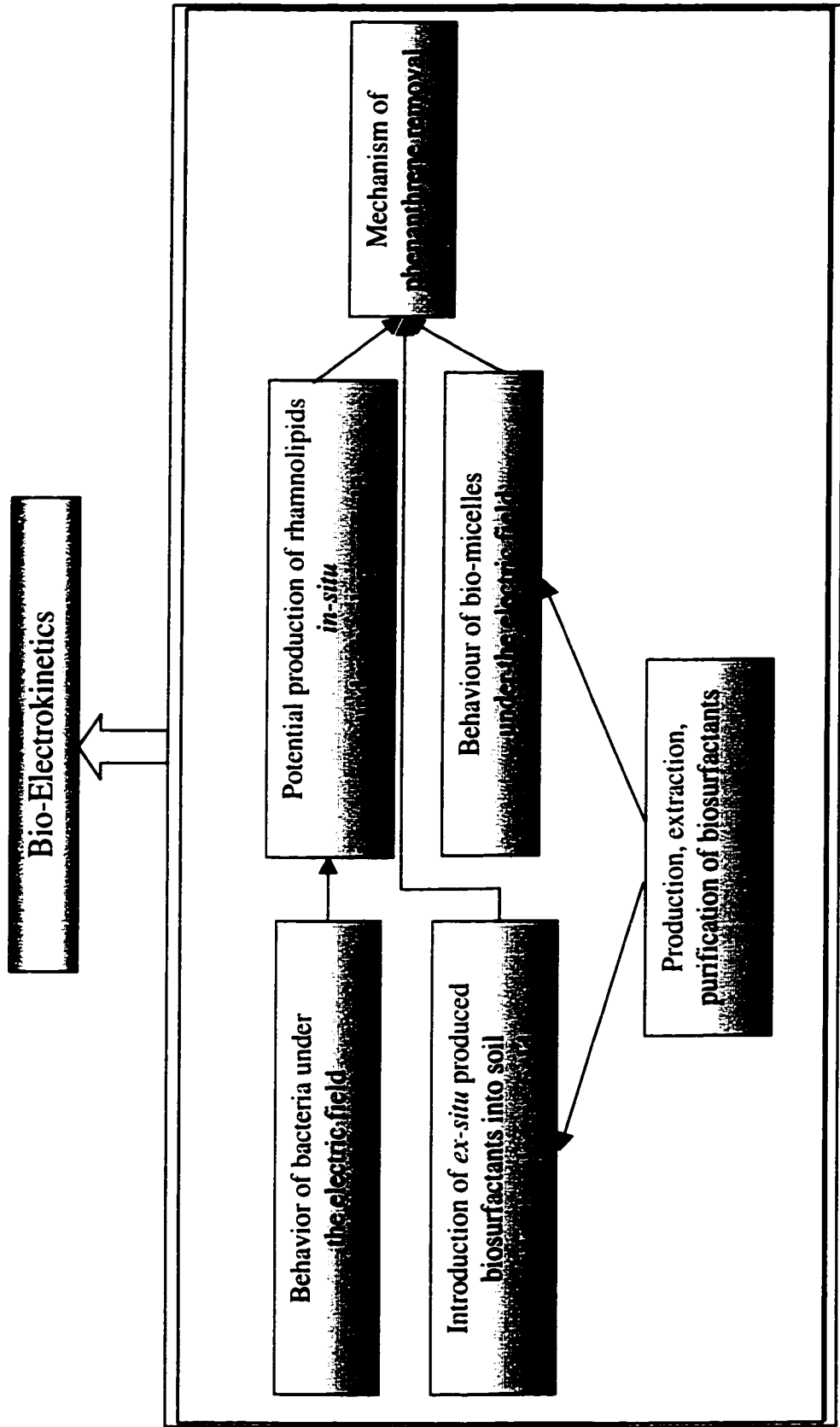


Figure 1.1 Scope of the research

## 1.3 Organization of thesis

The thesis is organized into eleven chapters encompass cover the research conducted. In this section, a general summary of these chapters is presented.

Chapter 1 consists of the problems which exist at present related to this research work, the objectives of the thesis, and the scope of research. Chapter 2 covers a literature review of this research in which a discussion related to electrokinetic remediation process, phenanthrene and biosurfactant characteristics, and a review of past studies on surfactants and biosurfactants enhanced remediation have been dealt with. Chapter 3 summarizes the principles of electrokinetics. Aspects of electrokinetic phenomena are divided into three parts: electroosmosis, electrophoresis, and electromigration, which are discussed in detail. All laboratory testing, conducted methodology and materials are present in chapter 4. In this chapter, design of bench-scale experiments is presented. The procedure of production, purification, and identification of biosurfactants is also described. The characterization of materials including soil specimens and phenanthrene was presented in Chapter 5. The schemes of these test results and discussion are separated into four chapters. The results from experiments related to the behavior of bacteria under the electric field are shown and discussed in Chapter 6. In Chapter 7, results related to the potential production of biosurfactants *in-situ* are addressed. The introduction of biosurfactants into the electric field to investigate the removal efficiency of phenanthrene from clayey soil are shown in Chapter 8. The study of the removal mechanisms of phenanthrene from clayey soil, in the presence of biosurfactants and under the electric field are presented in Chapter 9. Finally, the conclusions derived from

this research are highlighted and recommendations for further research are addressed in chapter 10.

## **1.4 Contributions**

Research on the efficiency of biosurfactants for the removal of PAHs (phenanthrene) from clayey materials under the electric field can result in the establishment of a new methodology in soil bioremediation: bio-electrokinetics. The following statements represent a summary of the entire research accomplishment:

- Research permitted the discovery that even under extreme pH conditions created by the electric field in clayey soil, bacteria can proliferate to a certain degree. That allows for the production of biosurfactants *in-situ* for soil bioremediation.
- The lab test confirmed that potential production of biosurfactants *in-situ* may become the breakthrough for the utilization of biosurfactants to enhance the solubility of PAHs *in-situ*, and facilitate their transport in a clayey soil environment, via electroosmosis and electrophoresis.
- The development of a methodology for the introduction of *ex-situ* produced biosurfactants into clayey soil by means of electrokinetics, in order to improve the efficiency of phenanthrene removal. The electrokinetic transport of biosurfactants enhances the solubility, mobility, and eventually bioavailability of PAHs in the low permeable soils.
- This is the first time description of the kinetics of bio-micelle formation in the presence of electrokinetic phenomena. Under the electric field, the change of pH resulted in different micelle structures. At the anode, the pH environment was favorable to the formation of lamellar micelles. In the cathode area, the micelles are



favor to form spherical micelles. The presence of clayey particles affected the formation stage. Supplementary force associated with electrokinetic phenomena was an important factor that affects on the transformation of bio-micelles.

- New analytical methods were developed: the application of Fourier Transform Infrared Spectrometers (FTIR) and Atomic Force Microscopy (AFM) to follow bio-micelle formation and the application of Supercritical Fluid Extraction (SFE) to enhance PAHs removal from clayey materials.

## **CHAPTER 2 LITERATURE REVIEW**

### **2.1 Organic contaminants: PAHs**

Polynuclear aromatic hydrocarbons (PAHs) are a special group of pollutants originating from natural or man-made sources. They are formed and released from the incomplete combustion of organic materials, such as coal, oil and gas, or other organic substances. Due to reduction and aromatization over extended periods of time, natural sources including diterpenes, triterpenes, steroids, and plant quinone pigments can form PAHs (Cookson, 1995). Human activity also increases the amount of PAHs in the environment. The major activities that result in the contaminated sites by PAHs are petroleum refining and coal distillation. Other industrial sources come from the production of solvents, pesticides, plastics, paints, resins, and dyes (Yong et al., 1991). PAHs may be found in burn pits, chemical manufacturing plants and disposal areas, contaminated marine sediments, disposal wells and leach fields, landfills and burial pits, leaking storage tanks, radiologic/mixed waste disposal areas, vehicle maintenance areas and wood preserving sites. At present, there are more than 100 different PAH compounds that have been found. Most concerned PAHs in the environment are fluorene, phenanthrene, anthracene, fluoranthene, pyrene, benz( $\alpha$ )anthracene, benzo( $\alpha$ )pyrene, perylene, and coronene.

With two or more fused benzene rings in linear, angular, or cluster arrangements, PAHs are hydrophobic organic chemicals. The molecular weight of PAHs range between naphthalene (128.16) to coronene (300.36). It has been found that PAHs are highly recalcitrant, persistent and tend to bioaccumulate (Cerniglia, 1984). Some of them are

known carcinogens and mutagens (Keith and Telliard, 1979). Therefore, PAHs are classified as priority pollutants by the U. S. Environmental Protection Agency (EPA).

PAHs can be present in various phases, such as water, air, soil or sediment. In the air, background levels of PAHs are 0.02-1.2 mg/m<sup>3</sup> in rural areas and 0.15-19.3 mg/m<sup>3</sup> in urban areas. Due to the fact that exposure to PAHs can cause cancer, the Occupational Safety and Health administration (OSHA) has established a legally enforceable limit of 0.2 mg/m<sup>3</sup> of all PAHs in the air. Alternatively, in drinking water, it ranges from 4 to 24 ng/l (U. S. Agency, 1990). Sims and Overcash (1983) reported that the background concentration of PAHs ranges from 0.01 to 88 µg/kg in soil and 1 to 10 µg/kg in plants. The Canadian Council of Ministers of the Environment (CCME, 1991) had recommended interim environmental-quality criteria for PAHs contaminated sites. These are summarized in Table 2.1. The application of these criteria is straightforward. Three concentration values (A, B, and C) are given for both soil and ground water. The A value represents background contamination with respect to contaminants found naturally. The B value represents a threshold when thorough analyses are necessary and decontamination may be or not carried out. However, proper remedial action must be taken at the C level, such as cleanup investigation and cleanup operation.

Humans may be exposed to PAHs by drinking water, swallowing food, breathing the air contaminated by PAHs, soil or dust particles that are contaminated by PAHs, and dermal exposure. PAHs have an affinity for fatty tissues, and tend to be stored monthly in kidneys, liver, with smaller amounts in spleen, adrenal glands and ovaries.

The fate of PAHs is derived by chemical oxidation, photolysis, hydrolysis, volatilization, bioaccumulation, adsorption to soil particles, leaching, and microbial

Table 2.1 Cleanup criteria for contaminated sites by PAHs in Canada (CCME, 1991)

Component	Threshold concentrations					
	Soil (mg/kg dry matter)			Ground water (µg/l)		
	A	B	C	A	B	C
Benzo(a)anthracene	0.1	1	10	0.01	0.1	1
Benzo(b)anthracene	0.1	1	10	0.01	0.1	1
Benzo(k)fluoranthene	0.1	1	10	0.01	0.1	1
Benzo(a)pyrene	0.1	1	10	0.01	0.1	1
Dibenzo(a, h)anthracene	0.1	1	10	0.01	0.1	1
Indeno(1,2,3-c,d)pyrene	0.1	1	10	0.01	0.1	1
Naphthalene	0.1	5	50	0.2	2	20
Phenanthrene	0.1	5	50	0.2	2	20
Pyrene	0.1	10	100	0.2	2	20

Note: A: Background value  
 B: Indicate value for elaborate investigation  
 C: Value for remedial action

degradation. Among them, due to natural reactions, biodegradation of PAHs has gained more attention. Microorganisms which can degrade PAHs include bacteria, filamentous fungi, yeasts, cyanobacteria, diatoms, and eukaryotic algae, which have an enzymatic capacity to oxidize PAHs that range in size from naphthalene to benzo(a)pyrene (Cerniglia and Yang, 1984; Cerniglia, 1984). Microbial transformation of PAHs is well documented. The five stages for transformation of PAHs include: 1) entry of the xenobiotic compounds into the cell; 2) manipulation of side chains and formation of substrates for ring-cleavage; 3) ring-cleavage; 4) conversion of products of ring-cleavage into amphibolic intermediates, and 5) utilization of amphibolic intermediates (Ashok and Saxena, 1995). Bioremediation is effective for anthracene and phenanthrene. However,

complete mineralization of higher molecular weight PAHs can be only achieved by a limited number of microorganisms (Cerniglia, 1992).

The degree of biodegradation of PAHs is a function of its solubility, number of fused rings, number, type, and position of substitution, and nature of atoms in heterocyclic compounds (Cookson, 1995). The rate-limiting step in the biodegradation of PAHs is the initial ring oxidation (Cerniglia and Heitkamp, 1989). PAHs have different half-lives in soil. In sandy soil, two-ring PAHs have half-lives of about 2 days. Three-ring PAHs, namely, anthracene and phenanthrene have half-lives of 16 and 134 days, respectively. In general, the four-, five- and six-ring PAHs have half-lives of over 200 days (Sims et al., 1988).

The environmental fate of PAHs depends upon many extrinsic and intrinsic factors which determine the rate and extent of their transformation and mineralization. These intrinsic factors include the physico-chemical properties of PAHs such as their structure, molecular size, nutrient status, water solubility, lipophilicity, and volatility. Various environmental extrinsic factors involve inorganic nutrients, water activity of soil, organic matter content, redox potential, soil structure, pH, temperature, oxygen availability, salinity, light intensity, and bioavailability. The indigenous microflora or the microbial ecology is also an important factor which should be taken into consideration for successful biodegradation. Among them, inorganic nutrients play an important role in the metabolism of PAHs by soil bacteria. For instance, the concentration of nitrogen and phosphorous may limit the microbial growth and biodegradation of PAHs. Manilal and Alexander (1991) and El-Nawawy et al. (1992) have reported increased rates of phenanthrene mineralization in soil amended with phosphate while it was found to

decrease with the addition of nitrate. Therefore, regarding *in-situ* bioremediation, introduction of nutrients into the contaminated site is a very important factor for a successful process. However, the introduction of nutrients in PAHs contaminated clayey soil has still shown to be a challenge.

Under optimized metabolic conditions, the major environmental factor affecting the degradation rates of PAHs is the sorption phenomena. Due to their hydrophobic properties with a higher log  $K_{ow}$  ( $>4$ ) (partition coefficient), PAHs have a higher affinity with the non-aqueous phase than water, and a significant portion of PAHs are sorbed on soil particles, especially to soil organic matter (Means et al., 1980). Meanwhile, if soil has a significant fraction of clay, associated with organic and inorganic amorphous materials, they can create high sorption conditions in soil (Elektorowicz et al., 1999). More researchers indicated that degradation of organics mainly took place in pore water. Consequently, the bioavailability of PAHs may be limited by their sorbed phase (Mihelcic et al., 1993).

Some typical values for bioremediation of PAHs were listed below. The soil moisture requirement for microbial activity ranges from 25 to 85% of water-holding capacity, and 30 to 90% for optimum PAH degradation (Dibble and Bartha, 1979). pH requirement for microorganisms ranges from 5.5 to 8.5, with a pH of 7.0 to 7.8 for optimum PAH degradation (Weissenfels et al., 1990). Aerobes and facultative anaerobes need a redox potential of larger than 50 mV and anaerobes smaller than 50 mV for biodegradation to occur. The designed C: N: P ratio in soil for microbial growth is approximately 120:10:1 (Wilson and Jones, 1993).

Phenanthrene is present in heating oil, and is commonly found in Canadian contaminated soil. Therefore, it was chosen in this research as a model PAH compound. Phenanthrene is an isomer composed of three benzene rings with molecular weight of 178. Its total surface area is  $198 \text{ \AA}^2$ , and density is  $1.174 \times 10^3 \text{ kg/m}^3$ . It has a very low water solubility (1.29 mg/l at 25°C), low vapor pressure ( $6.8 \times 10^{-4}$  mmHg at 20°C), high octanol/water partition coefficient ( $\log K_{ow} = 4.54$ ), and high organic carbon partition coefficient ( $\log K_{oc} = 4.46$ ).

Some of soil *Pseudomonas* can utilize phenanthrene as the sole carbon source, thereby allowing for its mineralization (Ghisalba, 1983). Keuth and Rehm (1991) reported that *Arthrobacter polychromogens* could degrade almost 50% of phenanthrene with the concentration of 150 mg/l in a solution. Due to cometabolism, doubling the starting concentration of anthracene or phenanthrene results in higher degradation rates (Wiesel et al., 1993).

The growth rates of bacteria on phenanthrene are related to the solubility of the hydrocarbon (Wodzinski and Johnson, 1968). In order to increase the solubilization of phenanthrene in soil, surfactants become a viable solution to reduce the sorption of phenanthrene in soil. Aronstein et al. (1993) reported that the nonionic surfactants Novel II 1412-56 enhanced the rate of phenanthrene mineralization, after a surfactant concentration of 10 µg/ml in water was pumped through the soil. Theoretically, Guha and Jaffa (1996) indicated that only a portion of phenanthrene that partitioned into the micellar phase of nonionic surfactants is directly bioavailable. Alternatively, biosurfactants can also assist the degradation of phenanthrene. Due to the addition of 3500 mg/l biosurfactant excreted by *P. aeruginosa* PRP 652, the apparent solubility of

phenanthrene increased from 1.2 mg/l to 34.4 mg/l (Hunt et. al, 1994). *Pseudomonas aeruginosa* was reported to produce a biosurfactant when grown on phenanthrene (Deziel et al., 1996).

In general, biosurfactants can be widely produced by a specific type of bacteria. In order to increase the solubility of phenanthrene, environmental friendly biosurfactants can be applied in a new remediation method.

## **2.2 Clay materials**

As it is mentioned in Chapter 1.1, the remediation of clayey soil presents a real challenge to soil remediation. Since the clayey materials create a habitat for microorganisms, and retain various contaminants (mainly complex hydrocarbon molecules), nutrients, the carbon energy sources, as well as water molecules (Yong, et al., 1992), the efficiency of remediation highly depends on a deep understanding of soil composition.

### **2.2.1 Soil components**

Soils are composed of inorganic and organic solid, water, and air (Figure 2.1). Soils are classified as primary minerals (derived from weathering of rock) and secondary minerals (transformed as fine particles). Primary minerals comprise a major portion of the sand and silt fraction. Common primary minerals include quartz as well as feldspar, amphiboles, pyroxenes. Because of larger particle size and low specific surface areas, they play less important roles in contaminant interaction and attenuation processes than



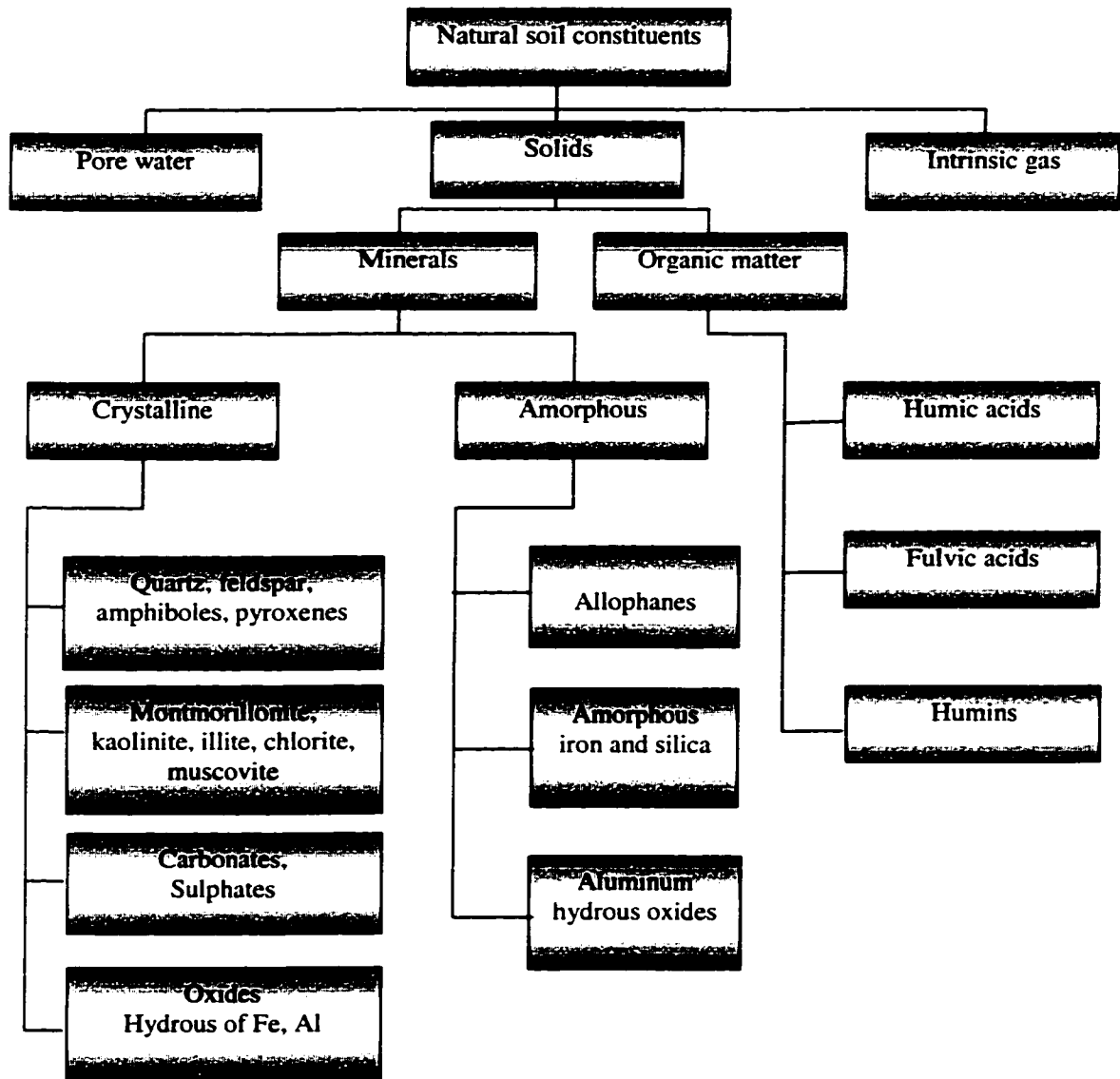


Figure 2.1 Natural soil composition (focus on solid phase)

phyllosilicates, which comprise the major portion of the clay-sized fraction material in soils. Pedologists define clay particles as being less than 2  $\mu\text{m}$  size and specify them in the group of colloids. The combination of high specific surface area and surface electrical charge makes the secondary minerals an important factor in defining the contaminant fate in the subsurface.

The properties of clay colloids are associated with their crystallographic structure. Clay minerals are composed of basic coordination units: tetrahedral sheets in which four oxygen atoms surround a silicon atom and octahedral sheets in which six hydroxyls form the corners, and where a cation (such as aluminum) resides in the center (Figure 2.2).

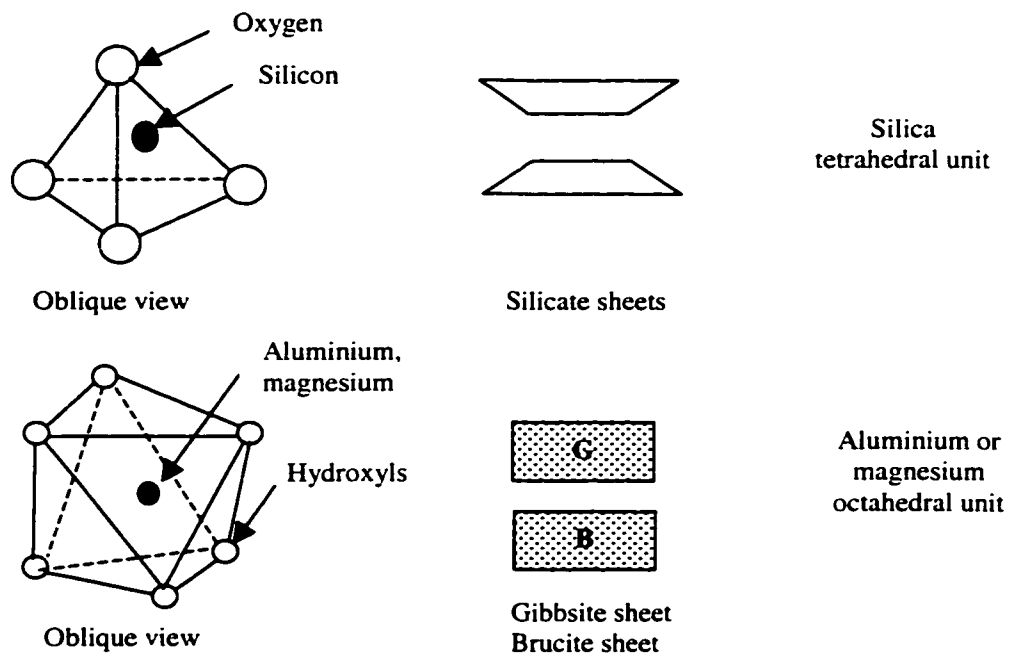


Figure 2.2 Schematic diagrams of clay basic coordination units (adapted from Yong and Warkentin, 1966)

Tetrahedral sheets have smaller metal ions such as silicon, contrary to the octahedral sheets which have larger metal ions such as aluminum ( $\text{Al}^{3+}$ ), magnesium ( $\text{Mg}^{2+}$ ), iron ( $\text{Fe}^{3+}$ ), and manganese ( $\text{Mn}^{2+}$ ). Stacking of layers formed by tetrahedral and octahedral sheets determines the type of clay mineral (Appelo and Postma, 1993). The commonly found clay materials are sub-divided into different groups of clays, e.g. montmorillonite, kaolinite, illite, muscovite, and chlorite.

Montmorillonite minerals endure isomorphous substitutions with magnesium or iron substituting for aluminum in the dioctahedral minerals (Figure 2.3). A layer of this clay consists of two silica sheets and one alumina sheet (also called a gibbsite sheet) (ratio of 2:1). Water enters easily between layers initiating the expansion of material. The swelling index of 0.9, is the highest among all types of clay minerals. Montmorillonite clays have a high plasticity limit over 97% and liquid limit up to 700% (Keedwell, 1984). Due to the surface charge, montmorillonite displays the ability to exchange ions and its CEC is 60-120 meq/100g of soil. Montmorillonite aggregates have a very large specific surface area (SSA) (up to 600 - 1390  $\text{m}^2/\text{g}$ ) (Das, 1994). These properties place montmorillonite in the group of extremely swelling and adsorptive minerals.

Kaolinite particle consists of alternating octahedral alumina and tetrahedral silica sheets (ratio of 1:1) (Figure 2.3). They are bound strongly by hydrogen bonding between hydroxyls from the alumina sheet on one face, and oxygens from the silica sheet on the opposite face of the layer. Due to these relatively strong forces, many layers are built up by preventing hydration between layers. The SSA of kaolinite situates between 10 to 20  $\text{m}^2/\text{g}$ , and its CEC (3 to 15 meq/100g) is the lowest among the clay minerals. Kaolinite has a low plasticity limit (26%), low liquid limit (52%) and low swelling index (0.06)

(Keedwell, 1984). Due to limited surface activity and affinity to water, kaolinite is recognized as a relatively poor adsorbent.

Illite minerals (also called K-mica) consist of an alumina sheet between two silica sheets in a repeating manner. The layers are held together by potassium ions (Figure 2.3). Due to its crystallographic structure, illite displays characteristics situated between montmorillonite and kaolinite: illite's structure limits the swelling index to 0.4, CEC is about 10-40 meq/100g, and SSA from 20 to 80 m<sup>2</sup>/g. Therefore, illite exhibits a behavior between kaolinite with low sorption activity and montmorillonite with a high sorption activity (Wilun and Starzewski, 1972; Yong et al., 1992).

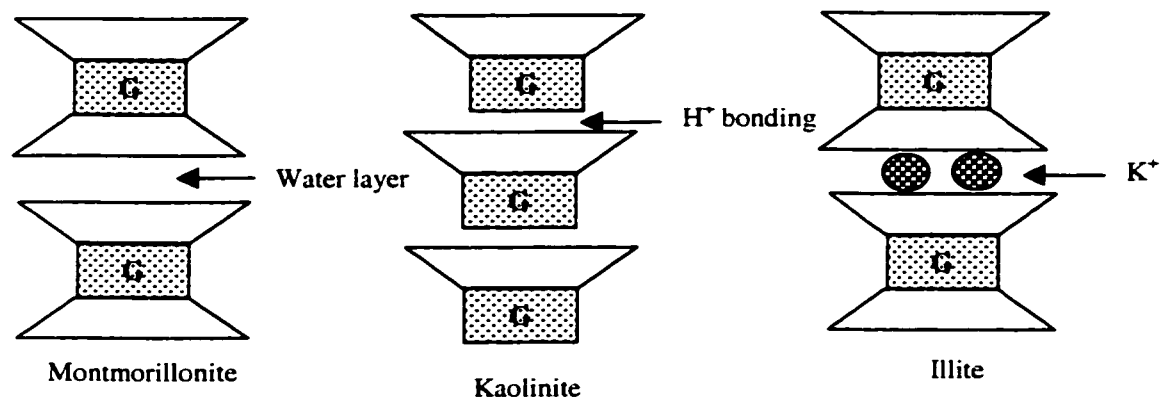


Figure 2.3 Scheme of clay mineral structure  
G: Gibbsite sheet  
(adapted from Yong and Warkentin, 1966)

Muscovite, hydrous potassium aluminum silicate, consists of a layered structure of aluminum silicate sheets weakly bonded together by layers of potassium ions (Figure 2.4). It is a member of the mica group. It is similar in the structure in illite, but containing more potassium between the aluminum silicate sheets.

Chlorite minerals are from such ferro-magnesium minerals as biotite, pyroxenes, and amphiboles (Marshall, 1964). They are composed of a silica sheet, an alumina sheet or brucite sheet (magnesium replacing the aluminum atoms in the octahedral units) in a repeating manner (Figure 2.4). A 2:2 ratio of silica and alumina sheets makes it different from kaolinite. The thickness of the repeating layer is 1.4 nm. In chlorite, silicon and aluminum can be substituted by other cations. Tetravalent silicon may be substituted by trivalent aluminum in the silica sheet, resulting in a negative charge. The CEC of chlorite is 10-40 meq/100g and SSA is 70-150 m<sup>2</sup>/g (Yong et al., 1992). Its behavior is similar to illite, however, the compounds are more difficult to penetrate into the repeating layer than illite due to their tight structure.

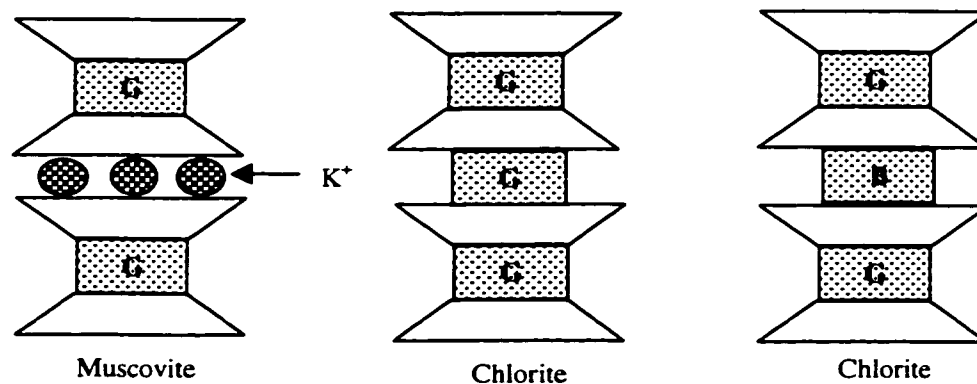


Figure 2.4 Scheme of clay mineral (muscovite and chlorite) structure  
 G: Gibbsite sheet  
 B: Brucite sheet  
 (adapted from Yong and Warkentin, 1966)

Other crystalline groups are called carbonates, which are most commonly found in arid and semi-arid regions. Calcium carbonate minerals are present in soil as particles or coatings. Sulphate minerals are also dominantly found in acid and semi-arid region

soils. Both carbonates and sulphates are characterized by relatively high water solubility and high sensitivity to the change of pH.

In soil, there are also non-primary and non-secondary crystalline inorganics (as indicated in Figure 2.1) that should be considered when dealing with the fate of contaminants. Among them, it is necessary to address the effect of organic carbon content on the bioavailability of PAHs. Organic carbon is one of the most important factors in determining the sorption of PAHs on soil. The soil organic carbon commonly represents a hydrophobic fraction with a strong binding affinity with hydrophobic compounds. In industrial area, the proportion of organic matter present in soil is as much as 0.5% to 8% by weight (Mitchell, 1976).

The major group of organic matter is humic substances, which comprise seventy to eighty-percent of the organic matter by weight found in most soils (Schnitzer, 1986). They have a higher capacity to bind water and nutrients than clay, and hence, have a larger impact on adsorption phenomena in soils. Humic substances include humic acids, fulvic acids, and humins which are typically found in sizes as low as 0.1  $\mu\text{m}$ . They are aromatic and aliphatic polymers with molecular weights ranging from a hundred to tens of thousands. The high molecular weights of organic matter create a larger tendency for van der Waals attraction with other soil components and contaminants. Therefore, humic substances can easily absorb organic compounds in their molecular structure.

The most common functional groups of organic matter are hydroxyls, carboxyls, and phenolic groups. Hydroxyls can develop positive or negative charges depending on pH of the soil. Carboxyls and phenolic groups contribute to high cation exchange capacity (CEC) up to 100-300 meq/100g (Yong et al., 1992), which can prevent removal

of inorganic contamination. Subsequently, the presence of organic matter can cause retardation of contaminants and prevent transport of contaminants in the soil. Grosser et al. (1994) reported that fulvic acid has been shown to decrease mineralization of pyrene. It was possible that the sorption of the compound with organic matter made it less bioavailable. However, Mahro et al. (1994) gave the opposite result of organic matter on the biodegradation of PAHs. Their research has shown that by the addition of organic matter (compost), biodegradation of PAHs increased significantly, possibly increasing the microbial activity.

Amorphous inorganics are another group of non-crystalline inorganics, such as allophanes, amorphous iron and alumina, and amorphous silica. SSA ranges between 300 and 700 m<sup>2</sup>/g, and their CEC are as high as 150 meq/100g. Compared to secondary minerals, they have a very little amount in soil and have a less influence on contaminant fate and environmental engineering.

Based on above description, an important property of clay minerals is evident. A net negative charge is caused by elements of similar size and charge replacing the ones in a perfect clay internal lattice during formation (isomorphous substitution), and leading to an overall charge deficiency in the mineral. Other reasons for charge deficiency are broken edges. The existence of natural organic species (such as humic acids) in the soil specimen also influences the available charge. The total electrical charge per unit surface area (surface charge density) increases as the specific surface area of the soil mineral increases. For example, the average surface density of the negative charges increases in the following order: kaolinite (25 Å<sup>2</sup>/electronic charge) < illite (50 Å<sup>2</sup>/electronic charge) < chlorite < montmorillonite (100 Å<sup>2</sup>/electronic charge) (Yong and Warkentin,

1966). The surface charge of clays is also a function of pH. When pH is below isoelectric point, it can provoke the change of soil surface charge. In the presence of a high pH soil solution, the surface concentration of OH<sup>-</sup> ions is high. Consequently, the surface charge density will tend to be negative. If the pH is increased, the charge density will become more negative (Yong et al., 1992). In the presence of a low pH, it will show the opposite phenomena on the surface of soil. When water is presented in clay, ions form a diffuse double layer around clay particles (Yong et al., 1992).

### **2.2.2 Effect of clay materials on the fate of contaminants**

Derived from the previous description, soil components that mainly influence the fate of contaminants and remediation process are secondary minerals and organic matter. Therefore, the interaction of main soil components with contaminants can create an understanding of the various processes, which control accumulation, transport, and fate of the contaminants.

One of main factors which affect the interaction between contaminants and soil is sorption. Sorption is defined as the process in which the solutes (ions, molecules, and compounds) are partitioned between the liquid phase and the soil particle interface (Yong et al., 1992). The soil mineral surface contains functional groups, which are responsible for adsorption. These functional groups on clay minerals are -Al-OH (octahedral) with a pKa (their respective log acidity) of approximately 5, -Si-OH (tetrahedral) with a pKa of approximately 9, and -Si-Al-OH<sub>2</sub> with an apparent pKa of approximately 6-7 (Evangelou, 1998). PAHs are nonpolar organics, with dipole moments less than 1, and dielectric constants less than 3 (Yong et al., 1992). Even though van der Waals forces between



these compounds and clay particles are very weak, they are additive, resulting in large total forces, and a less rapid decay with distance for large particles. It is thought that this is most likely responsible for the difficulty of the removal of hydrocarbon molecules from the aqueous medium. The value of  $K_{oc}$  for organic compounds can reflect the partitioning of the organic compounds between the adsorbed phase and the soil solution. The higher the  $K_{oc}$ , the lower is the water solubility. Yong and Rao (1991) proved that adsorption of hydrocarbons on clay surfaces occurs only when the solubility of the hydrocarbon is exceeded and when it exists in the micellar form. They noted that the lower the concentration of hydrocarbon in water, the greater is the tendency of the organic compound to adsorb to the clay minerals. Type and fraction of secondary minerals also influence sorption/desorption. A study by Elektorowicz and Ju (1997) showed different desorption rates from various clay materials, such as kaolinite, illite, and montmorillonite, under the same conditions. Tests of extraction of phenanthrene using supercritical fluid extraction (SFE) performed on above-mentioned soil demonstrated that the highest extraction rate (92%) was obtained from montmorillonite, the lowest from kaolinite (21%), and 52% from illite soil.

Another factor that should be taken into consideration is organic matter. As stated previously, organic material has high specific surface areas and ion exchange properties. Due to hydrophobic properties of nonionic organic compounds, they are primarily sorbed to the organic matter fraction of the soil. Interaction occurs on the hydrophobic surfaces of the organic matter in the soil. Hydrophobic active sites of humic substances include aliphatic side chains and lignin-derived moieties with high carbon content and small number of polar groups (Senesi and Chen, 1989).

In summary, the fate of contaminants in environment is dramatically influenced by the presence of clay colloids, associated organic matter and amorphous inorganic materials. In field conditions, clay material represents a major challenge. Therefore, design of a remediation operation for contaminated clayey soils must be preceded by exhaustive analysis of the clay fraction, its petrographical structure, organic matter content, and inorganic amorphous material – all associated with clay fraction (Elektorowicz et al., 1999). An accurate remediation technology has to take advantage of certain clay properties instead of challenging them.

## **2.3 Soil remediation and bioremediation**

*In-situ* soil remediation has obtained more attention than *ex-situ* technology by avoiding extraction and transportation of soil, preventing exposure of contaminated dust to residual areas, and allowing cost savings. There are physical/chemical soil treatment processes, such as pump-and-treat, soil washing, and electrokinetics. Biological soil treatment includes bioremediation, such as bioventing, enhanced bioremediation, land treatment, and phytoremediation. Some of the most common remediation technologies applied to PAHs contaminated sites are presented below.

- I. Soil vapor extraction (SVE) SVE is used for remediating subsurface soils contaminated by volatile and semivolatile organic compound with an applied vacuum, and thus enhancing the *in-situ* volatilization of contaminants. The contaminants typical treated are volatile organic carbons (VOCs). Soil porosity, soil structure and air permeability, are very important parameters that may influence the performance of SVE. Due to the low soil permeability of clay

materials, this methodology is not suitable for application in sites with high clay content. The Verorna Well Field Superfund site used a full-scale operation of an SVE system, for duration of 4 years. A total of 45, 000 pounds of VOCs were removed from the subsurface soil during the remediation (U. S. EPA, 1995a).

- II. Soil washing It involves the removal of organic or inorganic contaminants through the use of water or other suitable aqueous solutions. In this technique, fluid is used to wash contaminants from the saturated zone by injection and recovery systems. A solvent, surfactant solution, or water with or without additives is applied to soil to enhance contaminant release and mobility, resulting in increased recovery and decreased soil contaminant levels (Nash, 1987; U. S. EPA, 1994). This technology can be used to treat VOCs, PAHs, fuels, pesticides, and heavy metals. However, if the soil is heterogeneous or has low permeability, the contaminants are difficult to treat.
- III. Electrokinetics Electrokinetic remediation is one of the most promising *in-situ* techniques. Using the electrokinetic phenomena, electrodes are inserted into the contaminated clayey soil under an applied electric field, evoking a motion of a liquid and of the dissolved species. As a result, contaminants are transported to the electrodes, where they can be removed by an adapted collection or separating process (U. S. EPA, 1995b). Improved performance of electrokinetics can be attained by the introduction of surfactants. A detailed review related to this technology development is presented in Chapter 3.

The major group of *in-situ* treatment is bioremediation. Bioremediation is defined as treatment by which microorganisms directly use contaminants as energy and carbon

sources under optimal conditions, such as a suitable supply of oxygen and nutrients, controlled moisture, temperature and pH. Consequently, the contaminants can be broken-down to CO<sub>2</sub> and H<sub>2</sub>O if the biodegradation is complete. Bioremediation has gained interest during the last decade, as it may be applied *in-situ*, on-site or *ex-situ* for treating chemical spills and hazardous waste problems. The above-mentioned technologies are most advantageous when indigenous bacteria are considered for cleaning the contaminated site. In most cases, secondary pollution and health risks are minimized. In addition, low costs can be anticipated if biodegradation is complete. The disadvantage of *in-situ* bioremediation is that it is difficult to inject the nutrient and bacteria into the field, especially in clay material, which has very low hydraulic permeability. The fact that the contaminants are strongly sorbed to the clay soil prevents the efficiency of bioremediation. Bioremediation techniques have been applied for the sites contaminated by PAHs, solvents, pesticides, wood preservation, and other organic chemicals. A few examples of bioremediation methodologies have been discussed in detail.

- I. Bioventing Typically, bioventing involves the introduction of oxygen into contaminated unsaturated soils by extraction or injection of low airflow to enhance the performance of biodegradation and to support an active microbial population (U. S. EPA, 1995c). Process configuration is similar to those used for soil vapor extraction but the airflow rate is limited to the amount necessary for biodegradation. This technology has been widely used in the U.S. and Canada. However, it is a medium to long-term technology, and its efficiency is dependent on the specific site and its soil composition. If the soil has a high clay content, the effective application of bioventing is limited by a lack of nutrients in the

subsurface, low moisture content of the soil, and difficulty in achieving airflow through the contaminated zone.

- II. Enhanced bioremediation This technique applies the principle that indigenous or inoculated microorganisms, such as fungi, bacteria and other microorganisms, convert organic contaminants in soil to carbon dioxide and water under aerobic conditions, and methane, sulfide, nitrogen gas under anaerobic conditions. Oxygen, usually in the form of pure oxygen, or hydrogen peroxide is applied via an infiltration gallery, spray irrigation, injection or active barriers. The specific contaminants, site characteristics and environmental conditions will affect the rate of biodegradation, and duration of bioremediation. If the specific site contains high amounts of low permeability soil, such as clay materials, the injection of oxygen and nutrient to the contaminant site will become very difficult.
- III. Land treatment Land treatment is a full-scale bioremediation technique consisting of tilling techniques to enhance the interaction of waste, soil, oxygen and microorganisms to decompose organic hazardous waste. Upon enhanced biological activity, the contaminants in soil can be degraded, transformed, and finally mineralized. Diesel fuel, oily sludge, wood-preserving wastes (PCP, PAHs, and creosote), coke wastes, and certain pesticides have been successfully biodegraded by this technique (U. S. EPA, 1993). Nyer (1992) reported that pentachlorophenol (PCP) concentrations were reduced by 95 percent while PAH concentrations were reduced by 50 to 75 percent over a 5-month period in a land treatment system. Limitations to the process include: 1) large land-area

requirements, 2) dust, 3) the depth of tilling, 4) weathered contaminants which result in long term persistence, and 5) treatment time is relatively long.

IV. Phytoremediation Unlike enhanced bioremediation using microorganisms, phytoremediation involves plants to absorb, transfer, and degrade organic or inorganic contaminants in soil. Plants can supply nutrients to microorganisms through roots, translocate/accumulate (phytoextract) contaminants into plant roots, and mineralize the contaminants using enzymes, such as dehalogenase and oxygenase released by these plants. The typical contaminants that can be biodegraded by phytoremediation are metals, pesticides, solvents, explosives, crude oil, PAHs, and landfill leachates. However, a major limitation of this technique is the bioaccumulation of contaminants in animals through the ingestion of these plants. In addition, the remediation process can take years to reach regulatory levels, and therefore it requires a long-term commitment to maintain the system.

In summary, soil remediation and bioremediation is site specific. Up to now, there is no perfect method for the contaminated site with a large amount of clay material and high content of organic matter. The electrokinetics applied for heavy metal and PAHs contaminated clayey soil has been shown promising results (Acar et al., 1994; Pamukcu et al., 1995). This method seems to have potential to be applied in our study. In combination with biosurfactants to treat hydrophobic contaminants, enhanced electrokinetics represents a very promising *in-situ* technique for the removal of PAHs from clay materials.

## **2.4 Role of surfactants in remediation**

Surfactants, also called surface active agents, are amphiphilic molecules, having one polar moiety which has an affinity with water and other polar molecules, and another nonpolar moiety which is a hydrophobic part. Hydrophobic portions (tails) are usually hydrocarbon chains typically containing 12 or more carbon atoms. Hydrophilic portions (heads) are usually ionic, or polar. By concentrating at the air/water interface of the solution, the surfactant species are able to reduce the surface tension of a liquid medium, and then reduce the free energy of the system, thereby increasing their stability in the solution.

The mechanisms governing surface activity involve two processes in aqueous oil-surfactants-water solution: change of the structure of water, and the freedom of motion of the hydrophobic groups of surfactants. The hydrogen-bonding of water molecules tetrahedral arrangement may be disrupted by the presence of an amphiphilic molecule. The amphiphilic molecules are surrounded by water with the hydrophilic head group remaining in water and the hydrophobic portion extending into the gaseous or oil phase. The restriction of internal torsional vibration of the hydrocarbon chains results in the decrease of free energy upon the dissolution of the hydrocarbons. Therefore, the removal of the hydrophobic part from the aqueous solution will decrease the entropy. This is the reason that the amphiphilic molecules tend to accumulate at the air-water or oil-water interface. Because the forces of intermolecular attraction between water molecules and non-polar groups are weaker than those between two water molecules, the surface tension is reduced. Increasing the concentration of surfactant to reach a certain point with the lowest surface tension, called the critical micelle concentration (CMC), the monomers of

surfactants begin to aggregate into spherical, cylindrical or lamellar micelles. In other words, the CMC can be defined as the surfactant concentration at which the concentration of a free monomer ceases to increase and any further monomers added will form micelle structures (Myers, 1992). A micelle is usually an ordered, colloidal aggregate of 40 to 400 surfactant molecules in the liquid solution (Rosen, 1978). In the process of micelle formation, the surfactant molecules that aggregate to form micelles have the ability to surround insoluble molecules, thereby effectively dispersing or emulsifying them into the aqueous phase.

Surfactants are classified according to the nature of hydrophiles and hydrophobes. This results in the existence of anionic, cationic, zwitterionic (or amphoteric) and nonionic surfactants. The different types of surfactants are summarized in Table 2.2. Anionic surfactants, with the hydrophilic group carrying a negative charge, are the largest class of surfactants in use (70-75% of total consumption). Cationic surfactants, with the hydrophile bearing a positive charge, are very important roles as antiseptic agents, which can kill or inhibit the growth of many microorganisms (Myers, 1992). Zwitterionic (amphoteric) surfactants contain hydrophobic groups consisting of both negative and positive charges. Nonionic surfactants contain hydrophilic groups without charge (e.g. polyoxyethylenes).

Surfactants can be employed in detergency, emulsification, dispersion, coating, wetting, flotation, petroleum discovery, lubrication and adhesion. Recently, surfactants are used in technologies for the remediation of soil contaminated with hydrophobic organics, such as soil-washing, soil-flushing, pump-and-treat for increasing the solubilization of sorbed hydrophobic contaminants (Abdul et al., 1992; Fountain et al.,



1991; West and Harwell, 1992; Shieu et al., 1994; Robertson and Wilson, 1995; Volkering et al., 1995). The removal of petroleum hydrocarbons can be a few times higher where surfactants are added to the washing system (Ellis et al., 1985). Edwards et al. (1991) utilized four commercial nonionic surfactants to enhance the solubilities of naphthalene, phenanthrene, and pyrene. They found that the solubility of PAHs increased linearly with surfactant concentration above the CMC. Surfactant addition to PAH-contaminated soil have been demonstrated to be effective in the dissolution and desorption of PAHs from soil systems, resulting in higher mass transfer rates (Miller, 1995). Therefore, addition of surfactants into the soil can enhance the solubility and bioavailability of oil contaminants.

Table 2.2 Classification of synthetic surfactants

Type	Example	Molecular formula	Configuration
Anionic	Potassium laurate	$\text{CH}_3(\text{CH}_2)_{10}\text{COO}^- \text{K}^+$	
	Sodium dodecyl sulphate	$\text{CH}_3(\text{CH}_2)_{11}\text{SO}_4^- \text{Na}^+$	
Cationic	Dodecylamine hydrochloride	$\text{CH}_3(\text{CH}_2)_{11}\text{NH}_3^+ \text{Cl}^-$	
Ampholytic	N-dodecyl-N,N-dimethyl betaine	$\text{C}_{12}\text{H}_{25}\text{N}^+(\text{CH}_3)_2\text{CH}_2\text{COO}^-$	
Non-ionic	Polyoxyethylene p-tertoctylphenyl ether	$\text{C}_8\text{H}_{17}\text{C}_6\text{H}_4\text{O}(\text{CH}_2\text{CH}_2\text{O})_{10}\text{H}$	

## 2.5 Biosurfactants

As stated previously, in order to solve the remediation problem caused by PAHs properties, surfactants were presented as a feasible solution. However, Hunt et al. (1994) pointed out that the surfactants present some level of toxicity to the microorganisms due to their adsorption at interfaces and binding through hydrophobic interactions with proteins. They solubilize components of the membrane and this allows them to interact with cell membranes (which has very high protein/lipid ratio) and proteins-especially enzymes. Thus, surfactants disrupt normal cell functions and decrease enzymatic activity. Alternatively, rapid advances in biotechnology over the past decade have led to considerable interest in manufacturing surfactants by biological methods (so-called biosurfactants) on the industrial scale. Biosurfactants are a variable group of surface-active agents naturally produced by certain types of hydrocarbon-uptaking microorganisms. They exhibit both hydrophilic and hydrophobic structural moieties similar to a synthetic surfactant. A comparison of the surface-active properties of several microbial and synthetic surfactants are shown in Table 2.3 (Banat, 1995a).

Biosurfactants have special advantages over chemically synthetic surfactants, because of their small size (molecular weight less than 1500), their lower toxicity, structural diversity, biodegradable nature, effectiveness at extreme temperatures, pH, and salinity, and ease of synthesis, or perhaps even stimulation of *in-situ* production (Kosaric, 1993). Therefore, in recent years, significant interest in biosurfactants has been earned as a result of a wide application in environmental protection, crude oil drilling, pharmaceuticals, and food-processing industries (Fiechter, 1992; Klekner and Kosaric, 1993; Muller-Hurtig et al., 1003; Velikonja and Kosaric, 1993).

Table 2.3 The properties of biosurfactants and synthetic surfactants (Banat, 1995a)

Agent	Surface tension (mN/m)	Interfacial tension (mN/m)	Critical micelle concentration (mg/l)
<b>Synthetic surfactants</b>			
Span-20	32.0	5.0	10.0
Sodium dodecyl sulphate	30.0	0.01	2,500.0
Petroleum sulfonates	30.0	0.001	ND
<b>Biosurfactants</b>			
Cellobiose lipids	30.0	>1.0	20.0
<i>Rhamnolipid</i>	<b>40.0</b>	<b>1.5</b>	<b>50.0</b>
Sophorolipid	37.0	1.5	82.0
Trehalose dimycolate	30.0	18.0	0.7
Trehalose 6-mycolate	30.0	15.0	165.0
Hydroxy fatty acid	30.0	15.0	200.0
Surfactin	27.0	1.8	25.0
Corynomycolic acid	30.0	2.0	150.0
Protein-lipid-carbohydrate	35.0	15.0	1,900.0
PE-1006 product	30.0	5.6	70.0
ST-5 product	27.0	1.8	30.0
AB-2 product	28.0	1.5	35.0

- ND= Not detected

### 2.5.1 Characteristics of biosurfactants

Certain bacteria produce biosurfactants, and secrete these emulsifying hydrophobic compounds into the water phase, thereby increasing the hydrocarbon surface area in contact with the biodegrading microorganisms. Microbial surfactants include low-molecular-weight glycolipids, lipopeptides, and high-molecular-weight lipid-containing polymers such as lipoproteins, phospholipids, lipopolysaccharide-protein complexes, and polysaccharide-protein-fatty acid complexes (Koch et. al, 1991). Generally, the typical amphiphilic structure of biosurfactants has a hydrophobic moiety, which is either a long-chain fatty acid, alkyl or hydroxyl fatty acid. In addition, it has a hydrophilic moiety,

which can be a carbohydrate in glycolipids, an amino acid in lipoproteins, a phosphate in phospholipids, a carboxylic acid, an alcohol, etc. (Sreekala, 1994).

Biosurfactant molecules are cell wall associated and are also secreted into the surrounding media. Such molecules have the potential to promote cellular attraction to hydrophobic surfaces, to affect the distribution of cells between oil and water phases, to emulsify water-insoluble substances, and to mediate transport of hydrophobic substrate into the cell. Most biosurfactants are either neutral or negatively charged. The anionic character is due to the presence of carboxylic groups. A small number of cationic biosurfactants contain an amine functional group.

Recently, a considerable number of studies have been performed on biosurfactants produced by a wide variety of microorganisms such as bacteria, yeast and filamentous fungi. Different types of microorganisms produce a variety of biosurfactants (Table 2.4). The most commonly isolated and widely studied group of surfactants produced by microorganisms is glycolipids, which contain one or more monosaccharide residues linked by a glycosyl linkage to a lipid part and include trehalose lipids, rhamnolipid, and sophorolipids. Among them, rhamnolipids were the most widely researched.

Rhamnolipids, which was secreted into growth medium during the stationary phase of growth, contain two rhamnose units connected to  $\beta$ -hydroxydecanoic acid, or one rhamnose attached to the identical fatty acid (Figure 2.5). The monorhamnolipid has an average molecular weight of 504 (Zhang and Miller, 1992). Jarvis and Johnson (1949) first described the rhamnolipids, which were produced by *Pseudomonas aeruginosa*. The

Table 2.4 Various biosurfactants produced by microorganisms  
(adapted from Banat, 1995b)

Group	Microorganisms	Type of biosurfactants
Glycolipids	<i>Pseudomonas sp.</i>	Rhamnolipids (anionic)
	<i>Torulopsis sp.</i>	Sophorose lipids
	<i>Candida bogoriensis</i>	
	<i>Arthrobacter sp.</i>	Trehalose lipids
	<i>Mycobacterium tuberculosis</i>	
	<i>Lactobacillus fermenti</i>	Diglycosyl diglycerides
	<i>Ustilago zae, U. maydis</i>	Cellobiose lipids
Lipopetides	<i>Bacillus subtilis</i>	Surfactin, subtilisin, subsporin
	<i>Bacillus spp</i>	Lipopeptide antibiotics
	<i>Bacillus licheniformis</i>	various cyclic lipopeptides
	<i>Corynebacterium lepus</i>	Lipopeptide
	<i>Candida petrophilum</i>	Lipopeptide, protein emulsifier
Lipoproteins	<i>Pseudomonas rubescens</i>	Ornithine-containing lipid
	<i>Pseudomonas fluorescens</i>	Viscosin
Phospholipids	<i>C. alkanolyticum</i>	Lecithin, phospholipids
	<i>Thiobacillus thiooxidans</i>	Phospholipids
Polysaccharide lipid complexes	<i>Candida tropicalis</i>	Polysaccharide-fatty acid complex
	<i>Acinetobacter calcoaceticus</i>	Emulsan
	<i>Pseudomonas fluorescens</i>	Protein-carbohydrate complex

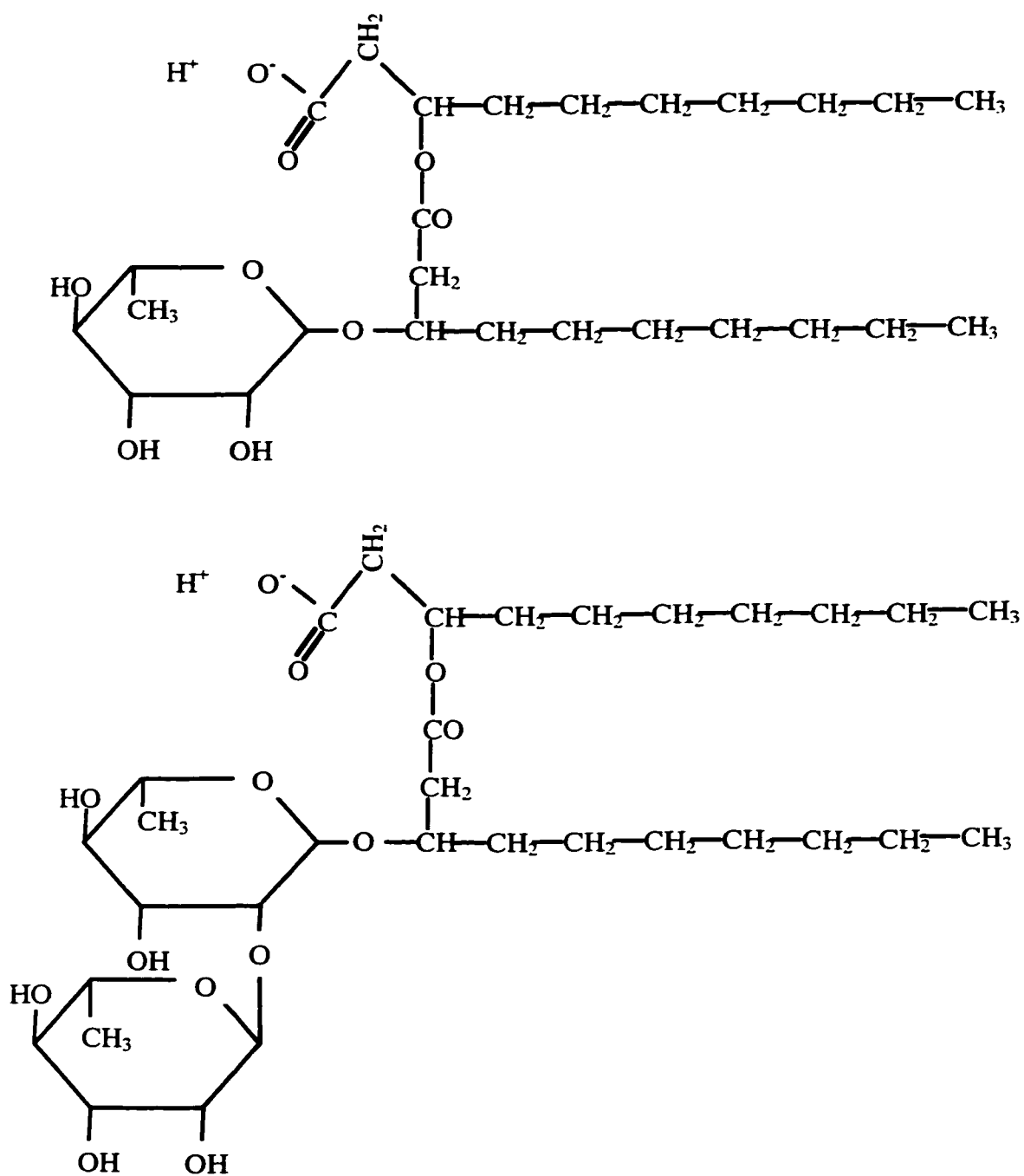


Figure 2.5 Structure of rhamnolipids (adapted from Zhang and Miller,1992)

genus of *Pseudomonas* is one of the most commonly found soil microorganisms. The complete enzymatic synthesis of rhamnolipid from the extracts of *Pseudomonas aeruginosa* ATCC 7700 was described by Burger et al. (1963). The structural and regulatory genes encoding the rhamnolipid synthesis pathway have been also isolated and characterized (Ochsner et al., 1995).

Rhamnolipid aggregates are predominantly small vesicles (50 nm in diameter), and micelles of 5 nm in diameter at pH > 6.0. The average surface tension of rhamnolipids is 40 mN/m. Rhamnolipid can lower the air/water surface tension for distilled water from approximately 72 mN/m to roughly 30 mN/m (Zhang and Miller, 1992). Previous work has shown that rhamnolipids can enhance soil flushing efficiency as well as the rate of biodegradation of non-aqueous phase liquid (NAPL) (Zhang and Miller, 1995; Miller, 1995; Bai et al., 1997), and desorption of heavy metals from soil (Herman et al., 1995; Mulligan et al., 1999). Therefore, they are of particular interest for use in *in-situ* remediation, since rhamnolipids are naturally biodegradable products that may be acceptable for being supplied to contaminated sites. Any new technology, which includes biosurfactants for the solubilization of PAHs instead of synthetic surfactants, needs to be further investigated.

### **2.5.2 Biosurfactant production**

In order to introduce biosurfactants into contaminated soil, the *ex-situ* production of biosurfactants is a necessary first stage of technology. Effective production and behavior of biosurfactants play an important role in achieving an efficient treatment technology. In this section, attention is paid to reviewing production of rhamnolipid

biosurfactants, which are used in this research. Production methods of rhamnolipids from *Pseudomonas spp.* are concluded in the below list:

- I. Growth-associated biosurfactant production There exists a parallel relationship between growth, substrate utilization, and biosurfactant production. Different carbon sources such as glycerol, glucose, and ethanol could be used for rhamnolipid production by *Pseudomonas spp.* (Robert et al., 1989). Reena and Desai (1997) dealt with the rhamnolipids produced from *Pseudomonas aeruginosa* GS3. When glucose was the substrate, maximum production (0.44 g/l) was observed during the stationary phase of growth. In addition, *Pseudomonas aeruginosa* GS3 can produce rhamnolipid biosurfactants during growth on carbohydrates, higher chain length n-alkanes and l-alkenes, petroleum crude oil and vegetable oils. Pilot-plant studies have shown that the production of rhamnolipids with a concentration of approximately 2.25 g/l was achieved (Reiling et al, 1986).
- II. Growing cells under growth-limitation conditions Due to the limitation of nitrogen, iron, and low phosphate concentration, the culture at the stationary phase of growth may increase the production of biosurfactants. Numerous investigators have demonstrated an overproduction of biosurfactants by *Pseudomonas spp.* when the culture reaches the stationary phase of growth due to the limitation of nitrogen and iron (Guerra-Santos et al., 1986; Mulligan and Gibbs, 1989; Ramana and Karanth, 1989). When bacterial cells were shifted from medium containing 36  $\mu\text{M}$  iron to a medium containing 18  $\mu\text{M}$  iron, rhamnolipid production dramatically increased three-fold (Guerra-Santos et al., 1986).



III. Production by resting cells In this method, although the bacterial cells continue to utilize the carbon source for the synthesis of biosurfactants, there is no cell multiplication. *Pseudomonas spp.* can produce the biosurfactants by resting cells. Syldatk et al. (1985) reported that the highest yield of rhamnolipids from n-alkanes produced by the resting free cells of *Pseudomonas spp.* DSM 2874 occurred at pH 6.6 and a temperature 37 °C. However, the biosurfactant production rate with resting cells was much lower than with growing cells. One of the advantages of using resting cells to produce biosurfactant is that it reduces the cost of product recovery (Reiling et al., 1986).

There are several nutritional and environmental factors, which affect biosurfactant production and should be considered in the development of the technology, including carbon, nitrogen, phosphate substrate, pH, temperature, oxygen concentration and salinity. Water-soluble carbon sources such as glycerol, glucose, mannitol, and vegetable oils were all used for rhamnolipid production by *Pseudomonas spp.* Ammonium salts and urea were selected as nitrogen sources for biosurfactant production. However, biosurfactant production in certain *Pseudomonas* species can be enhanced when cells are grown under low nitrogen conditions (Guerra-Santos et al., 1986). The research on rhamnolipid synthesis has shown that there are non-limiting concentrations of phosphate for the synthesis of rhamnolipids (Mulligan and Gibbs, 1989).

pH, temperature, and oxygen availability affect biosurfactant production through their effects on cellular growth or activity. Maximum rhamnolipid production in *Pseudomonas spp.* was in a pH range from 6 to 6.5 and decreased sharply above pH 7 in a continuous culture (Guerra-Santos et al., 1986). In addition, surface tension and CMC

of a biosurfactant product remained stable over a wide range of pH values, whereas emulsification had a narrower pH range (Abu-Ruwaida et al., 1991). The optimal temperature of synthesis for rhamnolipids is 31-34 °C. Below 30 °C or above 37 °C, the rhamnolipid yields were significantly reduced in continuous culture (Guerra-Santos et al., 1986).

### **2.5.3 Biosurfactants application in soil remediation**

Because biosurfactants are a naturally biodegradable product that may be acceptable into contaminated sites, they are of particular interest for use in *in-situ* remediation. Numerous researchers showed that the addition of biosurfactant could enhance the solubilization and bioavailability of hydrocarbons in batch scale studies. Jain et al. (1992) demonstrated that the addition of *Pseudomonas aeruginosa* UG2 biosurfactant to soil contaminated with a hydrocarbon mixture of tetradecane, hexadecane, pristane and 2-methylnaphthadene, followed by a 2-month incubation period, showed enhanced degradation of all hydrocarbons except 2-methylnaphthalene. Zhang and Miller (1992) showed that octadecane mineralization increased from 5 to 20% when the medium was supplemented with 0.3 g rhamnolipid/l. Van Dyke et al. (1993) reported that rhamnolipids from *Pseudomonas aeruginosa* increased 40 to 80% and 30 to 70% recovery of hydrocarbons from contaminated sandy-loam and silt-loam soil, respectively. The removal of hydrocarbons was approximately 10% more from a sandy loam soil (78% sand, 10% silt, and 12% clay) than from silt loam soil (54% silt, 30% sand, and 16% clay). Scheibenbogen et al. (1994) demonstrated that 56% of the aliphatic and 73% of the aromatic hydrocarbons were recovered from hydrocarbon-contaminated sandy-loam soil by treatment with rhamnolipids. A stimulatory effect of different types of

rhamnolipids on the degradation of hexadecane and octadecane by seven *Pseudomonas* strains has recently been presented (Zhang and Miller, 1995). Providenti et al. (1995) found that the addition of *Pseudomonas aeruginosa* UG14 rhamnolipid biosurfactants could enhance phenanthrene mineralization by 12% in a sandy loam (75% sand, 18% silt, 7% clay, 3.3% organic matter) and 19% in a silt loam (30% sand, 54% silt, 16% clay, 6.7% organic matter), respectively. Some researchers also reported that biosurfactants could form complexes with heavy metals. Miller (1995) and Herman et al. (1995) noted that in a soil experiment, the monorhamnolipid biosurfactant produced by *Pseudomonas aeruginosa* ATCC 9027 could remove 16%, 43% and 48% of the sorbed  $\text{Cd}^{2+}$ ,  $\text{Pb}^{2+}$  and  $\text{Zn}^{2+}$  from sandy soil (68% sand, 4.7% silt, 8.8% clay).

There are also a lot of promising uses of biosurfactant from *in-situ* remediation investigations. The removal of oil-contaminated gravel from the Exxon Valdez Alaskan oil spill was enhanced by biosurfactants that are produced by *Pseudomonas aeruginosa* SB30 (Harvey et al., 1990). Addition of 1% biosurfactant solution was found to consistently yield approximately twice the oil removal efficiency at temperatures from 10 to 80 °C. In Kuwait, oil-contaminated desert sand was treated by *in situ* and on site bioremediation. Through the introduction of specific nutrients and oxygen, indigenous microbial populations were encouraged to utilize hydrocarbons by the production of biosurfactants (Al-Awadhi et al., 1994).

To summarize, biosurfactants have similar properties to synthetic surfactant with added advantage of being biodegradable. Biosurfactant-producing bacteria can enhance the removal efficiency of PAHs from contaminated soil. Because this application is environmentally acceptable, biosurfactants are going to be applied in this research.

## **CHAPTER 3 PRINCIPLE OF ELECTROKINETICS**

### **3.1 Introduction**

Electrokinetics represents the viable methodology for the removal of inorganic contaminants from clay materials. Electrokinetic remediation (including bench-scale and pilot-scale tests) has demonstrated promising results in removing contaminants (Lageman, 1989; Acar et al., 1992; Pamukcu and Wittle, 1993; Probststein and Hicks, 1993; Runnels and Wahli, 1993; Acar and Alshawabkeh, 1996; Elektorowicz et al., 1995a, 1995b, 1996). Electrokinetics phenomena consist of electroosmosis, electrophoresis, and electrolytic migration in soils under an electric field in order to extract species from soils and to inject others into soils. This technique applies low voltage DC between anodes and cathodes. Due to oxidation-reduction processes, the pH decreases below 4 at the anode area, and increases above 10 at the cathode area (Elektorowicz et al., 1995a). Some research has been done to prevent the generation of extreme pH values by conditioning the anode and washing the cathode area with water (Reed et al., 1995; Elektorowicz and Hatim, 1999).

Lageman (1989) has used this technique successfully to remove more than 90% of heavy metals (arsenic, cadmium, cobalt, chromium, copper, mercury, nickel, manganese, molybdenum, lead, antimony and zinc) from clay, peat and argillaceous sand. Hamed et al. (1991) and Acar et al. (1994) presented the details of bench-scale laboratory test in order to demonstrate the feasibility of removing Pb, Cr, Cd, Ni, Cu, Zn, As, from fine-grained soils. The enhanced electrokinetic remediation done by Puppala et al. (1997) used acetic acid to neutralize the cathode electrolysis reaction and an ion selective membrane to prevent back-transport of the OH<sup>-</sup> generated at the cathode to remove the lead from

synthetic soil (40% illite, 8% kaolinite, 5% Na-montmorillonite and 47% fine sand). Wittle and Pamukcu (1993) and Chaudhury and Elektorowicz (1997) reported that the use of EDTA coupled electrokinetics could improve the solubility of lead and nickel in the natural soil.

A study by Bruell et al. (1992) has shown the possibility of removing benzene and toluene from clay by electrokinetics. They conclude that it appears to be a viable remediation technology for the removal of gasoline range hydrocarbons and chlorinated solvents from fine particle soils. Acar et al. (1992) and Elektorowicz et al. (1996) have reported 85-95% phenol removal from kaolinite. Probstein and Hicks (1993) also report high removal rates of phenol and acetic acid from kaolinite, up to 95%. Pamukcu et al. (1995) investigated the feasibility of transporting PAHs by electrokinetics from a manufactured gas plant site soil. Due to the formation of micelles by adding synthetic anionic surfactants (sodium dodecylbenzene sulfonate), the non-polar PAHs were transported. Lab scale tests have also demonstrated the removal of diesel fuel using PVC-carbon electrodes (Elektorowicz, 1995). All the studies have suggested or shown that electrokinetic remediation is an effective method of aiding the removal of contaminants from clay materials.

### **3.2 Fundamental theory of electrokinetics**

Electroosmosis, electrophoresis and electrolytic migration are the three major phenomena occurring in soil during the removal of contaminants under an electric field. Electroosmosis is caused by the migration of water towards cathode (i.e. by the movement of soil moisture from the anode to the cathode). Electrophoretic phenomenon

is observed when negatively charged colloid particles (such as soil particles, organic particles, droplets, microorganisms etc.) are attracted by the anode. Electromigration is the process by which transport of ionic species and ionic complexes in the pore fluid transport across the soil medium (Lageman, 1989). The following three sections describe the detailed principle of these phenomena.

### 3.2.1 Effect of electroosmosis on electrokinetic remediation

Electroosmosis is a significant process in electrokinetic soil processing. Electroosmotic phenomenon in a porous medium was first analytically treated by Reussa in 1807 (Wilun and Starzewski, 1967). Later the Helmholtz-Smoluchowski (H-S) theory was established. It describes electroosmotic velocity of a fluid with certain viscosity and di-electric constant, through a surface charged porous medium due to electrical gradient. This widely known theory has been applied for the description of water transport from the anode to the cathode through soil.

The driving force caused by electroosmotic flow is indicated by the coefficient of electroosmotic permeability ( $k_e$ ), which is defined as the volume rate of water flowing through a unit cross-sectional area due to a unit electric gradient under constant conditions and for a short duration of testing. The electroosmotic flow rate ( $q_e$ ) can be applied to evaluate the efficiency of the driving force. Assuming constant electrical potential gradient across the electrodes and neglecting the hydraulic gradients, the electroosmotic flow rate estimated in the laboratory (Casagrande, 1949), is expressed by

$$q_e = k_e i_e A = \frac{k_i}{\sigma} I \quad 3.1$$

where:

$q_e$  = electroosmotic flow rate ( $\text{cm}^3/\text{s}$ )

$k_e$  = coefficient of electroosmotic permeability ( $\text{cm}^2/\text{V}\cdot\text{s}$ )  
 $i_e$  = electrical potential gradient ( $\text{V}/\text{cm}$ )  
 $A$  = cross-sectional area ( $\text{cm}^2$ )  
 $k_i$  = coefficient of water transport efficiency ( $\text{cm}^2/\text{A}\cdot\text{s}$ )  
 $\sigma$  = electrical conductivity ( $\text{S}/\text{cm}$ )  
 $I$  = current (A)

The electroosmotic driving force is relatively insensitive to pore size (Shapiro and Probstein, 1993). Therefore, it allows for a more uniform flow distribution and a high degree of control in the direction of flow. The value of  $k_e$  has been found to be a function of zeta potential, viscosity of the pore fluid, porosity, and electrical permittivity of the soil medium.

Hunter (1981) displays that the zeta potential decreases linearly with a decrease in the logarithm of ionic concentration and /or the pH of the soil medium. It is hypothesized that the drop in pH of the soil due to electrokinetic processing will cause a decrease in the coefficient of electroosmotic permeability associated with the drop in zeta potential. In summary, the  $k_e$  value determined in one-dimensional tests is time-dependent, and is controlled by the electro-chemical process incited by electrical current. From Lageman's (1989) pilot-scale study, the average electroosmotic mobility has been calculated to be in the order of  $5 \times 10^{-9} \text{ m}^2/\text{V}\cdot\text{s}$ .

Accordingly, soluble species in the pore water may also be carried to the cathode following electroosmotic flow. Since clay can attract a cluster of excess cations close to the surface, under an electric field, the excess cations close to the surface move towards the cathode along with the movement of water molecules, thereby following electroosmotic flow in the same direction (Acar et al, 1993). They also indicated that this coupling effect may result in a high-conductivity region at the anode and a low-

conductivity region at the cathode, when applying a constant current (or variable voltage). A negative pore water pressure (suction) is expected to develop to compensate for the electroosmotic flux. For a constant current, the suction values will depend upon the ratio of electroosmotic permeability to the hydraulic conductivity ( $k_e/k_h$ ). The higher this ratio, the higher the suction. Therefore, the developed negative pore pressure will balance the electro-osmotic flow and hence decrease the net water flow, resulting in decreasing and eventually stopping at later stage of the process. Elektorowicz et al. (1995a) had solved the above-mentioned problem by the introduction of a water supply system near the electrode and barriers. Thus, in fine-grained soil, where the hydraulic conductivity is low, the major driving force for the water flow from the anode region towards the cathode was electroosmotic flow, which can be continuous during the test.

The fact that the theory does not always agree well with experimental results should be taken into consideration. The constant electrokinetic potential term in the H-S theory varies with soil pH and ionic concentration of the pore fluid, which does not remain constant during electrokinetic treatment of soils. When an electric field is applied to wet soil, the soil pH undergoes transient and spatial variation due to dissociation of water, which in turn affect soil surface properties such as cation exchange capacity, ion (cation and anion) adsorption capacity, and magnitude and sign of the electrokinetic potential. Even though phenanthrene is a non-polar insoluble organic compound, it is not totally insoluble. There is still soluble phenanthrene moving to the cathode following the electroosmotic flow.



### **3.2.2 Effect of electrophoresis on electrokinetic remediation**

Electrophoresis involves the movement of charged particles under the influence of an electric field (Mitchell, 1976). This definition includes all electrically charged particles like colloids, clay particles in pore solution, organic particles, droplets, microorganisms, etc. Within the pore solution, these particles transfer the electrical charges and affect the electrical conductivity and the electroosmotic movement. The electric force on the charged particle, is equal to the hydrodynamic frictional force on the particle by the liquid.

Clay minerals have two electrical polarity possibilities. One consists of the structure-based dipole moment, which depends on the atomic masses and has an orientation parallel to the longest axis of the clay particle. The second polarity exists at right angles to the first and is caused by the external electric field. It depends on the mode of polarization of the electrical double layer. The mobility of clay particles is a function of two moments and is less than the electroosmotic mobility. It varies between  $1 \times 10^{-10}$  and  $3 \times 10^{-9} \text{ m}^2/\text{V.s}$  (Lageman, 1989).

From the above-mentioned concept, electrophoresis is a very important mechanism in electrokinetic soil and slurry remediation when surfactants are introduced into the fluid to form micelles (charged particles) (Pamukcu and Wittle, 1992; Acar and Alshawabkeh, 1996). In addition, electrophoresis of clay colloids may play an important role in decontamination if the migrating colloids have the chemical species adsorbed on them. Electrophoretic movement can contribute to the transport of contaminants in the form of colloidal electrolytes or ionic micelles. Micelle formation is promoted as the concentration of the aggregating groups increase. Ionic micelles often carry a high charge

and exhibit high conductance in dilution. As the concentration of surfactant increases, a build-up of charge occurs due to further aggregation, and the conductance consequently increases. However, with many systems there is a sudden and sharp decrease of conductance at a critical concentration which is attributed to: 1) increasing association of the ionic colloids which results in increased fraction of neutral colloids; 2) retarding interionic forces which could be especially powerful with the large charges that these ionic micelles carry (Pamukcu et al., 1995).

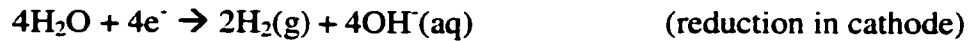
In this research, contaminant of concern is phenanthrene, which is a nonpolar insoluble organic compound. It is strongly sorbed to the clay particles or/and soil organic matter. Consequently, it cannot be effectively transported with electroosmotic flow. Therefore, introduction of surfactants to form ionic micelles, which are moved by electrophoretic forces and can enhance the removal of phenanthrene. Generally, the process may involve the micelle migration and electroosmotic flow in the action.

### **3.2.3 Effect of electromigration on electrokinetic remediation**

Electrolytic migration (also called electromigration) is the movement of ions and ion complexes within the soil moisture or groundwater, other than the movement of water or particle transport. The cations move toward the cathode, and the anions toward the anode. The average mobility of ions lies around  $5 \times 10^{-8} \text{ m}^2/\text{V.s}$ , which is ten times greater than that of the electroosmotic mobility (Lageman, 1989).

Electrolysis reactions at the electrodes need to be considered together with the mass flux of species that occurs in the electric field. Due to the application of direct electric current, oxidation occurs at anode, generating an acid front, while reduction at the

cathode, producing a base front. The reactions are shown below at the anode and the cathode, respectively.



The hydrogen (protons) and hydroxyl ions generated at the electrodes by the electrolysis reactions may transport to the opposite electrode. In the unenhanced electrokinetic remediation, the protons with hydroxyl group can be transported across the soil mass, and generate water (Acar and Alshawabkeh, 1993).

Meanwhile, clay particles in suspension are strongly influenced by pH. Clay particles may have hydroxyl ( $\text{OH}^-$ ) exposed on their surfaces and edges. The tendency for the silica hydroxyl ( $\text{SiOH}$ ) to dissociate  $\text{SiO}^-$  and  $\text{H}^+$  is strongly influenced by pH. The higher the pH, the greater the tendency for the  $\text{H}^+$  to go into solution, and the greater the effective negative charge of the particle. As a consequence, a low pH promotes a positive edge to negative surface interaction, often leading to flocculation from suspension. Stable suspensions or dispersions of clay particles often require high pH conditions.

Other possible transport mechanisms during electrokinetic remediation are hydraulic convection and ionic diffusion. Hydraulic convection can be neglected in the case of low permeability soils (Acar and Alshawabkeh, 1996). Diffusion transport of ions can occur when concentration gradients exist or are produced by reactions between the various species present, by electrode reaction or any solid/liquid interface phenomena (sorption, precipitation, dissolution, and complexation).

In general, the electrokinetic remediation technique is a controlled use of electroosmosis, electrolytic migration, and electrolysis reactions for the extraction of

species from soils. Electrolytic migration dominates transport in most soils once the species are released into the pore fluid by the prevailing dissolution reactions. In high water content and low activity clays, mass transport by electroosmosis may be on the same order of magnitude as mass transport by electromigration. Electrophoresis becomes a more important phenomena when surfactants are involved in the electrokinetic process.

In summary, due to surface charge of the clay material, electrokinetics offers the possibility of inducing a greater flow through clayey soil, and driving contaminant movement. Therefore, electrokinetically controlled processes on contaminant transport in heterogeneous soil have significant implications regarding the potential efficiency of *in-situ* remediation technologies.

## CHAPTER 4 METHODOLOGY AND MATERIALS

The experiments were divided into four test series, which allowed for the determination of several unreported phenomena, which affected bio-electrokinetic technology. For this reason, four different types of experiments were dealt with. These tests allowed for the investigation of:

- I. Bacterial behavior in contaminated clayey soil under the electric field;
- II. Potential *in-situ* production of biosurfactants under the electric field;
- III. Introduction of biosurfactants produced *ex-situ* into clayey soil by means of electrokinetics;
- IV. Bio-micelles formation process, kinetics of bio-micelles' mobility, and effectiveness in phenanthrene removal within the microcosm of soil environment.

The detailed experimental procedures are highlighted in Figure 4.1. These experiments encompassed the preparation of soil, production of biosurfactants in a lab scale, characterization of materials, protocol of analytical methodology and setup of electrokinetic cells.

### 4.1 Preparation of soil specimens

Phenanthrene was used as a model for PAH contamination in soil. Phenanthrene (98% purity), an isomer composed of three benzene rings, was purchased from Fisher Scientific, Rochester, NY. Phenanthrene was dissolved in hexane to obtain the required concentration.

Soil used in all experiments are clay materials, purchased from Canada Brick Limited (Laval, QC), under the manufacture name "Sealbond". In order to characterize

the soil properly, all soil specimens were passed through the No. 200 sieve. Total organic carbon content, moisture content, pH, carbonates, sulphates, chloride, total Kjeldahl Nitrogen (TKN), and cation exchange capacity (CEC) of soil were measured before the experimentation. Mineralogical analyses for soil specimens were performed by X-ray diffraction.

Prior to all experiments, the soil specimens were dried in the oven at 105 °C for 24 hrs to allow for the removal of pore water. Moisture content was adjusted to 40-45% using distilled water. In all tests related to bacteria, the soil specimens were dried in an oven at 105 °C for 24 hours and autoclaved for 30 min at 103 kPa and 121 °C to ensure sterility. The autoclaved soil was confirmed to be sterile by plating autoclaved soil on *Pseudomonas* agar P plates (content of culture presented in Chapter 4.2). The soil was then dried at 105 °C for 24 hours and adjusted to a desired moisture content by sterilized water. The soil was placed into the electrokinetic cells by layers in order to prevent gap and air pockets within the soil specimen.

In order to investigate the efficiency of biosurfactants on the removal of the phenanthrene from clay soil, the soil was spiked with a solution containing phenanthrene and hexane. The concentration of phenanthrene applied in this experiment was 250 mg/kg soil. This value belongs to level C, which indicates that the soil is contaminated and cannot be used for the residential and industrial purposes. Therefore, remedial action is necessary.

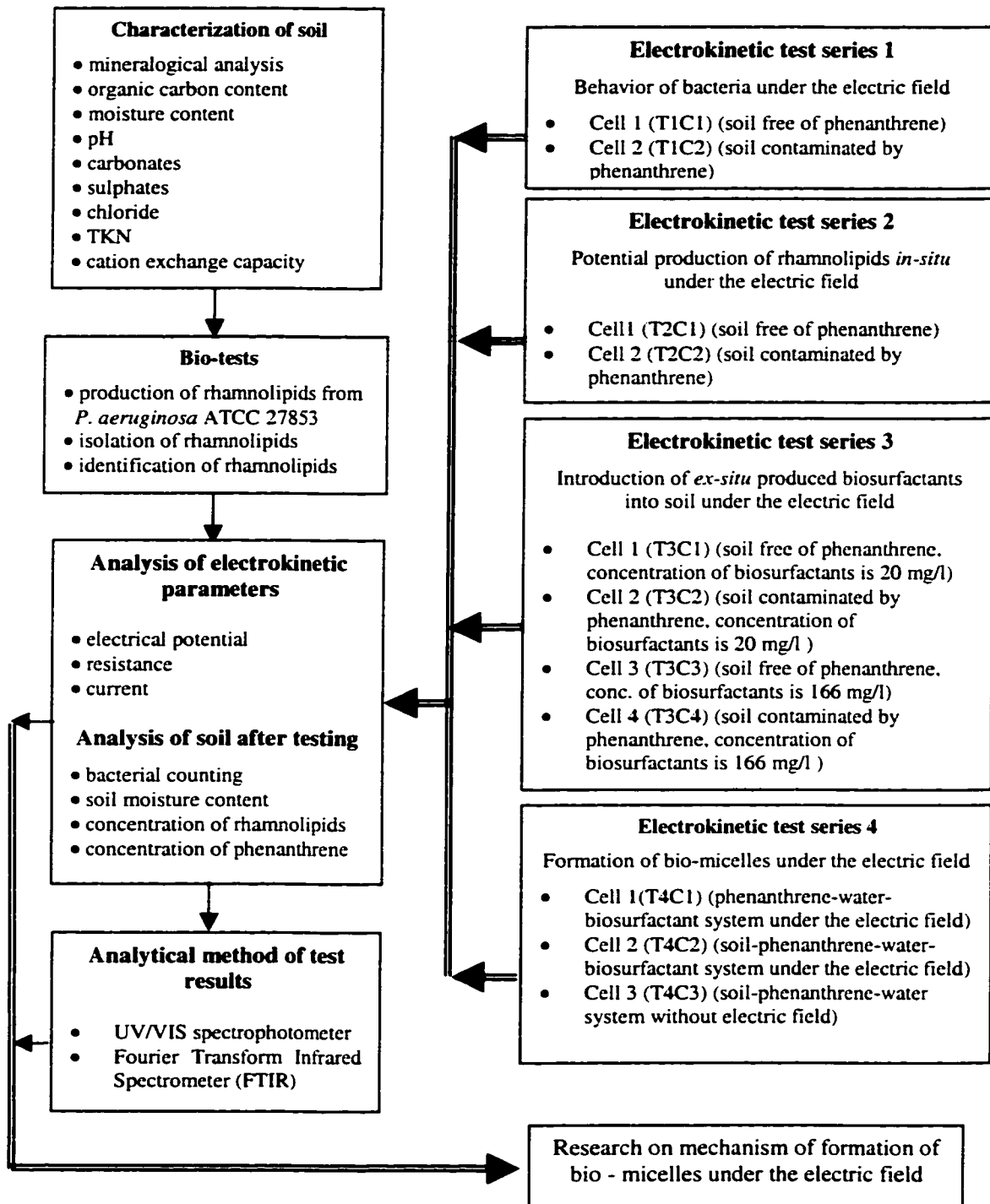


Figure 4.1 Scope of experiments

## 4.2 Preparation of microorganisms

Due to its biosurfactants production capacity, *Pseudomonas aeruginosa* was chosen as the target bacteria in this research. *Pseudomonas aeruginosa* ATCC 27853 was obtained from the American Type Culture Collection (Rockville, MD) and stored at 4°C on *Pseudomonas* agar P plates and transferred to a fresh agar plate each month. The culture contents of *Pseudomonas* agar P consist of 20 g/l proteose peptone, 15.0 g/l agar, 10.0 g/l glycerol, 10.0 g/l dipotassium hydrogen phosphate ( $K_2HPO_4$ ), and 1.4 g/l magnesium chloride hexahydrate ( $MgCl_2 \cdot 6H_2O$ ). They are gram-negative bacteria, which are chemoheterotrophs using organic compounds containing more than one carbon atom as energy and carbon sources. They depend on oxygen as a terminal electron acceptor. These bacteria do not require additional growth factors. A blue phenazine pigment, pyocyanin, is characterized as the species *P. aeruginosa*.

The procedure of counting the viable number of bacteria in soil dilutions followed the traditional methodology, namely dilution plate counts for bacteria in soil. A 1 g soil sample from the experiment was weighed into a dilution tube containing 10 ml of sterilized distilled water. The tube was capped, placed on a mechanical shaker, for 3 hours at 200 rpm at room temperature (23 °C). The tube was centrifuged at  $5000 \times g$  for 20 min, and a  $10^{-1}$  dilution was obtained. A 1 ml from the supernatant was transferred to a 9 ml dilution in a capped tube, and shaken well. This procedure was repeated until  $10^{-8}$  was reached. A 0.1 ml suspension from the dilution was spread on the *Pseudomonas* agar P surface with a sterile glass spreader for each plate. Triplicate plates per dilution were prepared. The culture plates were incubated in a dark, aerobic environment of 28 °C for



24 hrs. Plates containing 30 to 300 colonies were considered (presented as Colony-Forming Units (CFU)/g soil).

### **4.3 Production from bacteria, extraction and identification of biosurfactants**

In this research, isolated rhamnolipid (biosurfactant) was used to perform the enhanced electrokinetic experiment. *P. aeruginosa* ATCC 27853 was reported to have the ability to produce rhamnolipids during growth on a medium of protease peptone-glucose-ammonium salts (Cheng et al, 1970).

The procedure for the production of biosurfactant from *Pseudomonas aeruginosa* ATCC 27853 is described below. *P. aeruginosa* was inoculated into 25 ml of Kay's minimal medium (Warren et al., 1960) in a 125-ml flask. This medium included 1.5 g/l of monobasic ammonium phosphate ( $\text{NH}_4\text{H}_2\text{PO}_4$ ), 1.0 g/l dipotassium hydrogen phosphate ( $\text{K}_2\text{HPO}_4$ ), 1.0 g/l glucose, 0.5 mg/l iron (II) sulfate ( $\text{FeSO}_4$ ), and 0.5 g/l magnesium sulfate heptahydrate ( $\text{MgSO}_4 \bullet 7 \text{H}_2\text{O}$ ). The culture was incubated with shaking at 200 rpm for 24 hours at 37°C, and then 2 ml was transferred into 200 ml of protease peptone-glucose-ammonium salts medium (PPGAS) in a 1,000 ml flask. The contents of PPGAS consist of 1.1 g/l ammonium chloride ( $\text{NH}_4\text{Cl}$ ), 1.5 g/l potassium chloride (KCl), 0.12 M Tris (hydroxymethyl) hydrochloride (Tris-HCl), 5 g/l glucose, 10g/l protease peptone, and 0.2 g/l magnesium sulfate ( $\text{MgSO}_4$ ). This flask was incubated at 37°C with shaking at 200 rpm for 60 hours, at which rhamnolipids were harvested at the maximum level (Zhang and Miller, 1992). In addition, the culture suspension was used for extraction, purification and identification of rhamnolipids.

For isolation and purification of rhamnolipid from bacterial culture, the culture suspension was centrifuged at  $5,000 \times g$  for 20 min to remove cells (Canlab Medifuge 5415, CA). The supernatant was removed from the centrifuged tube, then added to concentrated HCl to achieve a final pH of 2.0 in order to promote the precipitation of rhamnolipid, and centrifuged at  $14,000 \times g$  for 20 min (IECB-20A centrifuge, U.S.A). The precipitate was dissolved in 0.05 M sodium bicarbonate, reacidified, and recentrifuged at  $14,000 \times g$  for another 20 min. The precipitate was extracted with chloroform-ethanol (2:1) three times in a separator funnel. The equivalent volume of distilled water was also introduced into the funnel to separate the chloroform layer (containing the lipids) from the water-soluble phase. The organic solvent was removed with the aid of a rotary evaporator (Buchi 001, Switzerland), and the residue was dissolved in 0.05 M sodium bicarbonate (pH 8.6).

Identification of the glycolipid fraction was performed by Fourier Transform Infrared Spectrometers (FTIR) with Bomem-Gramps/386 spectrometer operating Win-Bomen Easy software packages (Bomem, Inc. QC). This equipment has one accessory, called Gemini, which combines two sampling technologies in one device: horizontal attenuated total reflectance (with Zinc Selenide crystal as a sampling plate) and diffuse reflectance (with six macro diffuse sampling cups mounted on a diffuse reflectance cartridge). The former provides a horizontal sampling surface to allow for the analysis of the liquid samples. The latter is used to analyze the solid samples and rough surfaces. In this study, the liquid sample of biosurfactants was directly placed in the ZnSe plate, dried in the air-flow hood for 6 hours, and placed back into the spectroscopy. Fifty scans were applied with a resolution of  $4 \text{ cm}^{-1}$ . The spectral data were interpreted by examining the

literature values of infrared absorption (Little et al., 1966).

In order to investigate the formation of bio-micelles by biosurfactants and phenanthrene, NanoScope Atomic Force Microscopes (AFM) (Dimension 5000 SPM, California) was applied. AFM measures the attractive or repulsive forces between tip and sample, and obtains topography by mechanically moving a shape probe across the sample to “feel” the contours of the surface. Samples are not disturbed by preparation process. The image obtained was three-dimensional and of high resolution.

#### **4.4 Determination of pH, moisture content, and concentration of rhamnolipids and phenanthrene in soil**

Analysis of pH values for the soil was performed using standard pH experiments. 3.0 g of air-dried soil from each soil specimen was placed in a 15 ml tube. 7.5 ml distilled water was added to the soil. The tube was shaken for 1 hour and allowed to settle for 0.5 hours. The pH of the supernatant was obtained once the reading became stable.

In order to measure the moisture content in soil, a 1 g soil specimen was placed into a pre-weighted porcelain dish and dried in the oven at 105 °C for 24 hours. After that, it was put into a desiccator to cool down and then weighed. The difference between these weights divided by the original weight of the soil was multiplied by 100% to obtain the moisture content in soil.

For the isolation of rhamnolipids from the soil, in order to test the concentration of biosurfactants, one gram of soil specimen was extracted with 5 ml diethyl ether in a 15 ml centrifuge tube. The tube was then centrifuged at 5000 × g for 20 min. The rhamnolipids in the supernatant was pooled, dried, and resuspended in 1 ml of 0.05 M sodium bicarbonate. And then the concentration of rhamnolipids was estimated using the

modified L-rhamnose measurement technique (orcinol assay) (Chandrasekaran and Bemiller, 1980). A 100  $\mu$ l sample was treated with 900  $\mu$ l of 100 mg orcinol (in 53%  $H_2SO_4$ ) and heated for 20 min at 80°C. After cooling at room temperature for 15 min,  $A_{421}$  was measured. Rhamnolipid concentrations were calculated from standard curves prepared with L-rhamnose (obtained from Sigma, St. Louis, MO.) and expressed as rhamnose equivalents (in mg/l).

In order to determine phenanthrene concentration in the soil, one gram of soil specimen after testing was mixed with 5 ml of hexane in 15 ml centrifuge tube, and shaken for 2 hours at 150 rpm. Then, the tube was centrifuged at  $5000 \times g$  for 20 min. The supernatant was used for the determination of phenanthrene concentration by UV-VIS spectrophotometer (PYE PU8600, Philips). The absorbance of UV was compared with a prepared standard curve of phenanthrene to obtain the concentration.

## **4.5 Electrokinetic cell configuration**

Figure 4.2 shows a schematic diagram of the container used in bench-scale test series 1 and test series 2. The container was made of rigid polyethylene for electrical insulation and resisting the lateral compaction pressure. Inner dimensions of the container were chosen to be 5.0 cm in width, 4.0 cm in height, and 11.4 cm in length for test series one and two (T1 and T2) (Figure 4.2). For test series three (T3), inner dimensions of the container were chosen to be 5.0 cm in width, 2.0 cm in height, and 11.4 cm in length (Figure 4.3). The inner side of the container was sealed with silicon sealant paint. The configuration of the electrokinetic cell for test series four (T4) was 8.0 cm in width, 6.0

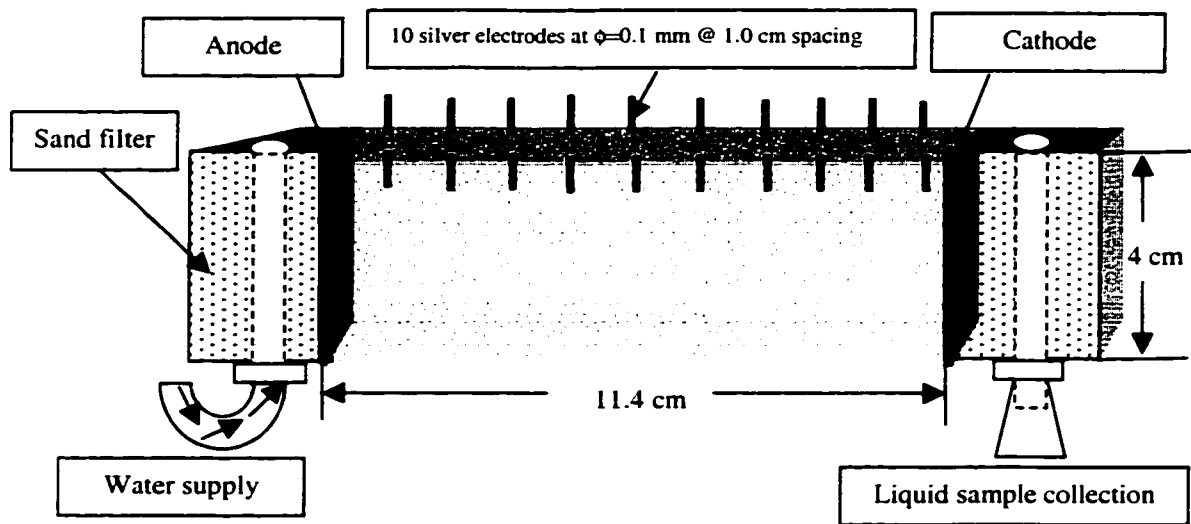


Figure 4.2 Schematic diagram of experimental setup for cells T1C1, T1C2, T2C1, and T2C2

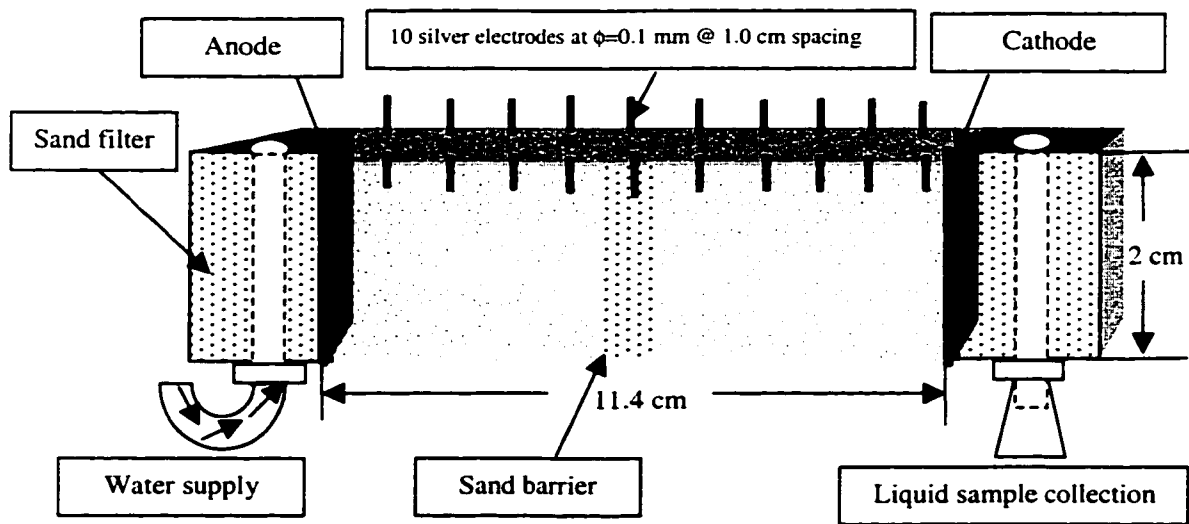


Figure 4.3 Schematic diagram of experimental setup for cells T3C1, T3C2, T3C3 and T3C4

cm in height, and 3.0 cm in length (Figure 4.4). In order to measure differential electrical potentials along the electrokinetic cell, ten silver probe electrodes with a diameter of 0.10 mm and spacing of 1.0 cm were inserted in the soil between electrodes.

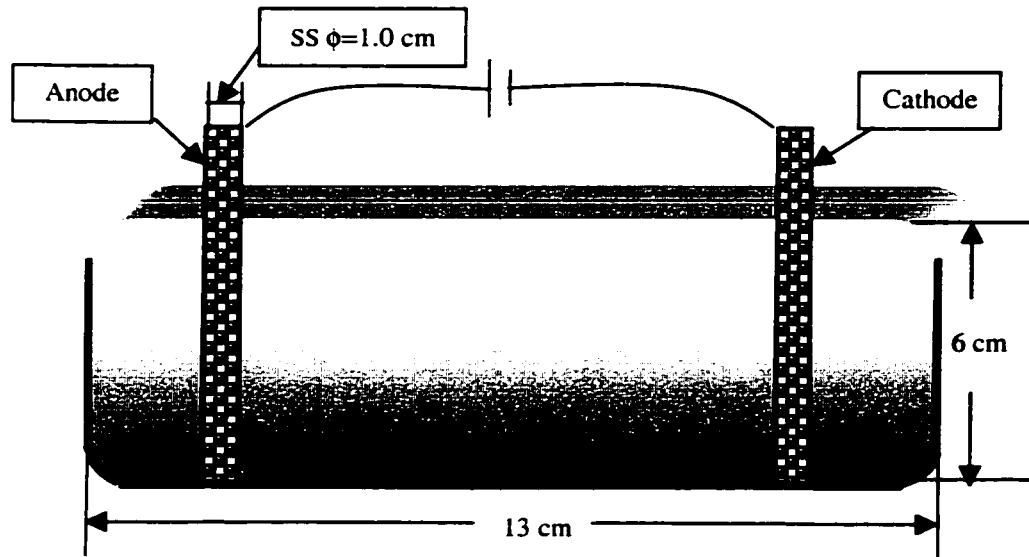


Figure 4.4 Schematic diagram of experimental setup for cells T4C1, T4C2 and T4C3

For series T1, T2 and T3, two plates made of stainless steel mesh, which allowed the uniform distribution of electrokinetic flow, were used at both the anode and the cathode (Figure 4.5). They were cut into a size that matched the cross section of the cell, which was 5 cm × 4 cm for T1 and T2, and 5 cm × 2 cm for T3. The platinum wires (0.05 mm in diameter) were wrapped around the top of stainless steel mesh in order to take advantage of their electrochemical inertness. They were connected in parallel to a power supply using silver wires. For series T4, the perforated stainless steel electrode (with diameter of 1.0 cm) was used as the cathode and the anode, fixed to the cell at a distance of 8.0 cm (shown in Figure 4.4).

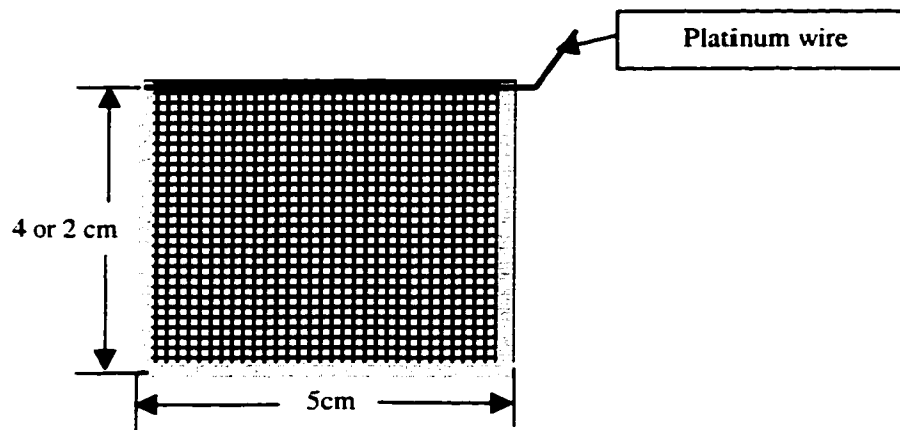


Figure 4.5 Stainless steel mesh electric plate

#### 4.5.1 Test series 1: Behavior of bacteria under the electric field

In order to improve the efficiency of bio-electrokinetic remediation, the response of bacteria under an electric field is still under research. Through the application of electrokinetics, pH control is very important because extreme pH values could eliminate inoculated degradative bacteria or indigenous bacteria for bioremediation (DeFlaun and Condee, 1997). In order to investigate the behavior of biosurfactant-producing bacteria under the electric field, two cells were setup, and designated as TIC1 and TIC2. Their dimensions were identical. The cell configuration is shown in Figure 4.2.

The experiment duration for this test series was 14 days. The electrode mesh, tubes, and containers were thoroughly rinsed before using them in the next electrokinetic cell. DC regulated power supplies (TES 6230, CA) were used to apply a voltage continuously across the electrodes for the experimental duration. The applied electrical potential between the two electrodes was 5.70 V at a distance of 11.4 cm to achieve the value of 0.5 V/cm. The design specifications for the power supply and the associated

electrical circuit are such that they are able to perform independent experiments in parallel electrokinetic cells.

It is important to monitor the voltage distribution across the electrokinetic cells as a function of time, since the electrical gradient is the primary driving force for the transport of species during the electrokinetic process. It can help to better understand the development of the process. In order to measure differential electrical potentials along the electrokinetic cell, ten silver probe electrodes with a diameter of 0.10 mm and spacing of 1.0 cm were inserted in the soil between electrodes. This design made it possible to measure the actual electrical potential change using TES Scientific Multimeter (Model 155, CA), with an input impedance of 100 M $\Omega$ . Potential measurements were obtained every 24 hours, at each probe location for the entire 14 days of the experiment. The uncertainty in each measurement was estimated to be lower than  $\pm 5\%$  of the reading. At the same time, the electric current in the system was also recorded by a TES Scientific Multimeter, with a sensitivity of 0.01 mA. These allowed for the determination of the resistance distribution within the soil and permitted to monitor the electrokinetic phenomena during the experiments.

Sterilized water from a reservoir was introduced through a perforated tube (a plastic PVC tube at  $\phi$  0.5 cm) directly into the porous sand filter, which adjacent to the anode plate was used in order to uniformly distribute water into the electric field. The volume of water supplied was connected to a graduated reservoir for daily measurement. The supplied water level in each cell was kept at 5 mm below the soil surface in order to avoid overflow. A plastic wrap covered the clay in the cells in order to minimize evaporation. The collection of the liquid was performed by placement of perforated tubes



in the sand filter adjacent to cathode. Liquid samples were collected in a 20 ml vial on a daily basis and subjected to analysis. The pH of the liquid from the cathode was measured by directly inserting the multi-electrode pH/voltmeter (Hanna Instruments, HI8418).

At the end of the experiment, the soil was sampled in approximately equal thickness and at known distances from the middle row around the electric probe and electrodes. Ten samples were obtained from each cell. This sampling protocol allowed for the verification of different parameters and their variation with distance. Final analysis of soil moisture content, pH in soil, and bacterial counting in soil were carried out for the soil specimens in each cell.

#### **4.5.2 Test series 2: Potential *in-situ* production of biosurfactants under the electric field**

In order to conduct the experiments related to potential production of biosurfactants *in-situ*, test series 2 was setup. The configuration of two electrokinetic cells T2C1 and T2C2 were presented in Figure 4.2. Their dimensions were identical. Medium (PPGAS) with bacterial cells from an exponentially growing culture were uniformly incorporated into sterilized soil for both electrokinetic cells. Approximately, 9.00 log CFU/g soil dry wt. of bacteria was applied. The applied culture was used to promote rhamnolipids production (culture content shown in Chapter 4.3).

Electrokinetic cells connected to a power supply at 5.7 V were run for 14 days. DC regulated power supplies applied a voltage of 5.7 V at a distance of 11.4 cm across the electrodes to achieve a value of 0.5 V/cm. In order to measure differential electrical potentials along the electrokinetic cells, ten silver probe electrodes at the diameter of 0.10

mm and space of 1.0 cm apart were inserted in the soil of cells, in order to measure the electrical potential difference at each probe location every 24 hours. A plastic wrap covered the clay in order to minimize evaporation. The electric current in the system was also recorded at the same time. This allowed for the determination of the resistance distribution within the soil and permitted the monitoring of the electrokinetic phenomena during the experiments.

The water supply system followed the description in Chapter 4.5.1. The collection of the liquid was done at the placement of perforated tubes in the sand filter adjacent to the cathode. Liquid samples were collected into 20 ml vial on a daily basis and subjected to analysis.

At the end of the experiment, the soil was sampled in approximately equal thickness and at known distances from the middle row around the electric probe and electrodes. Ten samples were obtained from each cell. Final analysis of soil moisture content, soil pH, bacterial number in soil, and concentrations of phenanthrene and rhamnolipids in soil were carried out for the soil specimens in each cell, which followed the analytical procedure indicated in Chapter 4.4.

### **4.5.3 Test series 3: Transport of biosurfactants under the electric field**

Due to the anionic properties of rhamnolipids, it was hypothesized that the negatively charged biosurfactants would be transported in the soil via electrolytic migration to the anode region due to the application of a DC current on the soil specimen. The negatively charged micelle of phenanthrene and rhamnolipids would be also transported to the anode area. In this manner, it was also hypothesized that biosurfactants

would be able to desorb phenanthrene from the soil surface and the phenanthrene could be transported in the aqueous solution to the cathode by electroosmosis. However, under the complex electrokinetic conditions, the transport of biosurfactants under the electric field is still unknown. In order to investigate the behavior of biosurfactants under the electric field, test series 3 was performed. Four identical electrokinetic cells (referred as T3C1, T3C2, T3C3, and T3C4) were used in test series 3 (Figure 4.3). This setup allowed for the study of the fate of biosurfactants injected through a unique point in the middle between the electrodes. For this purpose, a sandy supply zone, with a thickness of 1.0 cm and the same cross-sectional dimensions of the electrokinetic cell, was located in the middle of the electric cell in test series 3 in order to supply the biosurfactant solution uniformly. After the electrokinetic cells were connected to the electrical power supply, the biosurfactants were introduced. The biosurfactants (rhamnolipids) used were produced on a lab scale (seen in Chapter 4.3). The solution of biosurfactants was introduced in a volume of 4 ml into the center of sand barrier every 24 hours during 8 days of experimentation.

In order to investigate the impact of rhamnolipid concentration, two concentrations (below and above CMC, which is 50 mg/l after Zhang and Miller (1992)) were applied. The concentration of biosurfactants used was 20 mg/l, which represents the value below the CMC, and was introduced into cell T3C1 (free of phenanthrene in soil) and cell T3C2 with phenanthrene contaminated soil. The biosurfactant concentration of 166 mg/l, representing the value above the CMC, was introduced into cell T3C3 (free of phenanthrene in soil) and cell T3C4 containing phenanthrene contaminated soil. The concentration of phenanthrene used in the soil was 250 mg/kg soil.

Ten monitoring electrodes were installed along the electrokinetic cell. The silver monitoring electrodes were advanced 2 cm into the specimens prior to testing. During 8 days of experimentation, a constant voltage of 5.7 V was applied between anode and cathode to achieve the value of 0.5 V/cm. Electric current and voltage at each of the ten monitoring probes along the cell were recorded every 24 hours. Liquids were collected daily at the cathode and subjected to pH analysis.

After testing, the clay specimens were extruded and sliced into 10 sections, following the sampling methods described in Chapter 4.5.1. The value of pH, moisture content, concentration of phenanthrene and biosurfactants of each slice were measured. The chemical analysis of component was described in Chapter 4.4.

#### **4.5.4 Test series 4: Investigation on bio-micelles under the electric field**

In order to describe the kinetic formation of bio-micelles (micelle created by biosurfactant and phenanthrene), test series 4 was conducted. It is important to answer the formation of bio-micelles in soil microcosm environment since the stability of micelles has an impact on the efficiency of PAHs removal. Consequently, special experiments were prepared to simulate this phenomena within the contaminated soil pores. In order to describe the dynamics of interaction among phenanthrene, biosurfactants, soil and water under the electric field, experimental work was conducted to compare the three system: phenanthrene-water-biosurfactants in cell T4C1, and soil-phenanthrene-water-biosurfactants in cell T4C2 under the influence of electric field, and soil-phenanthrene-water in cell T4C3 without application of the electric field.

The dimension of the polyethylene cell was 8.0 cm width, 6.0 cm height, and 13.0 cm length with the cover at the top of the cells. Two perforated stainless steel electrodes (with a diameter of 1.0 cm) were placed into the cell with a distance of 8.0 cm (Figure 4.4). These electrodes are connected by a DC power supply at the level of 6.5 V to achieve the value of 0.5 V/cm.

The biosurfactants (rhamnolipids) applied in this test were produced and extracted on a lab scale, as described in Chapter 4.3. For the preparation of the phenanthrene-water-biosurfactant system, 7.5 mg of phenanthrene and 40 ml of 1.0 g/l biosurfactants was added to 260 ml of distilled water to achieve the concentration of approximately 160 mg/l, and gently shaken for 2 hours. For the preparation of soil-phenanthrene-water-biosurfactant system, phenanthrene, dissolved in hexane, was spiked on 30 g soil to obtain a concentration of 250 mg/kg. The hexane in the stock was allowed to evaporate over a period 24 hours prior to the addition of 260 ml of distilled water and 40 ml of 1.0 g/l biosurfactants, after which the medium was gently shaken for 2 hours. For the preparation of soil-water-phenanthrene, following the same spiking procedure, 300 ml of distilled water was added, and gently shaken for 2 hours.

Before the test, the pH of solution, concentration of biosurfactants and phenanthrene in the mixture were determined. During the 7 day test, the samples were taken from the top (1.5cm from top), middle (3.5cm from top), and bottom (5.5cm from top) in the central area of the electrokinetic cell. In order to follow the kinetics of micelle formation, the samples were taken at time interval of 0 hour, 1 hour, 2 hours, 5 hours, 8 hours, 11 hours, 14 hours, 17 hours, 20 hours, 48 hours, 72 hours, 96 hours, and 168 hours. After the test, for T4C2 and T4C3, the sediment was dried in the fume hood for 24

hours. In total, 150 samples were collected.

The mixture and sediment sampled from different locations were analyzed by FTIR using a ZnSe plate for liquid sample and diffuse sampling cups for solid samples. The samples were dried in the air-flow hood for 6 hours before mounted into the spectroscopy. Fifty scans were applied with a resolution of  $4\text{ cm}^{-1}$  for each sample. The spectral data were interpreted by examining the literature values of infrared absorption (described in Chapter 5.3).

# CHAPTER 5 CHARACTERIZATION OF MATERIALS

## 5.1 Characterization of soil

The mineralogical analytical results, performed by X-ray diffraction are presented in Figure 5.1. It clearly showed that the main primary minerals in the soil specimen were quartz. In addition there were small fractions of the primary minerals - amphibole and pyroxene. The main secondary minerals found in the soil specimen were chlorite and muscovite, which belong to mica minerals. Muscovite is similar in structure to illite (as described in Chapter 2.2).

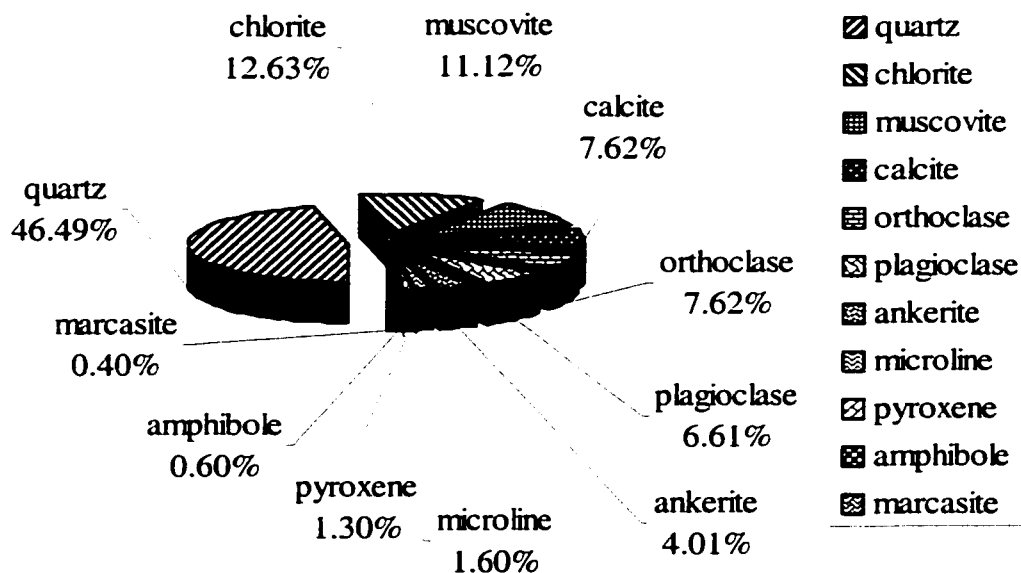


Figure 5.1 Mineralogical analysis of soil specimens

Soil specimens were also subjected to the physical and chemical characterizations. Table 5.1 contains the results of the analysis for the characterization of soil specimens. As shown in the table, the CEC of the soil specimens was 21 meq/100g,

which is in the region typically for illite. The high CEC value may cause the binding of phenanthrene with soil. The carbonate content of the soil specimen was relatively high with a value of 7.5% as CaCO<sub>3</sub>. It contributed to the high pH level of the soil, affected precipitation, and also increased the soil buffer capacity. The soil contained organic carbon, which indicated that soil specimens possessed a certain level of humic content.

Table 5.1 Initial physical and chemical properties of soil specimen

<b>Parameter tested</b>	<b>Value</b>
<b>Specific gravity</b>	2.65
<b>Total Organic Carbon</b>	2.7% wt
<b>Moisture content</b>	8.6%
<b>pH</b>	7.8 ± 0.05
<b>Carbonates</b>	7.5% CaCO <sub>3</sub>
<b>Chloride</b>	245 ppm
<b>Sulphates</b>	12.3 ppm as SO <sub>4</sub> <sup>2-</sup>
<b>Total Kjeldahl Nitrogen (TKN)</b>	0.005%
<b>Cation Exchange Capacity (CEC)</b>	21 meq/100g

In summary, characterization of soil specimens was able to show the chemical, physical and mineralogical properties of the soil. The soil predominantly contained a significant level of clay fraction. As described in Chapter 2.4, clay mineral and organic matter are mainly attributed to retardation of the transport of organic compounds in the soil.



## 5.2 Characterization of materials by means of FTIR

FTIR (Bomem-Gram) combines the horizontal attenuated total reflectance and diffuse reflectance technology into one Gemini device, which enable to obtain the spectra from liquid and solid sample. This method is often non-destructive. Therefore, in this research, clayey soil, phenanthrene and biosurfactants spectra were obtained through FTIR.

The soil samples, which were stirred in hexane solution, were recovered by placing the sample on diffuse sampling cup and evaporating the supernatant solvent in an air-flow hood for 6 hrs. The diffuse reflectance FTIR spectra of the soil specimens were obtained (Figure 5.2). An OH stretching vibration is presented at a narrow band of  $3614\text{ cm}^{-1}$  and a broad band of  $3414\text{ cm}^{-1}$ . The former is related to hydroxyls linked to  $\text{Al}^{3+}$ ,

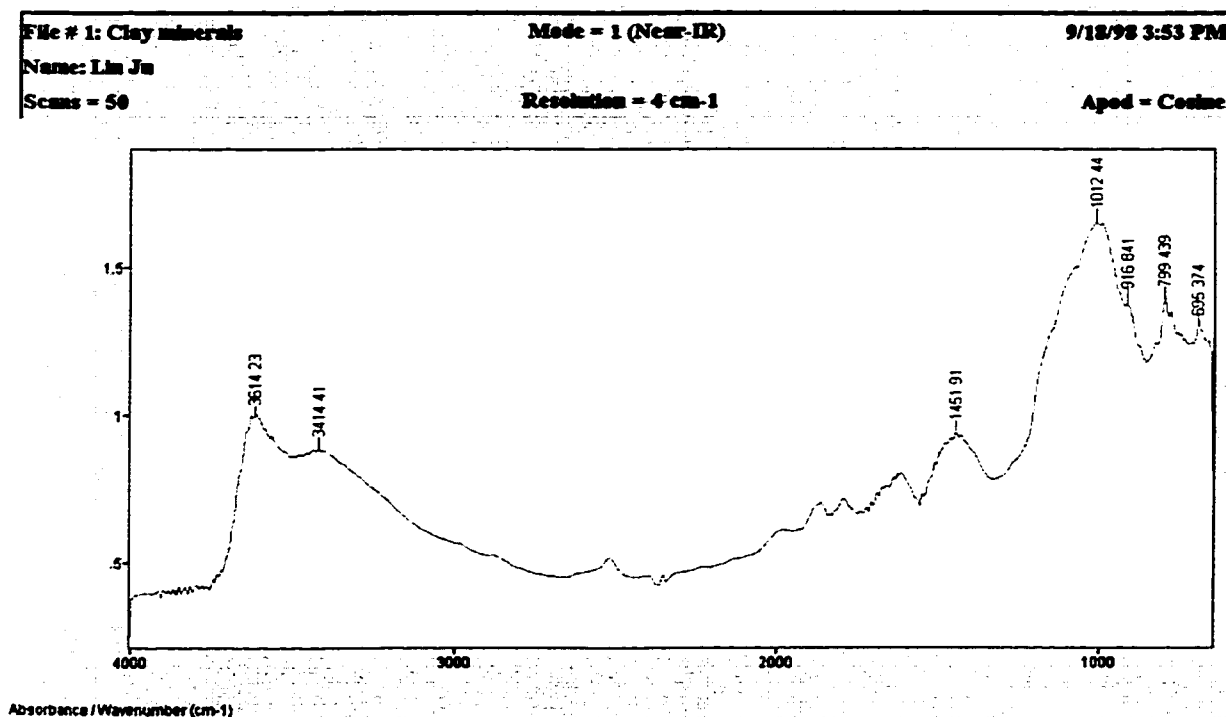


Figure 5.2 The FTIR spectroscopy spectrum of clay minerals with 50 scans at a resolution of  $4\text{ cm}^{-1}$

and the latter is related to hydroxyls in H<sub>2</sub>O (hydration sphere). These values were similar to those in the spectrum of illite (Van Olphen, 1979). He discussed that it was caused by a highly disordered illite. Skeletal Si-O and Al-O vibration were evident below 1400cm<sup>-1</sup>. The strong band at 1012 cm<sup>-1</sup> is clearly attributable to Si-O stretching vibration. It should be noted that the typical peak for soil Si-O is at 1159 cm<sup>-1</sup> (Van Olphen, 1979). Farmer and Russel (1967) stated that the spectra of clays are mostly sensitive to the regularity of the silicon lattice, degree of distortion, and Al-for-Si substitution. Therefore, the stretching vibration at 1012 cm<sup>-1</sup> can shift and split into components.

Aromatic compounds give rise to a large number of very sharp, characteristic bands, so that their identification by infrared methods is usually straightforward. Furthermore, the changes in certain regions that result from substitution are largely independent of the nature of the substitutes, therefore it is possible to determine the degree and type of substitution present. Figure 5.3 shows the spectra, which was obtained by placing pure phenanthrene with KBr (1: 9 by weight) into the diffuse sampling cup. A typical aromatic-type structure is best recognized by the presence of the =C-H stretching vibration-sharp absorption near 3030 – 3058 cm<sup>-1</sup>. The spectra showed that the =C-H stretching unit was at 3053.2 cm<sup>-1</sup> which is consistent to the reference number of 3053.5 cm<sup>-1</sup> (Keller, 1986). The C=C vibrations were presented between 1500-1600 cm<sup>-1</sup>. In these regions the absorption bands are slightly affected by the substitution pattern. However, a study of the C=C region can give information related to the nature of substitution in certain cases, and to the presence of conjugation with the double bonds of the ring. In the spectra of aromatic materials, strong bands appear in the region 650-1000 cm<sup>-1</sup>, which is caused by the out-of-plane deformation vibrations of the hydrogen atoms

remaining on the ring. The very high intensity of these bands makes them particularly well suited for quantitative work.

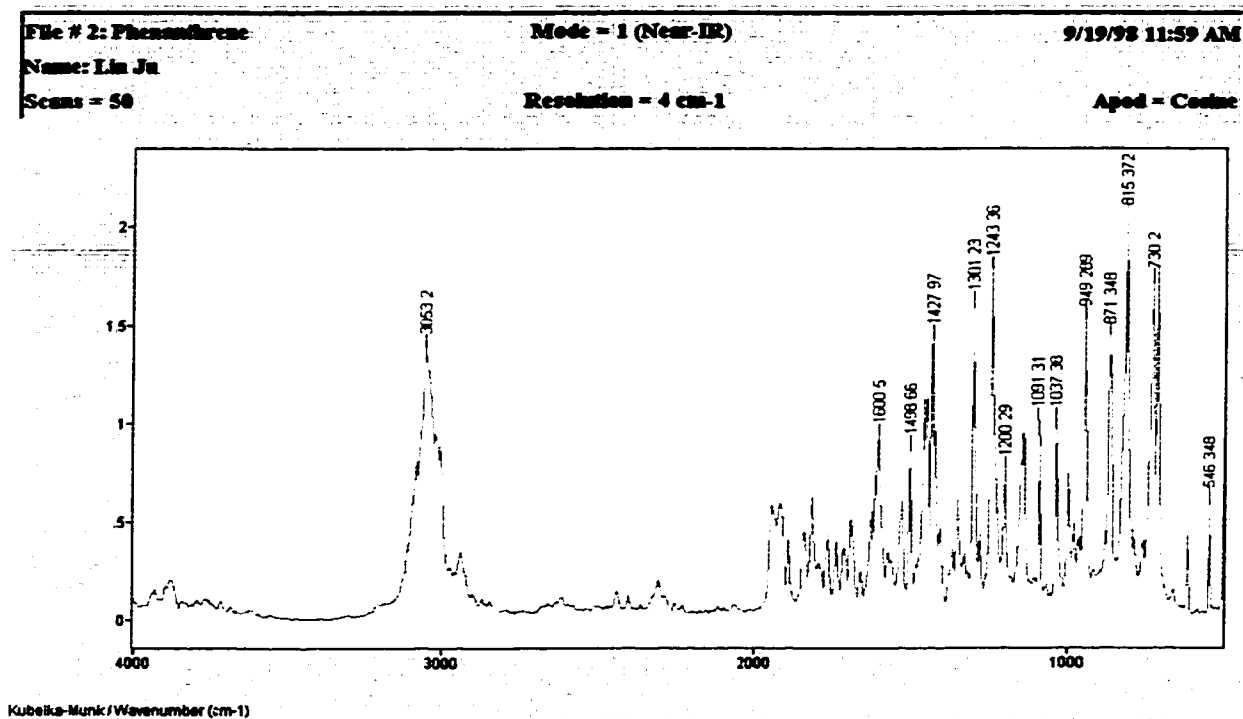


Figure 5.3 The FTIR spectroscopy spectrum of phenanthrene with 50 scans at a resolution of 4 cm<sup>-1</sup>

The FTIR spectra of biosurfactants (rhamnolipids) are presented in Figure 5.4. The biosurfactants were dried on the ZnSe plate in the air-flow hood, and then put into the spectroscopy. A broad OH stretch was presented between 3000-3700 cm<sup>-1</sup> and OH bending vibration was at 3304 cm<sup>-1</sup>. The highest peak in this figure was at 2925.76 cm<sup>-1</sup>, which was attributed to CH stretching vibration in aliphatic CH<sub>2</sub>-bonds. This agreed with the reference which indicated that CH<sub>3</sub> is in the range between 2872-2962 cm<sup>-1</sup> (Nakanishi, 1977). Carboxylic acids (-C=O-O<sup>-</sup>) exist normally in dimeric form with very strong hydrogen bridges between the carbonyl and hydroxyl groups of the two molecules,

which has two ranges from  $1610\text{ cm}^{-1}$  to  $1550\text{ cm}^{-1}$ , and  $1420\text{ cm}^{-1}$  to  $1300\text{ cm}^{-1}$ . Therefore, in Figure 5.4,  $1731$  and  $1577\text{ cm}^{-1}$  clearly belong to C=O vibration of acid and ester groups. Another strong band at the range of  $1319$ - $1390\text{ cm}^{-1}$  is attributed to CH vibration in the sugar  $\alpha$ -ring (Nakanishi, 1977). This is confirmation of the molecular structure of rhamnolipids.

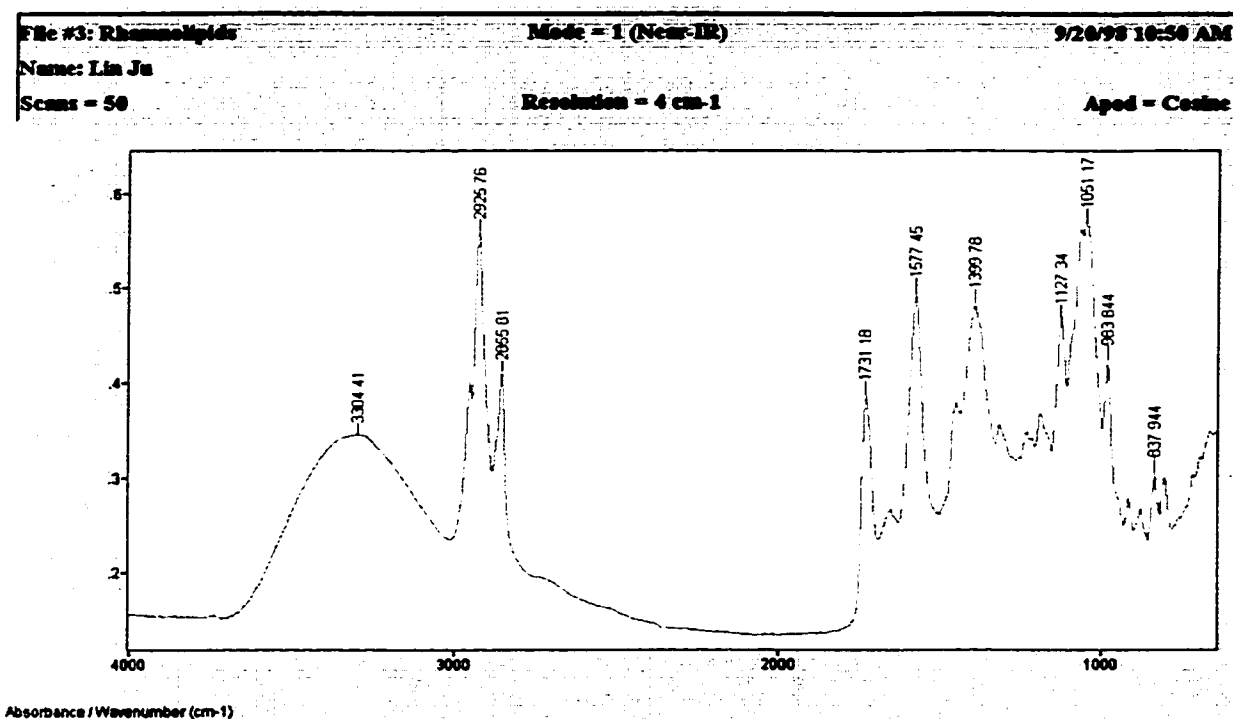


Figure 5.4 The FTIR spectroscopy spectrum of rhamnolipids with 50 scans at a resolution of  $4\text{ cm}^{-1}$

To summarize, the spectra of clay minerals, phenanthrene and biosurfactants are very useful tool to identify these compounds. The analysis of relative optical density of these components can be used for quantitative evaluation in test series 4.

## **CHAPTER 6 RESULTS AND DISCUSSION FOR TEST SERIES 1: Behavior of bacteria under the electric field**

The purpose of this series of experimental work was to investigate the behavior of biosurfactant-producing bacteria when growing on the hydrocarbon (phenanthrene) as the sole carbon source in clayey soil, under the electric field. Results from laboratory tests conducted in this research are presented and discussed in this chapter.

This experiment is designed to investigate the behavior of biosurfactant-producing bacteria under the influence of electric field. The objective of this test is to eventually find a suitable situation for the survival of bacteria and the optimum condition for the potential production of biosurfactants *in-situ* under the electric field.

Based on the experimental protocols, electrokinetic test series 1 (T1) was performed on a clay soil specimen, where cells were referred to as “T1C1” containing soil free of phenanthrene and “T1C2” containing soil with phenanthrene. Bacterial cells from an exponentially growing culture were uniformly incorporated into soil in cell T1C1 testing soil. In cell T1C2 soil, only bacteria in a mineral salt medium were incorporated with soil in order to allow the bacteria to utilize phenanthrene as a sole carbon source. Before the test setup, the preparation of culture medium and soil were described in Chapter 4.2. Fluid flow, electrical potential, electrical current, and pH of collected liquid were measured during 14 days’ test. After the experiment, soil pH, moisture content, and bacterial count in soil were also obtained. The method of analysis was described in Chapter 4.3.

## **6.1 Electrical potential and resistance distribution**

The electrical potential distribution in the soil specimens for both cells showed a similar pattern during the electrokinetic process (Figure 6.1A and B). The electrical potential dropped along the electrokinetic cell from 4.02 V to 2.05 V in TIC1 and from 4.41V to 1.40 V in TIC2 at the beginning of the experiment, respectively. At the end of the test, the lowest value obtained was 1.38 V (probe 10, at 336h) in TIC1 and 1.41 V (probe 10, at 336h) in TIC2. A general linear decreasing trend was observed from the anode to the cathode during testing. The electrical potential difference was generally constant with time at each probe. It demonstrated a uniform distribution of electrical potential gradient across the electrokinetic cells. Two cells showed similar distribution patterns. Therefore, they were comparable.

The resistance for cells TIC1 and TIC2, was calculated from Ohm's law ( $V=IR$ ) and is also showed graphically versus distance in Figure 6.2A and B. It clearly showed that the resistance tended to decrease from the anode to the cathode. Near the anode, the resistance increased with time from the beginning in cell TIC1 of 0.4 kOhm to 1.2 kOhm and in cell TIC2 from 0.5 kOhm to 1.6 kOhm in TIC2. Therefore, it is visible that the highest resistance was mainly at the anode/soil interface. Near the cathode, 0.5 kOhm in TIC1 and 0.8 kOhm in TIC2 were observed at the end of test, respectively. The overall resistance in phenanthrene contaminated soil consistently was 0.3 kOhm higher than comparative values in soil free of phenanthrene.

Due to electroosmotic flow, water can be transported from the anode to the cathode through the soil specimen. Acar and Alshawabkeh (1993) stated that applying a constant current or various electrical gradient (V/cm) and neglecting the hydraulic

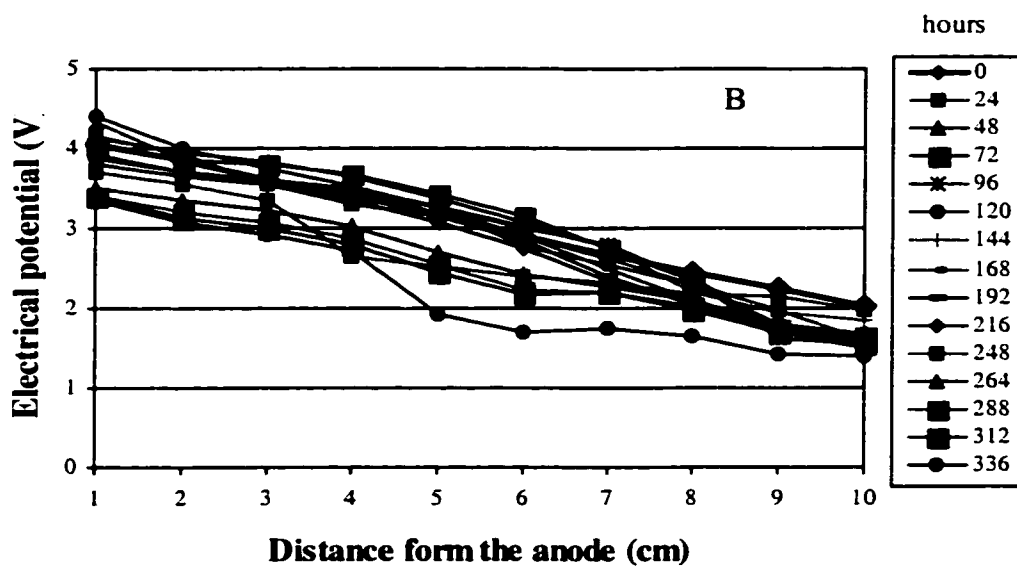
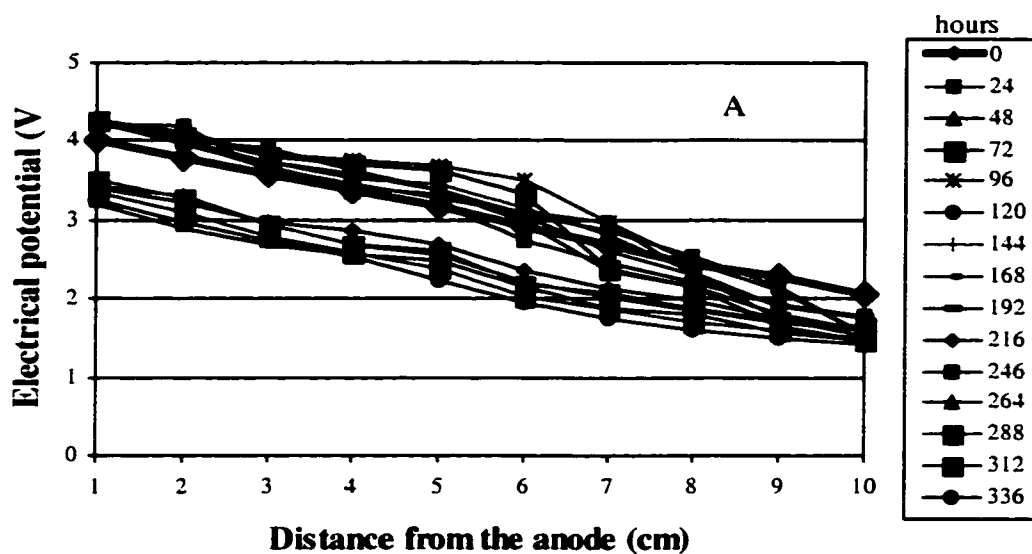


Figure 6.1 A. Electrical potential distribution in cell TIC1  
 B. Electrical potential distribution in cell TIC2

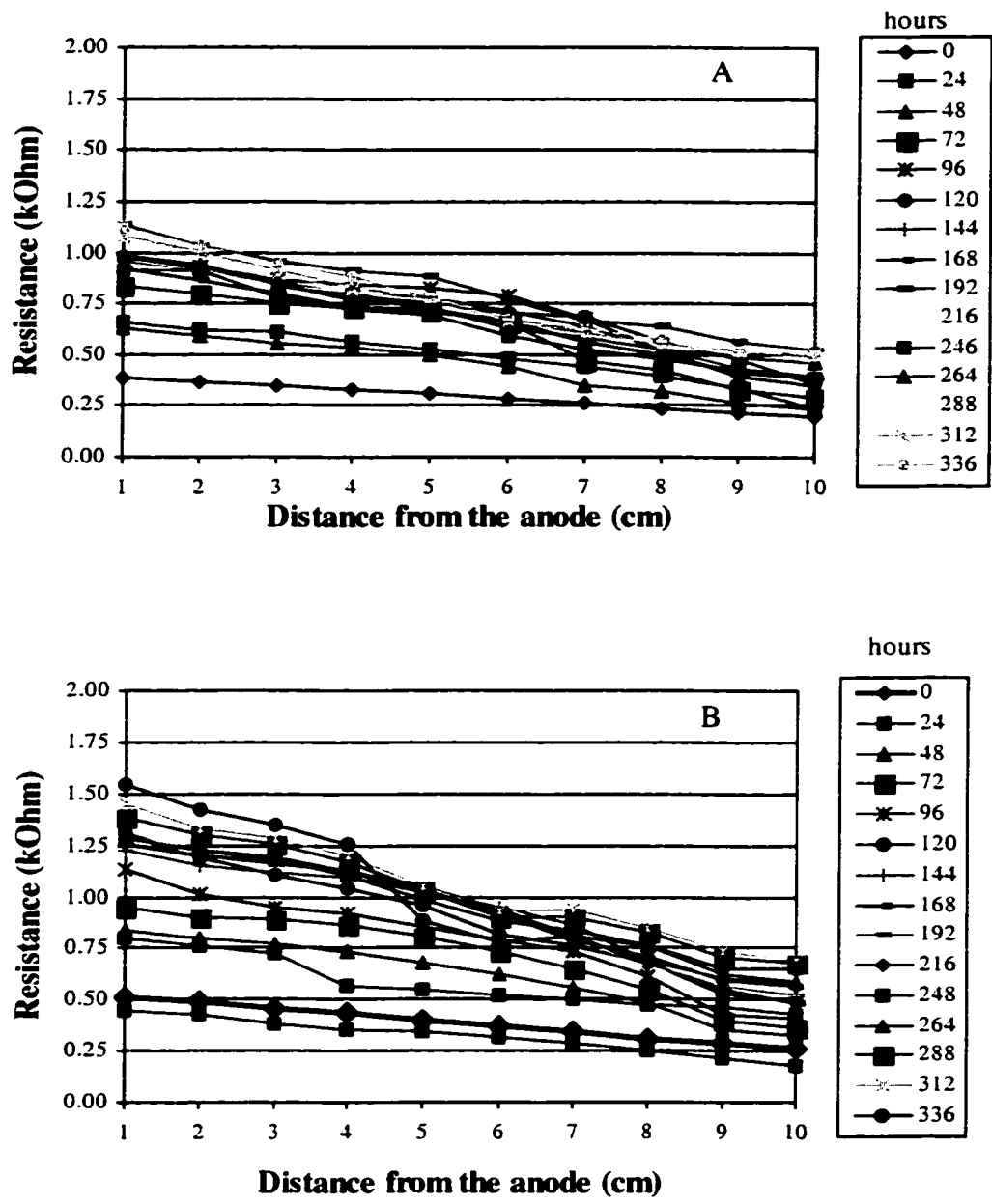


Figure 6.2 A. Resistance distribution in cell T1C1  
 B. Resistance distribution in cell T1C2



gradients, may result in a high conductivity region at the anode and a low-conductivity region at the cathode. The electrical potential dropped along the soil specimen during testing. At the cathode, the higher electrical gradient will cause higher electroosmotic flow than at the anode region. From the experimental results, the resistance increase with time, may be due to negative pore water pressure (suction) (Acar et al., 1995), which balanced the electroosmotic flow and eventually led to its decrease. However, in this research, water was supplied near the anode. The suction and its tendency to decrease the electroosmotic flow were not major factor.  $k_e$  (see Chapter 3.2.1) also changed with time, due to movement of ions, dissociation process of water, and carbonate precipitation, etc. The average  $k_e$  calculated from this test series was  $8.5 \times 10^{-10} \text{ m}^2/\text{V.s}$ . The main reason for the increase of resistance is probably caused by the oxidation process, resulting in the accumulation of oxygen in soil pores.

In summary, the applied voltage dropped uniformly across the specimens. The uniform distribution of electrical potential gradient across the electrokinetic cells was clearly shown. These results agreed with West et al. (1999) experiments. There is little variation in voltage gradient at each probe during the experiment's period. As time progressed, decreased water flow was observed as reflected by a decrease in the volume of collection liquid.

## **6.2 Moisture distribution**

Moisture content was analyzed after 14 days of electrokinetic experiments for both cells, which is shown in Figure 6.3. It is demonstrated that moisture in the range of 26% to 54% for the soil without phenanthrene (TIC1) and 37% to 46% for the soil with

phenanthrene (T1C2) from anode to cathode, respectively. The lowest value of moisture content (26%) occurred in the middle of cell T1C1. For contaminated soil, moisture content was more uniformly distributed than that in soil free of phenanthrene.

In general, moisture content of the soil strongly influences biological activity – microbial growth. Therefore, under an electric field, the moisture content in the electrokinetic cell remained around 40%. Most bacterial metabolism occurs at values of less than 3 bar of matric potential. They are situated in the range of optimal matric potential around 0.3 bar (Cookson, 1995). This is clay matric potential, which is different from sandy soil. Due to the average moisture content of 38 % in T2C1 and 41% in T2C2, the matric potential of water is around 0.1 bar. High moisture content close to the electrodes (above 50%) in T1C1 does not seem to improve the biomass growth condition due to extreme pH condition in these regions. In T1C2, the moisture content tended to be more uniform than in T1C1. However, this tendency did not follow the pattern of bacterial distribution.

To summarize, from the obtained data, the soil maintained the significant level of moisture content. A higher moisture content was encountered near the cathode region. This was due to transport of water from anode to cathode by electroosmotic flow under the electrical gradient. The results showed a good moisture condition for bacterial growth in soil, as a result of controlling the moisture via electrokinetics. It could create a matric potential which assists the bacteria to secrete extracellular substances for using phenanthrene as a sole carbon source.

### **6.3 pH distribution**

At the termination of the experiment, the soil was sampled and analyzed for pH. The distribution of pH along the electrokinetic cell is presented in Figure 6.4 for cells T1C1 and T1C2. The final pH of the soil near the anode dropped to 3.5 in cell T1C1, due to the oxidation process under the electric field. At the cathode, the value of pH was raised to 10.4 for both cells due to the reductive reaction under the electric field. However, the pH value near the anode was not extremely low with a value of 7.1 in cell T1C2. It is speculated that the presence of contaminants directly affected the change of pH within the anode area. It created better conditions for bacterial proliferation near the anode than in cell T1C1. No ideal conditions were obtained close to cathode. Elektorowicz and Hatim (1999) designed a new type of electrodes, which allowed for the decrease of pH in the cathode area. Therefore, due to application of a multifunctional electrokinetic system, the control of bacterial growth conditions and subsequent production of biosurfactants are possible.

### **6.4 Bacterial response to electric field**

Correspondingly, the bacterial count showed that 2.24 log CFU/g soil dry wt. was in T1C1 soil and 5.60 log CFU/g soil dry wt. in T1C2 soil near the anode (Figure 6.5A and B). In addition, 1.48 log CFU/g soil dry wt. in cell T1C1, and no bacterial detection in cell T1C2 was observed near the cathode. A pH value of 10.7 caused the amount of bacteria to decrease dramatically. Although the low pH value was evident at the anode, there were still 1.5 times and 5.6 times more bacteria detected at the anode area than the

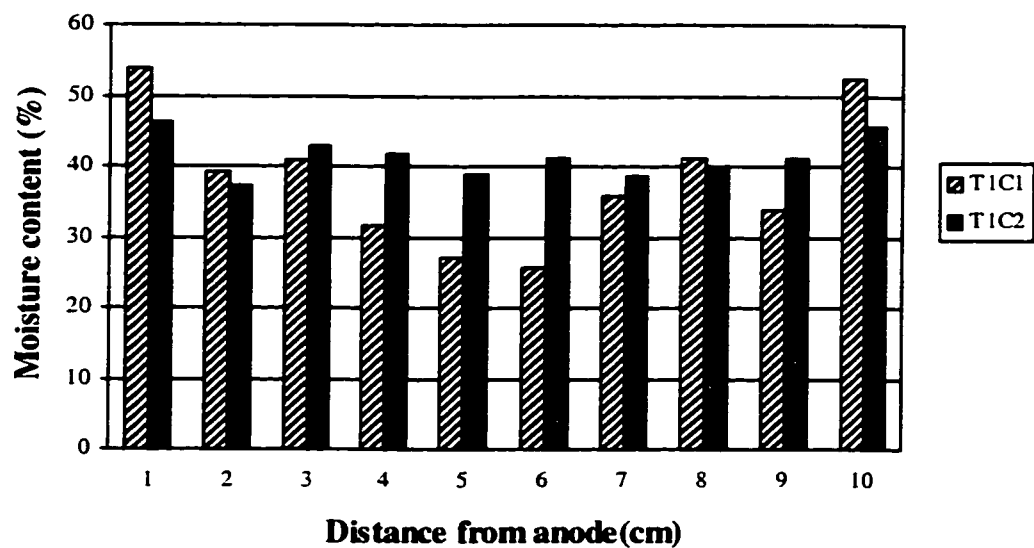


Figure 6.3 Moisture content distribution in cells TIC1 and TIC2

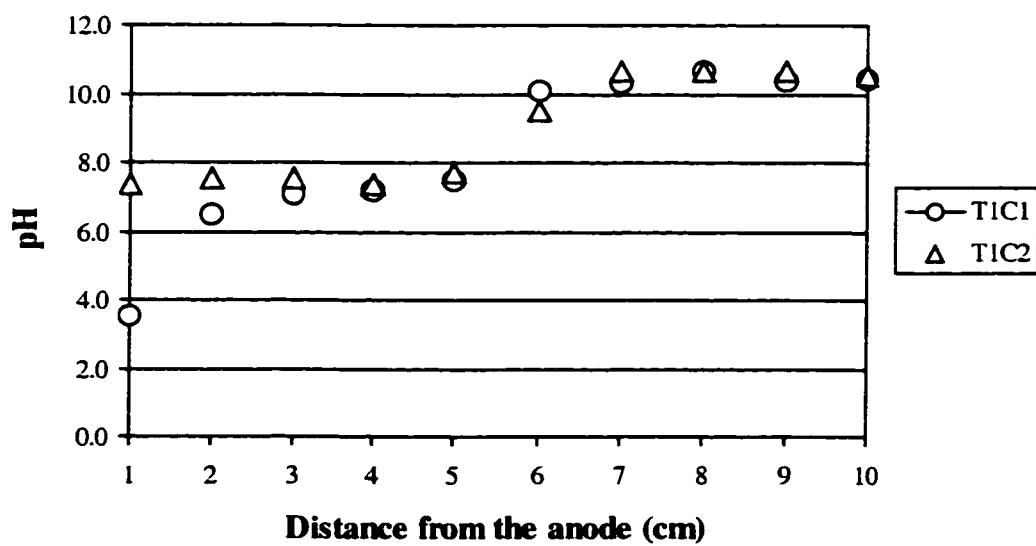


Figure 6.4 pH distribution in cells TIC1 and TIC2

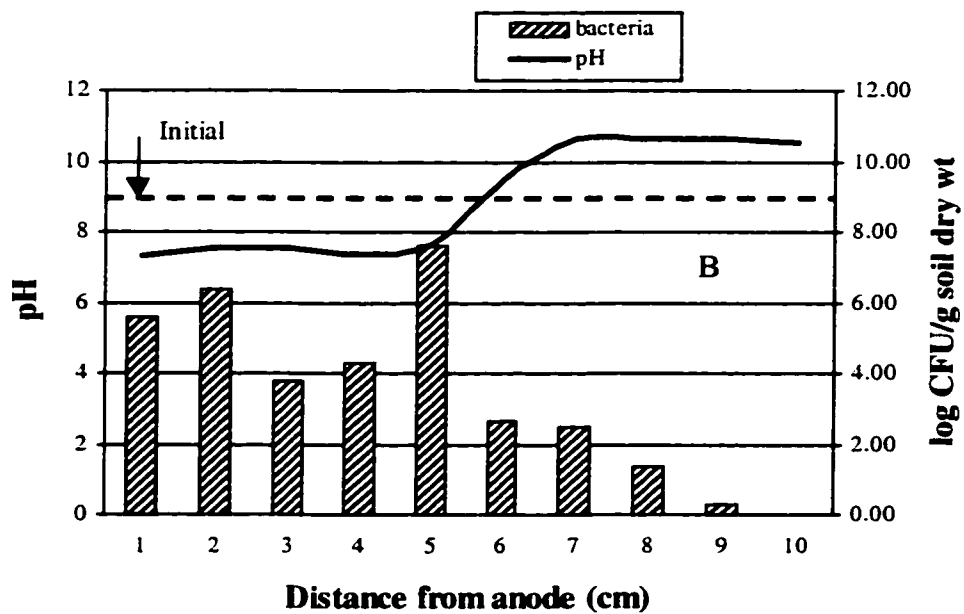
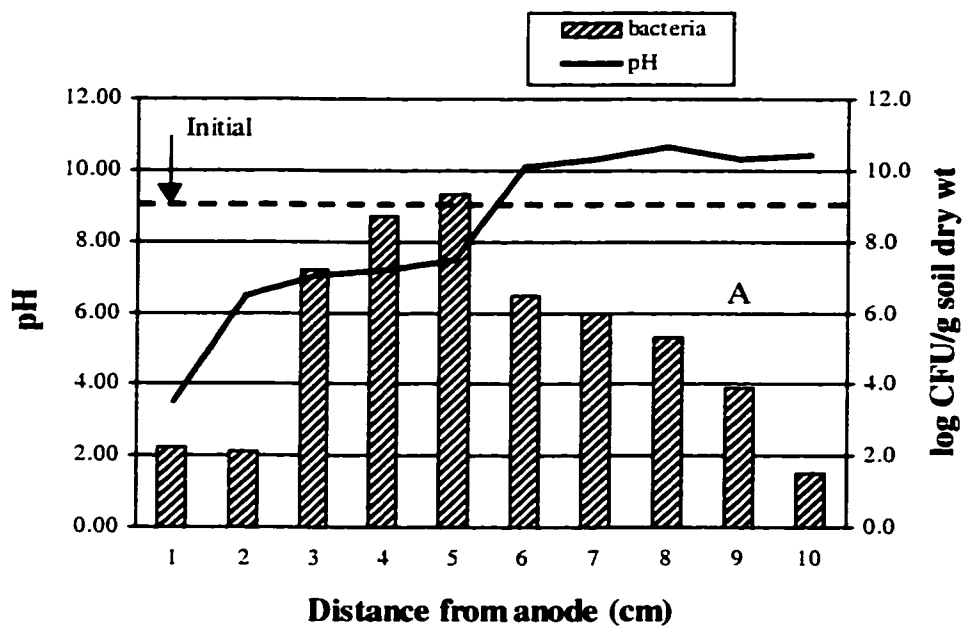


Figure 6.5 A. pH and bacterial distribution in cell TIC1  
 B. pH and bacterial distribution in cell TIC2

cathode area in cell TIC1 and in cell TIC2, respectively. On the other hand, although phenanthrene was used as a sole carbon source, 7.6 log CFU/g soil dry wt. was observed in TIC2. This indicated that bacteria could uptake phenanthrene as a carbon source and multiply.

The maximum value of 9.32 log CFU/g soil dry wt. in cell TIC1 and 7.6 log CFU/g soil dry wt. in cell TIC2 were achieved at a distance of 5 cm from the anode where neutral pH was measured. It appeared that the electric field did not extensively inhibit the growth of bacteria. Sale and Hamilton (1967), who were working on electrical disinfection, showed that the elimination of bacterial cells required high pulsed voltages (25 kV/cm and 40-100  $\mu$ s pulse duration) under a direct effect of the current on the cells. In this research, the voltage applied was 0.5 V/cm. It can be concluded that under the low electric field and under neutral pH conditions, the bacteria could multiply normally in clayey soil. In soil, the normal amount of existing bacteria is 7 to 9 log CFU/g dry wt. Therefore, this amount of bacteria is suitable to participate in the biodegradation of contaminants in soil.

Another reason for the distribution of bacterial numbers may be due to the transport of bacteria. Jenkins and Lion (1993) demonstrated the possibility of transport of the bacteria and PAHs in the sandy soil. However, the complexity and heterogeneity of soil ecosystems have made it difficult to distinguish the movement or microbial adhesion. Bacterial surfaces in most natural environments are negatively charged like most other colloids, and bacterial density is slightly greater than that of water (Kim and Corapcioglu, 1987). However, the adhesion between bacteria and soil is evenly strong. Stenstrom (1989) reported that the presence of negatively charged groups on the bacterial surface

has no effect on the electrostatic repulsion forces between the bacteria and clay minerals. The surface electrokinetic potential becomes more influential for more hydrophilic cells and concluded that this allows the bacteria to adhere to the minerals (Van Loosdrecht et al.,1995). Since no accurate method for the bacterial transport detection was invited, the research performed in this thesis support the hypothesis of bacteria movement under the electric field. And also the bacteria can form biofilm on the soil surface, which can also enhance the adhesion in clay minerals. When bacteria are incorporated into soil, they are captured on the surface of the soil matrix by the van der Waals force. After a bacterium stays for some critical residence time on the soil surface, the attachment or anchoring begins, resulting in the formation of biofilm (Characklis, 1984). This action is biological in nature and is mainly attributed to the production of extracellular polymeric substances. In order to uptake phenanthrene as a sole carbon in cell TIC2, extracellular substances – biosurfactants were produced and then the micelles were formed. The solubility of phenanthrene can be increased by the formation of micelles.

In general, the available large surface area of clay materials is certainly much greater, and actually could be utilized as bacterial habitat, since bacteria were located within the soil matrix and increased the protective effect. However, under the electric field, the force driving water from anode to cathode could cause the bacteria to disperse through the soil. In addition, the negatively charged bacteria near the cathode area may be transported towards the anode by electrophoresis (DeFlaun and Condee, 1997). Therefore, under the electric field, when bacterial culture is incorporated into clayey soil, it is possible that the bacteria could be transported towards the anode area (Elektorowicz

et al., 1999). This is probably one of the reasons that the bacterial count in the cathode area was much lower than that in the anode area, especially in contaminated soil.

Results related to pH values suggest that the optimal condition for the survival of bacteria are in the middle area of the electrokinetic cell, and even in the worse cases (at anode and cathode) there are still metabolically viable bacteria. Clay presents a good habitat for bacteria survival. It is necessary to control the pH in the electric field by increasing the pH at the anode and decreasing the pH at the cathode in order to maintain optimal conditions for bacterial proliferation. Therefore, the bacteria under a low electric field can survive to a certain extent, which means that the method of introduction of bacteria into the electrokinetic cell and production of biosurfactants *in-situ* is potentially possible. It appeared that oxidation-reaction, production of a free O<sub>2</sub> electron acceptor, can improve the growth condition for microorganisms close to the anode. The reduction condition at the cathode does not help the survival of bacteria. However, the production of extracellular substance –biosurfactants in contaminated soil enhanced the mobility of bacteria and phenanthrene, which could be transported toward the anode area. The results also showed that when a low electric current is applied into clayey soil, bacteria can thrive, thereby provoking the process of contaminant biodegradation.



## **CHAPTER 7 RESULTS AND DISCUSSION FOR TEST SERIES 2: Potential *in-situ* production of biosurfactants under the electric field**

Since the previous results demonstrated bacterial growth under the electric field, it was necessary to test the potential production of biosurfactants by indigenous microorganisms. Electrokinetic test series 2 was performed on a clay specimen free of phenanthrene and contaminated by phenanthrene. The test's cells were referred to as "T2C1" for the cell with non-contaminated clay and "T2C2" for the cell containing clay with phenanthrene, respectively. The electrokinetic test duration was 14 days. Before the test setup, the preparation of culture medium and soil were described in Chapter 4.2. Fluid flow, electrical potential, electrical current, and pH of collected liquid were measured every 24 hours during the 14 days test. After the experiment, soil pH, moisture content, bacterial count, and concentration of phenanthrene and biosurfactants in the soil were also obtained. The method of analysis was described in Chapter 4.3.

### **7.1 Electrical potential and resistance distribution**

Measurements related to electrical potential at each probe and current supplied in each cell were performed. The electrical potential difference from the anode along the electrokinetic cell is displayed in Figure 7.1 for cell T2C1, and in Figure 7.2 for cell T2C2. The range of the electrical potential was approximately from 4.0 V to 1.8 V in cell T2C1 and from 4.1 to 1.8 V in cell T2C2 along the electrokinetic cell, respectively. Therefore, the general pattern of the electrical potential for this test is that as time progressed, the electrical potential decreased along the electrokinetic cells. A general linear pattern was obtained. This pattern could initialize the electroosmotic flow from the

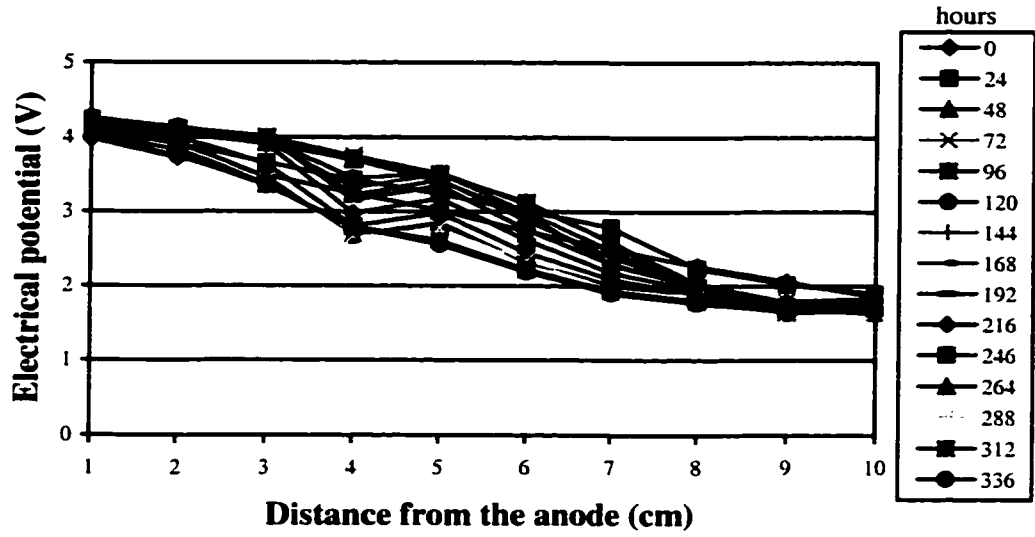


Figure 7.1 Electrical potential distribution in cell T2C1 during two weeks test

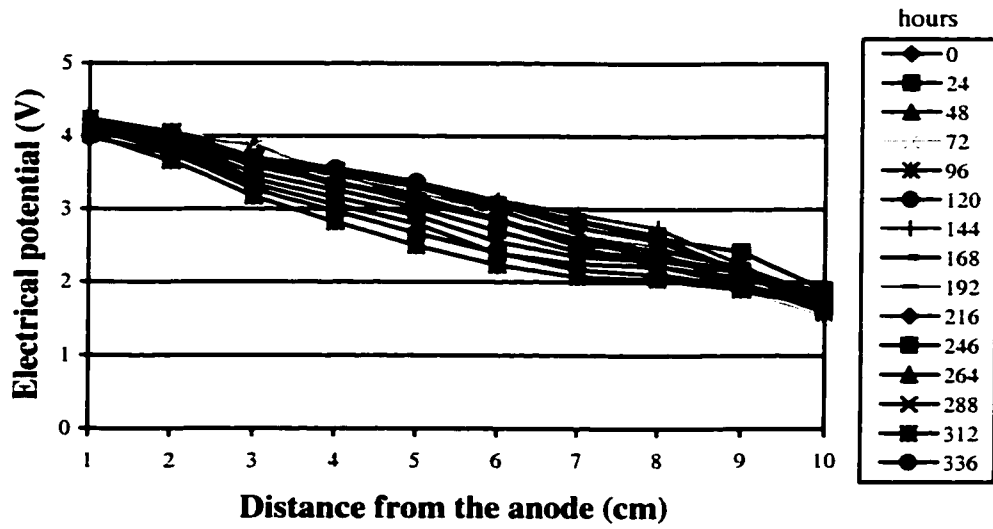


Figure 7.2 Electrical potential distribution in cell T2C2 during two weeks test

anode to the cathode. For each electrical probe, the electrical potential remained relatively constant during the test. It demonstrated the uniform distribution of electrical potential gradient across the electrokinetic cells in both cells.

The resistance versus distance for cells T2C1 and T2C2 are also shown graphically in Figure 7.3 and Figure 7.4. During the experiment, it was clearly showed that the resistance tended to decrease from the anode to the cathode. For each probe, the resistance increased with time from the beginning of 0.8 kOhm to 2.5 kOhm in T2C1 and from 0.6 kOhm to 2.5 kOhm in cell T2C2 near the anode. The highest resistance was mainly at the anode/soil interface. Near the cathode, 1.0 kOhm in T2C1 and 1.1 kOhm in T2C2 were observed at the end of the test, respectively. The overall resistance of T2C2 was similar to the value of T2C1. As time progressed, the resistance in both cells increased accordingly, due to the electroosmotic flow from the anode to the cathode, thereby decreasing the conductivity of the soil in the anode region. Both cells present the same pattern of resistance distribution that permit to include this information to all comparative analysis of both cells.

The electrical potential difference is also significant in estimating the power and energy expenditure. The rate of species transport under electric fields depends on the electrical gradient profile across the soil. Alsbawabkeh and Acar (1996) showed that a relatively linear distribution of electrical gradient was obtained due to the uniform electric conductivity distribution across the soil, which was observed in these experiments. The electroosmotic flow decreased at the end of the test as observed by the decreased volume of collected liquid. It should be considered that the value of  $k_e$  (equation 3.1) is a function of zeta potential, viscosity of the pore fluid, porosity, and

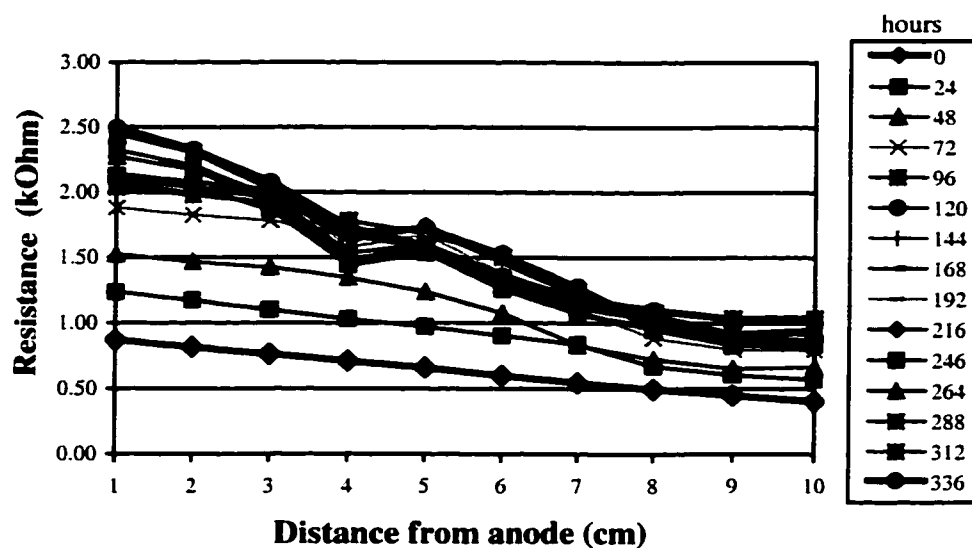


Figure 7.3 Resistance distribution in cell T2C1 during two weeks test

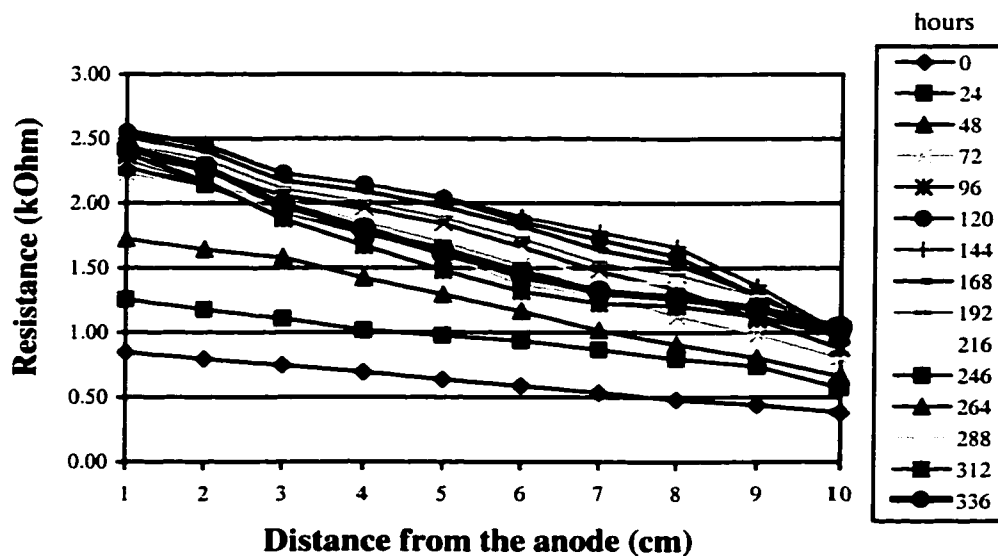


Figure 7.4 Resistance distribution in cell T2C2 during two weeks test

electrical permittivity of the soil medium (Acar et. al., 1993). Hunter (1981) pointed out that the zeta potential decreased linearly with a decrease of pH within the soil medium. Respectively, it is hypothesized that due to electrolysis, the drop of pH at the anode region will cause a decrease in the  $K_e$  associated with the drop in zeta potential. Since, in this research, the water was continuously supplied near the anode area, therefore, the flow would not stop at the latter stages of the experiments, it was beneficial for the transport of the species in the cells.

## **7.2 Moisture distribution**

Moisture distribution in the soil after 14 days of experimentation for both cells is presented in Figure 7.5. It shows that moisture range from 37% to 56% in cell T2C1 and from 34% to 65% in cell T2C2. The average moisture content for cell T2C1 is 46% and 51 % for cell T2C2. It appears that the level of the moisture content is suitable to create a good environment for bacterial development (as discussed in Chapter 6.2). It also shows that moisture content in contaminated soil was generally higher than that in soil free of phenanthrene. The highest bacterial count of 7.59 log CFU/g soil dry wt. occurred at a moisture content of 52%.

In summary, the soil maintained a significant level of moisture content, which tended to be uniformly distributed. The highest levels occurred near the cathode region in cell T2C2 where they reach values up to 63%. It was caused by the transport of water from anode to cathode by electroosmotic flow under the electrical gradient and also due to continuously supplying water in the anode area. The results showed optimal moisture conditions for bacterial growth and biosurfactants production.

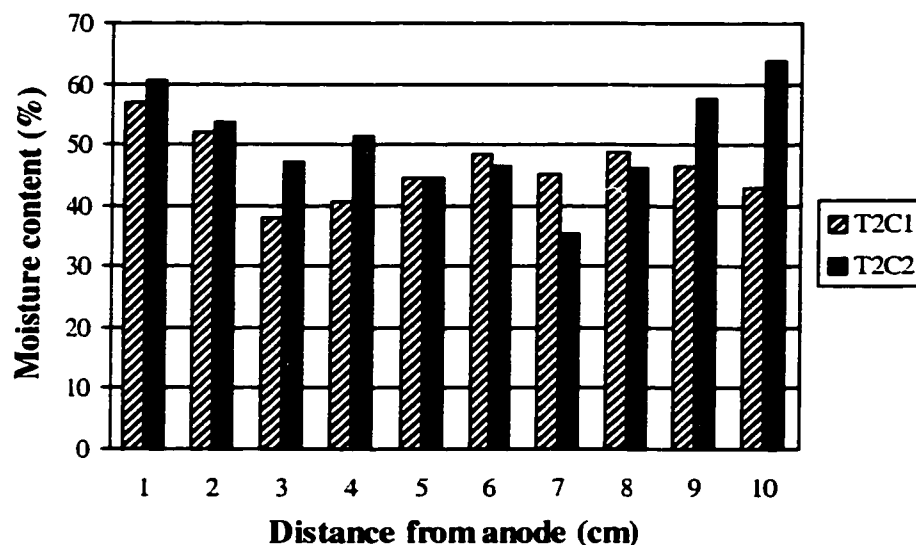


Figure 7.5 Moisture content distribution in cells T2C1 and T2C2

### 7.3 pH distribution

A significant pH gradient developed as a result of electrolysis reactions (Figure 7.6). Near the anode, due to the oxidation process, the pH value dropped to 2.8 for cell T2C1 and 6.3 for cell T2C2 at the end of experiment. Near the cathode, due to the reduction process, the pH value increased to 10.1 in cell T2C1 and 10.2 in cell T2C2. This agrees with bench-scale and pilot-scale experiments, which demonstrated that a pH in the cathode region reaches values as high as 10-11 (Hamed and Bhadra, 1997; Elektorowicz, 1995a). However, it was evident that the pH value near the anode was not extremely low with a value of 6.2 in contaminated soil. This agrees with the test series 1 (Chapter 6.3). It can be speculated that the presence of phenanthrene modified the

oxidation process. As mentioned above in Chapter 6.3, a modified pH-controlling system in the cathode area can improve the bacterial growth and production of biosurfactants.

In cell T2C2, the average pH value was higher than that in T2C1. It is possible that due to the production of biosurfactants at the anode, most of the generated  $H^+$  at the anode was reacted within the transformation of phenanthrene associated with oxidative process, resulting in a pH increase near the anode in T2C2. Subsequently, bacteria survival up to 6.8 log CFU/g soil dry wt. near the anode area was observed.

Overall, the results of the pH experiments suggest that the optimal condition for the survival of bacteria was in the middle of the electrokinetic cell. Even in the worse conditions (at the anode and cathode), bacteria was still metabolically active. It seems that the presence of clay creates a good habitat for the bacteria.

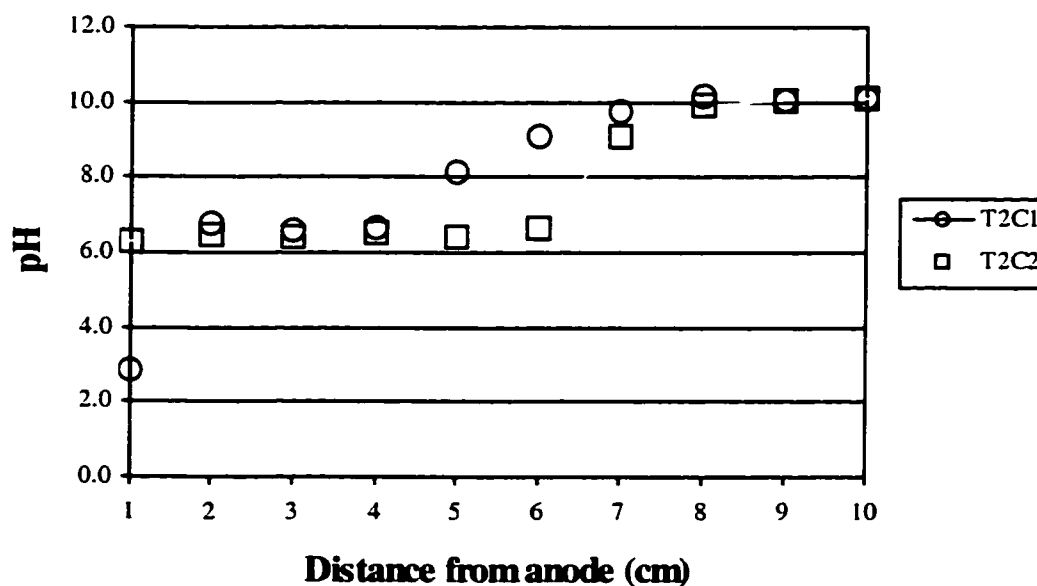


Figure 7.6 pH distribution in cells T2C1 and T2C2

## 7.4 Bacterial response to electric field

The bacterial count showed 0.3 log CFU/g soil dry wt. in cell T2C1 and 6.8 log CFU/g soil dry wt. in cell T2C2 near the anode at the end of the test (Figure 7.7 and Figure 7.8). Despite the low pH value present at the anode, there were still certain numbers of bacteria at the anode in T2C1. Due to the pH value in T2C2 which was close to neutral, the number of bacteria was raised to 6.8 log CFU/g soil dry wt., five times higher than the cathode area. In the middle of the cells, the pH value was close to neutral for both cells. Maximum values of 6.2 log CFU/g soil dry wt. in the T2C1 and 7.9 log CFU/g soil dry wt. in the T2C2 were achieved, respectively. Near the cathode, the pH value was raised to 10.1 for both cells due to the reductive reaction. The amount of bacteria dramatically decreased to 1.7 log CFU/g soil dry wt. in T2C1 and 1.48 log CFU/g soil dry wt. in T2C2.

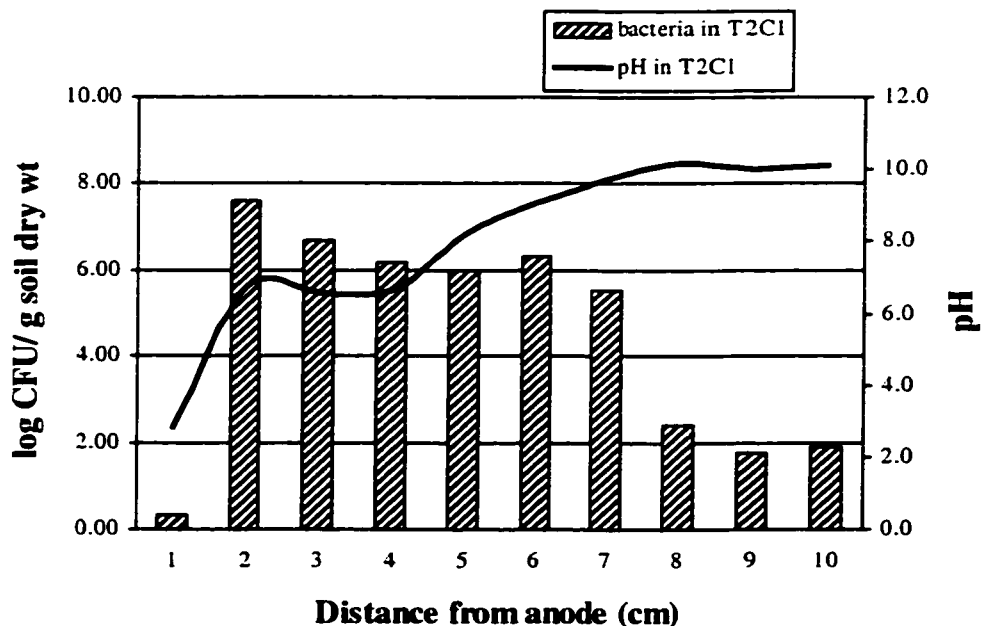


Figure 7.7 Bacteria and pH distribution in cell T2C1



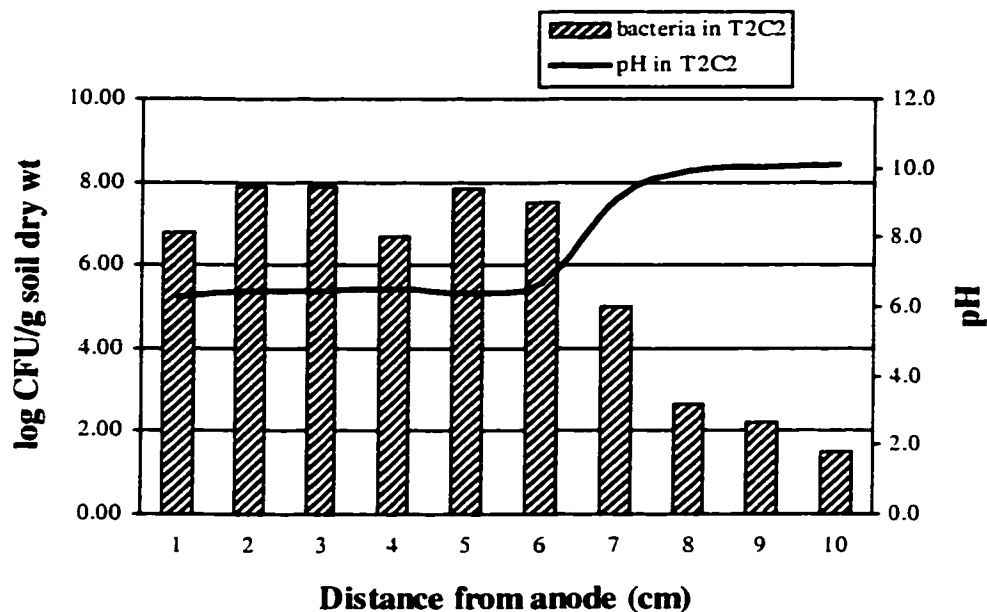


Figure 7.8 Bacteria and pH distribution in cell T2C2

### 7.5 Biosurfactant production under the electric field

The profiles of biosurfactant production in soil without phenanthrene (T2C1) and with phenanthrene (T2C2) under the electric field are shown in Figure 7.9. It seems that the soil contaminated with phenanthrene enhanced the bacteria to produce more biosurfactants into the aqueous phase than in the soil without contaminants. In T2C2, bacteria could use phenanthrene as their carbon source, therefore, in order to use insoluble phenanthrene, the excretion of more biosurfactants was provoked. The highest production (25 mg/l) occurred in the middle of the electrokinetic cell T2C2. Bacteria in cell T2C2 produced 2 times at the anode and 1.4 times at the cathode more biosurfactant than T2C1, respectively. Another reason for more biosurfactants production could be

attributed to the pH condition in the middle of the cell. It is favorable for growth of viable bacteria and for the production of biosurfactants under the electric field.

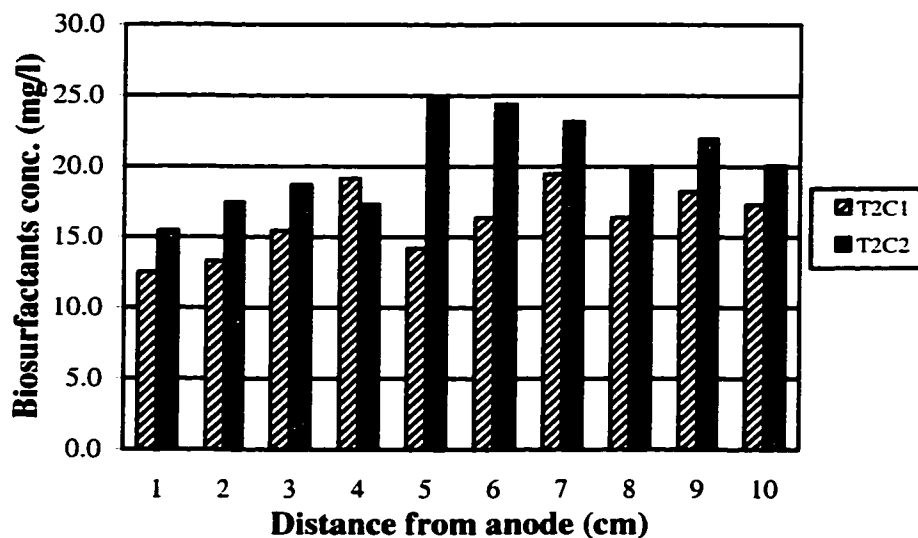


Figure 7.9 Biosurfactants distribution versus distance in cells T2C1 and T2C2 after the test

The research demonstrated that, under the electric field, the distribution of biosurfactants tended to be uniform rather than follow the bacterial distribution profile. In the middle of the electrokinetic cell, more biosurfactants could be produced due to the highest amount of bacteria (7.8 log CFU/g soil dry wt. in cell T2C2). Biosurfactants may have been transported to the anode due to their anionic properties. However, at the same time, due to water supply close to the anode, the electroosmotic flow was so high that biosurfactants produced across the soil could be transported toward the cathode.

## 7.6 Phenanthrene removal due to *in-situ* produced biosurfactants

In order to evaluate the efficiency of phenanthrene removal\* corresponding to the production of biosurfactants, three distinctive zones along the electrokinetic cell in T2C2 could be observed (Figure 7.10). The first zone, “A” (close to the anode), was characterized by uniform biosurfactant distribution and uniform removal of phenanthrene. Zone “B” (at the middle part) was characterized with the higher production of biosurfactants and the lower removal value. Probably the formation of anionic bio-micelles transported phenanthrene that was incorporated into micelles toward the anode. In the meanwhile, micelles could also follow the electroosmotic flow toward the cathode.

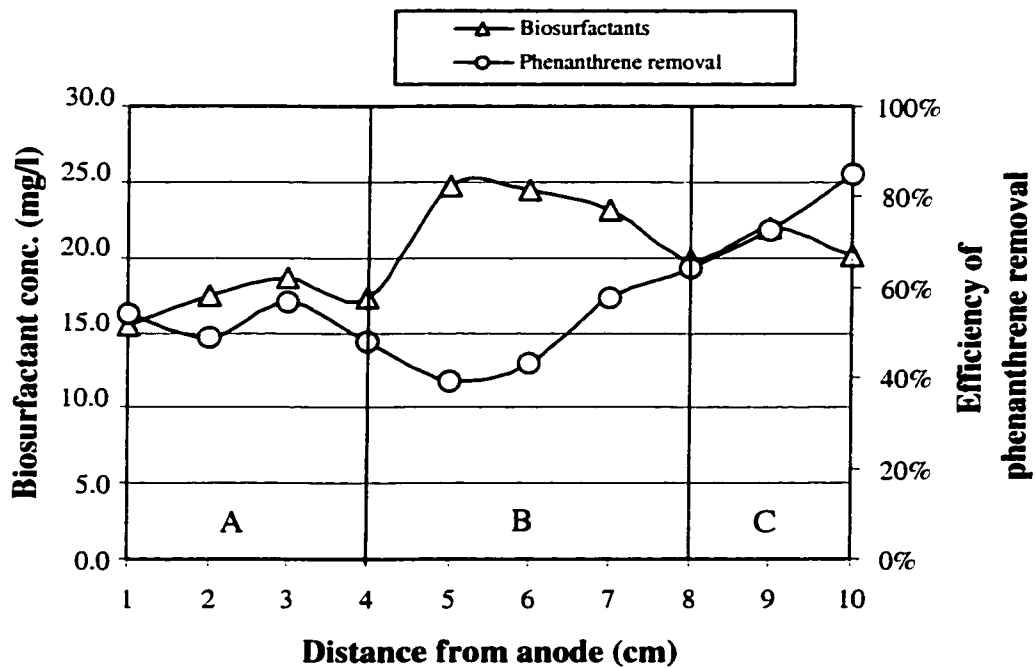


Figure 7.10 Biosurfactants and phenanthrene removal distribution versus distance after the test in T2C2

\*  $[(\text{initial conc. of phenanthrene} - \text{final conc. of phenanthrene}) / \text{initial conc. of phenanthrene}] \times 100\%$

Therefore, the middle of the electrokinetic cell became the location of transition for the transport of phenanthrene. Zone “C” (close to the cathode) had a very high removal of phenanthrene (up to 85%) and uniform production of biosurfactants. The general removal of phenanthrene increased from 38% to 85% along the electrokinetic cell in T2C2 (Ju and Elektorowicz, 1999).

From the above-mentioned results, it can be concluded that the electric field does not disturb the biosurfactant production. Instead, the application of electrokinetics can help in the uniform distribution in clayey soil due to the following evidences:

- I. It was observed that the highest production of biosurfactants was in the area of the highest bacterial activity (in the middle of electrokinetic cells);
- II. The high amount of biosurfactants was also found in both anode and cathode areas. It was concluded that the high value of biosurfactant in the anode area can be caused by the ionic migration of biosurfactants micelles under the electric field in addition to the *in-situ* produced biosurfactants. However, in the cathode area, the high value of biosurfactants is associated with the electroosmotic flow.
- III. The significant level of bio-micelles in the electrokinetic cells did not follow the pattern of bacterial distribution;
- IV. The short period of the experiment probably did not permit transport of the micelles from Zone B. Therefore, this area showed lower efficiency for phenanthrene removal;
- V. Removal of phenanthrene from the collecting areas (electrodes) was successful. The mobility of phenanthrene was enhanced by the produced biosurfactants under the electric field. The highest removal was achieved at the cathode area (up to

85%). The mechanism of this phenomenon was probably caused by kinetics of bio-micelles formation. It was necessary to proceed the further investigation in this domain, which was undertaken in test series 4.

To summarize, this experiment has determined the possibility of production of biosurfactants to enhance the efficiency of phenanthrene removal within *in-situ* clayey soil under the electric field. Since the production of biosurfactants took place, it increased the solubility of PAHs into the aqueous phase, which in turn it increased the mobility of phenanthrene.

This investigation displayed the potential of increasing the solubility of PAHs in the aqueous-phase and improving desorption from soil, thereby making them amenable to the biodegradation by microorganisms using *in-situ* produced biosurfactants. This increases the efficiency of bio-electrokinetics in the context of increased desorption and mobility of phenanthrene as well as its bioavailability. *In-situ* production of biosurfactants associated with the electrokinetic nutrients supply, could complete previous work (Elektorowicz, 1995a) and lead to the development of new technology – bio-electrokinetics.

## **CHAPTER 8 RESULTS AND DISCUSSION FOR TEST SERIES 3: Transport of biosurfactants under the electric field**

Following the primary conclusion of test series 2, supplementary tests (test series 3) regarding transport of biosurfactants where electrokinetic phenomena are applied were designated. The second objective of these tests was to investigate the feasibility of introducing *ex-situ* produced biosurfactant to soil medium using only electrokinetic method. Subsequently, the investigation on the electrokinetic introduction of *ex-situ* produced biosurfactants was performed in cells T3C1, T3C2, T3C3, and T3C4. During the 8 days experimentation, fluid flow, electrical potential, electrical current, and pH of collected liquid were measured every 24 hours. At the end of the experiment, soil samples were subjected to analysis for pH, moisture content, and concentration of phenanthrene and biosurfactants. The method of analysis was described in Chapter 4.3.

### **8.1 Electrical potential and resistance distribution in cells T3C1 and T3C2**

The electrical potential was measured before and immediately after daily introduction of biosurfactants into the supply zone situated in the middle of the cells. Figure 8.1, Figure 8.2, Figure 8.3 and Figure 8.4 present a profile of electrical potential across the soil specimen of cells T3C1 and T3C2 before and after daily introduction of biosurfactants, respectively. As shown in Figure 8.1 and 8.2, the electrical potential drop was realized mostly after the supply zone toward the cathode region, causing higher electroosmotic flow in that region. The electrical potential difference was 3.02 V between probe 1 and probe 2 at the beginning of testing and 3.14 V after 8 days for both cells. Within the 8 days of testing, the electrical potential difference showed no significant

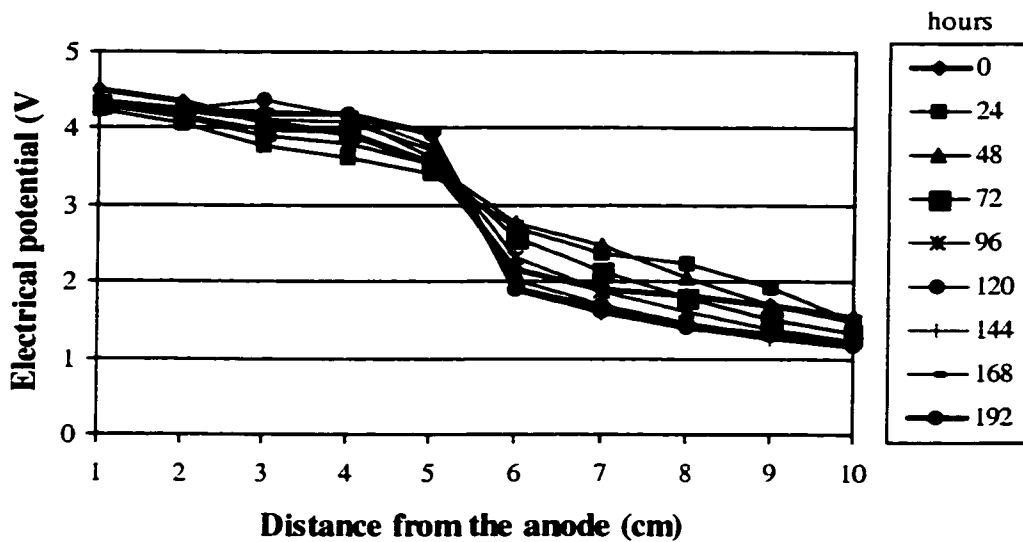


Figure 8.1 Electrical potential distribution in cell T3C1 before daily introduction of biosurfactants

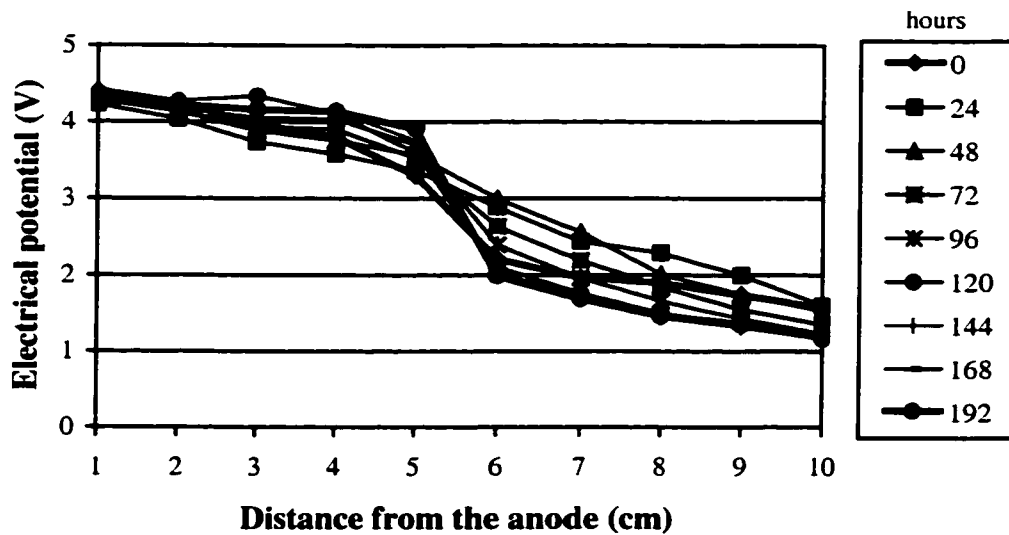


Figure 8.2 Electrical potential distribution in cell T3C1 after daily introduction of biosurfactants with a concentration of 20 mg/l

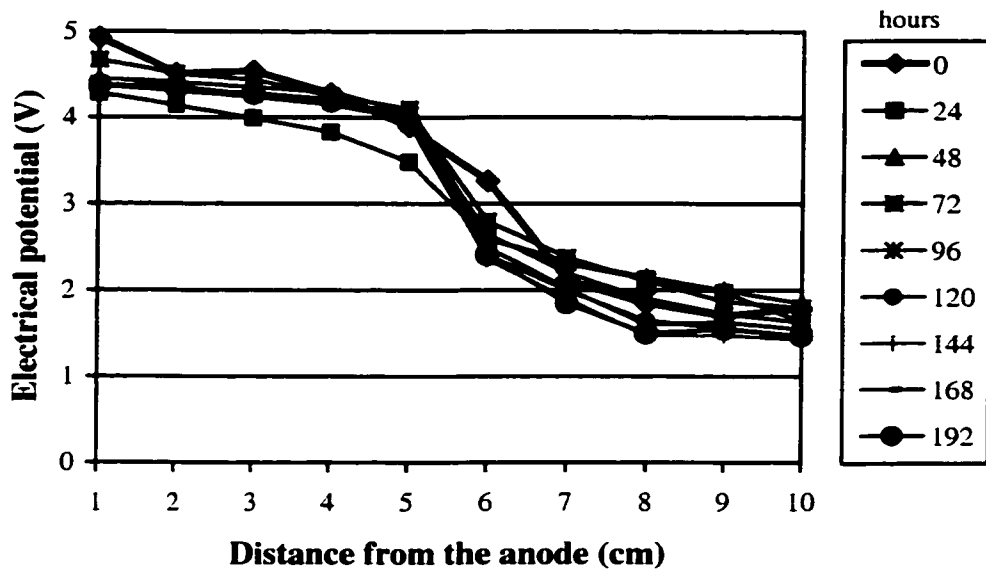


Figure 8.3 Electrical potential distribution in cell T3C2 before daily introduction of biosurfactants

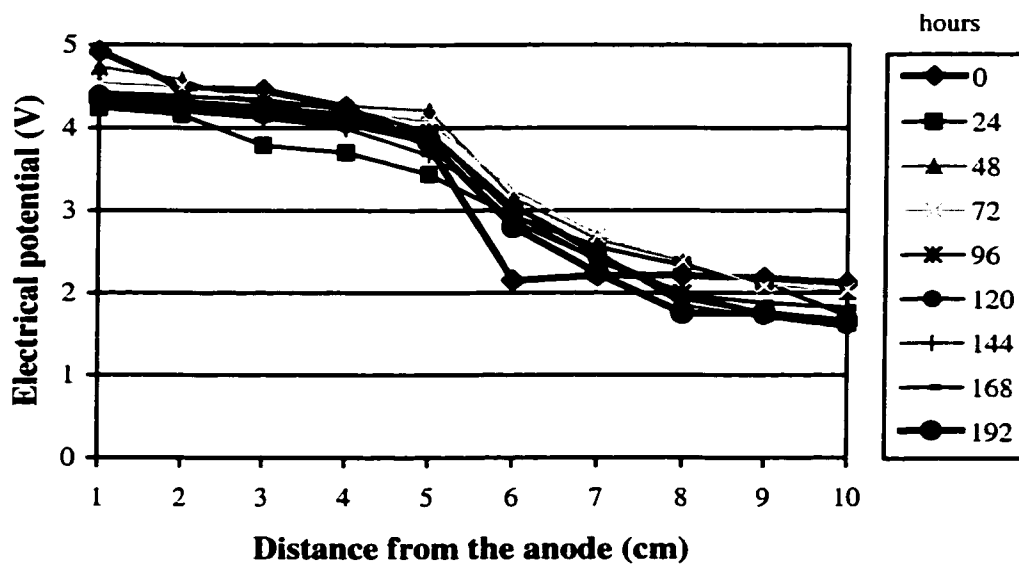


Figure 8.4 Electrical potential distribution in cell T3C2 after daily introduction of biosurfactants with a concentration of 20 mg/l



change at each measured point across the cells. Supply zone showed higher electric gradient with time. It is visible that the introduction of a low concentration of biosurfactants into the non-contaminated soil and contaminated soil did not cause significant changes in the electric gradient. Both cells had a similar electric gradient distribution. The existing electric gradient could provoke the electroosmotic flow, along with the transport of species in the soil pores.

The resistance in cells T3C1 and T3C2 was presented in Figures 8.5 to 8.8. In order to describe the distribution of resistance in cells, the cells were divided into three zones. Each zone had shown different behavior during the experiments. Zone A is designated from the anode to the supply zone. Zone B represents the supply zone, and zone C is designated after the supply zone toward the cathode area. The summary of all the resistance changes in the three zones was shown in Table 8.1. At each measured probe, the resistance increased dramatically with time in zone A. The difference in resistance was 6.7 kOhm in cell T3C1 and 4.1 kOhm in cell T3C2 at probe 1. However, after the introduction of biosurfactants, the difference in resistance decreased for both cells. The value in cell T3C1 was almost two times higher than that in cell T3C2. Zone B represented the transition of the change of resistance. It showed that the difference of resistance decreased dramatically for both cells. After the supply zone, the difference of resistance for both cells was similar, at a much lower level of resistance when compared to zone A. It indicated that there was more electroosmotic flow in zone C.

In summary, the introduction of biosurfactants and a supply zone had an impact on the resistance distribution. No significant change of voltage was evident close to the electrode during 192 hours of experiment.

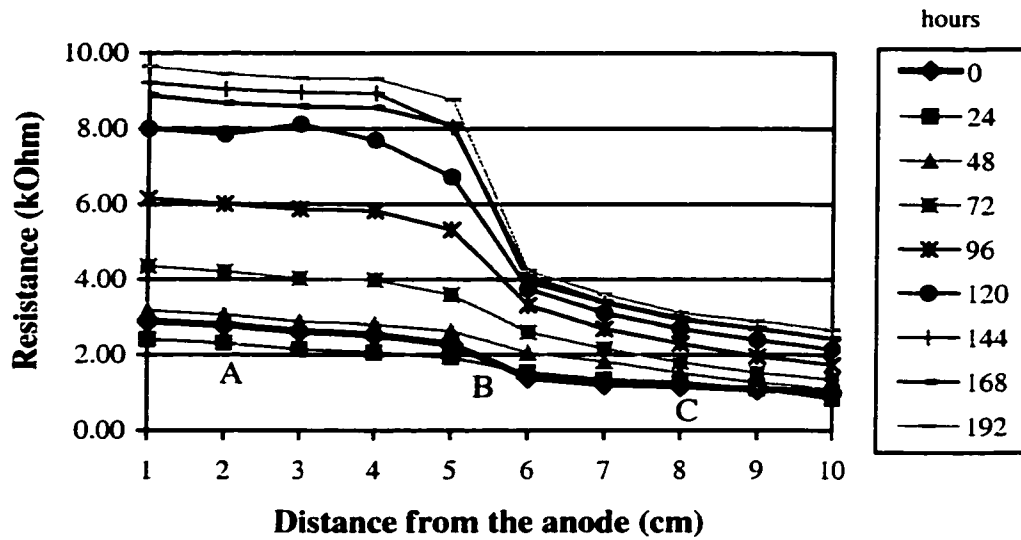


Figure 8.5 Resistance distribution in cell T3C1 before daily introduction of biosurfactants

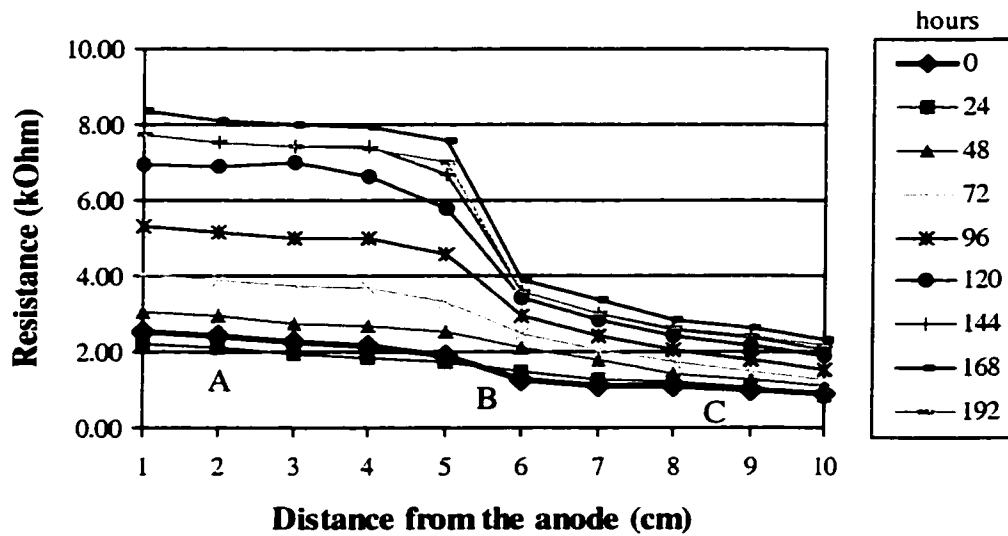


Figure 8.6 Resistance distribution in cell T3C1 after daily introduction of biosurfactants with a concentration of 20 mg/l

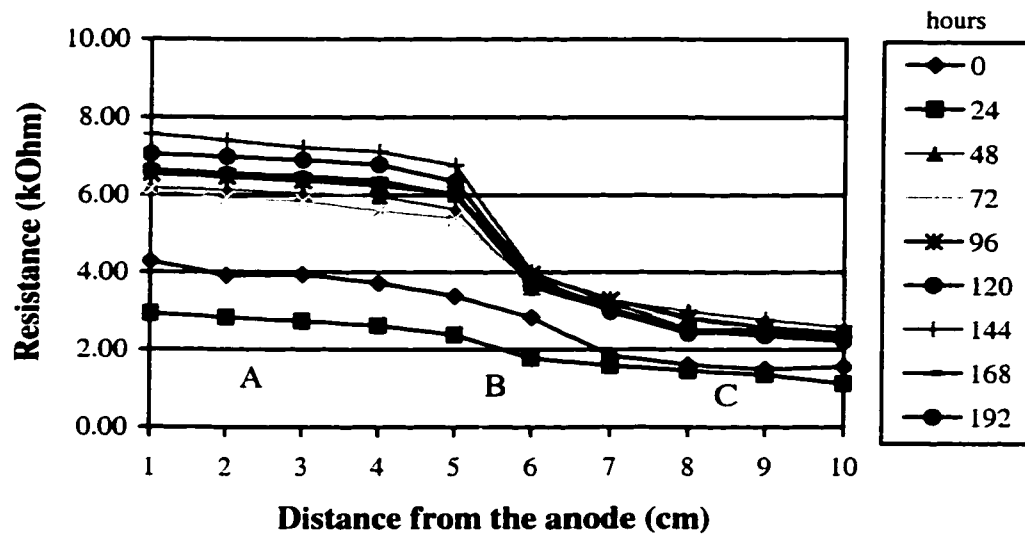


Figure 8.7 Resistance distribution in cell T3C2 before daily introduction of biosurfactants

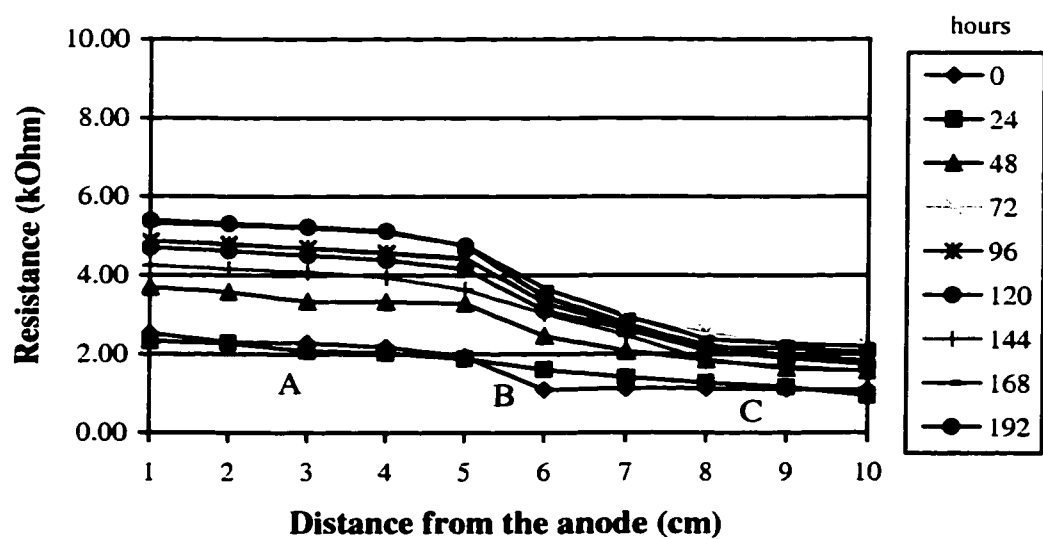


Figure 8.8 Resistance distribution in cell T3C2 after daily introduction of biosurfactants with a concentration of 20 mg/l

Due to the anionic properties of the rhamnolipids, the soil conductivity increased, hence the resistance decreased after the introduction of biosurfactants in both cells. This caused more electroosmotic flow from the supply zone to the cathode. Considering the contaminated soil and the non-contaminated soil, it was showed that cell T3C2 had a much lower resistance difference than cell T3C1. It indicated that the presence of phenanthrene on the surface of the clay, due to the introduction of biosurfactants, dissolution, suspension and emulsification processes increased conductivity in the electric cell.

Table 8.1 Resistance difference in cells T3C1 and T3C2

Electrokinetic cells of test series 3		Resistance difference between the value at the beginning of test and at the end of test (kOhm)					
		Zone A		Zone B		Zone C	
		1 cm	5 cm	5 cm	6 cm	6 cm	10 cm
T3C1	Before	6.7	6.5	6.5	2.8	2.8	1.6
	After	5.8	5.9	5.9	2.7	2.7	1.3
T3C2	Before	4.1	4.0	4.0	2.1	2.1	1.5
	After	3.1	2.7	2.7	2.4	2.4	1.2

Note:

Zone A : from 1 cm to 5 cm away from anode;

Zone B : from 5 cm to 6 cm away from anode;

Zone C : from 6 cm to 10 cm away from anode;

Before : Before daily introduction of biosurfactants;

After : After daily introduction for biosurfactants;

## **8.2 Electrical potential and resistance distribution in cells T3C3 and T3C4**

Figures 8.9 to 8.12 present a profile of electrical potential across cells T3C3 and T3C4 before and after daily introduction of biosurfactants, respectively. These cells were supplied in the middle zone with a high concentration of rhamnolipids (at 3.5 times higher than the CMC). As shown in Figures 8.9 and 8.10, the electrical potential drop was realized primarily after the supply zone toward the cathode region, causing higher electroosmotic flow in that region than in the anode region. The electrical potential difference was 3.1 V between the electrodes at the beginning of testing and 3.1 V after 8 days for both cells. Within the 8 days of testing, the electrical potential difference had no significant change at each measured point across the cells. The supply zone showed higher electric gradient with time. It is visible that the introduction of a high concentration of biosurfactants into the non-contaminated soil and contaminated soil had not caused a significant change in the electric gradient. Both cells had a similar electric gradient. Comparing to cells T3C1 and T3C2, the same pattern of electric gradient were obtained. The existing electric gradient can provoke the electroosmotic flow, along with the transport of species in the soil pores.

The resistance in cells T3C3 and T3C4 was presented in Figure 8.13 through to Figure 8.16. In order to describe the distribution of resistance in these cells, they were divided into three zones as described in Chapter 8.1. The summary of all the resistance changes in the three zones was shown in Table 8.2. At each measured probe, the resistance increased dramatically with time in zone A. The difference in was 5.7 kOhm resistance in cell T3C3 and 12.1 kOhm in cell T3C4 at probe 1. However, after the introduction of biosurfactants, the difference of resistance was similar for both cells. The

value in cell T3C3 was almost 1.2 times higher than that in cell T3C4. Zone B represented the trisection of the change of resistance. It showed that the difference of resistance decreased dramatically for both cells. After the supply zone, the difference of resistance for both cells was similar and at a much lower level, when compared to zone A. However, the values before the introduction of biosurfactants were 2.5 times in cell T3C3 and 6.2 times in cell T3C4 higher than after the introduction at the cathode area. It indicated that there was more electroosmotic flow in zone C.

Table 8.2 Resistance difference in cells T3C3 and T3C4

Electrokinetic cells of test series 3		Resistance difference between the value at the beginning of test and at the end of test (kOhm)					
		Zone A		Zone B		Zone C	
		1 cm	5 cm	5 cm	6 cm	6 cm	10 cm
T3C3	Before	5.7	5.8	5.8	3.6	3.6	2.2
	After	2.8	2.7	2.7	1.4	1.4	0.9
T3C4	Before	12.1	6.3	6.3	4.1	4.1	2.5
	After	2.2	1.5	1.5	1.6	1.6	0.4

Note:

- Zone A : from 1 cm to 5 cm away from anode;
- Zone B : from 5 cm to 6 cm away from anode;
- Zone C : from 6 cm to 10 cm away from anode;
- Before : Before daily introduction of biosurfactants;
- After : After daily introduction for biosurfactants.

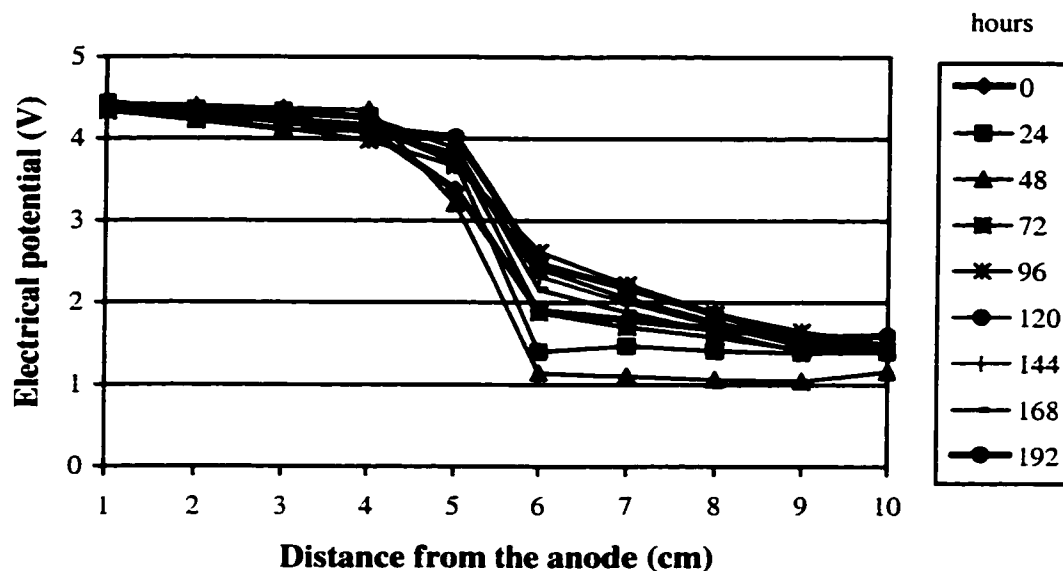


Figure 8.9 Electrical potential distribution in cell T3C3 before daily introduction of biosurfactants

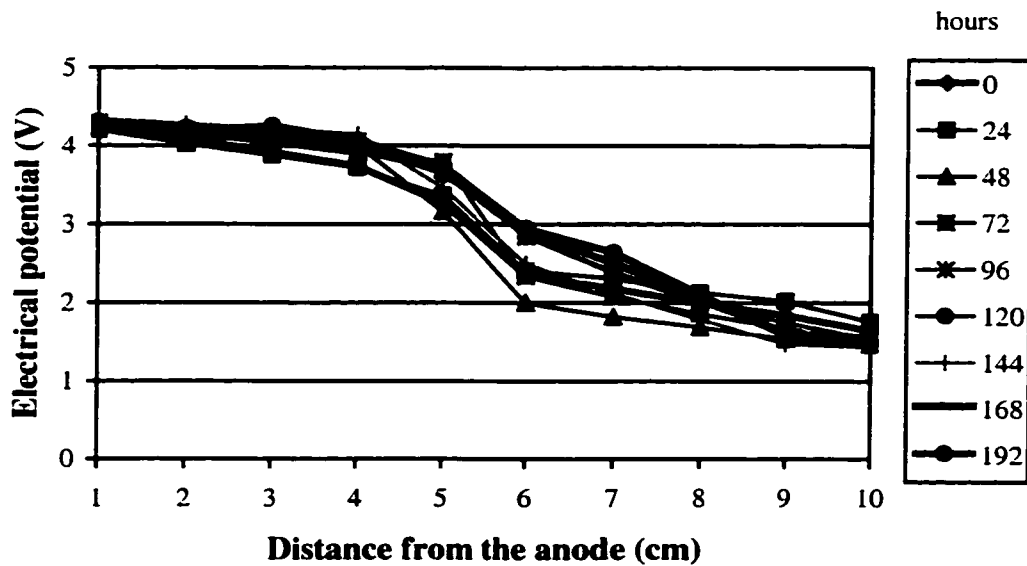


Figure 8.10 Electrical potential distribution in cell T3C3 after daily introduction of biosurfactants with a concentration of 166 mg/l

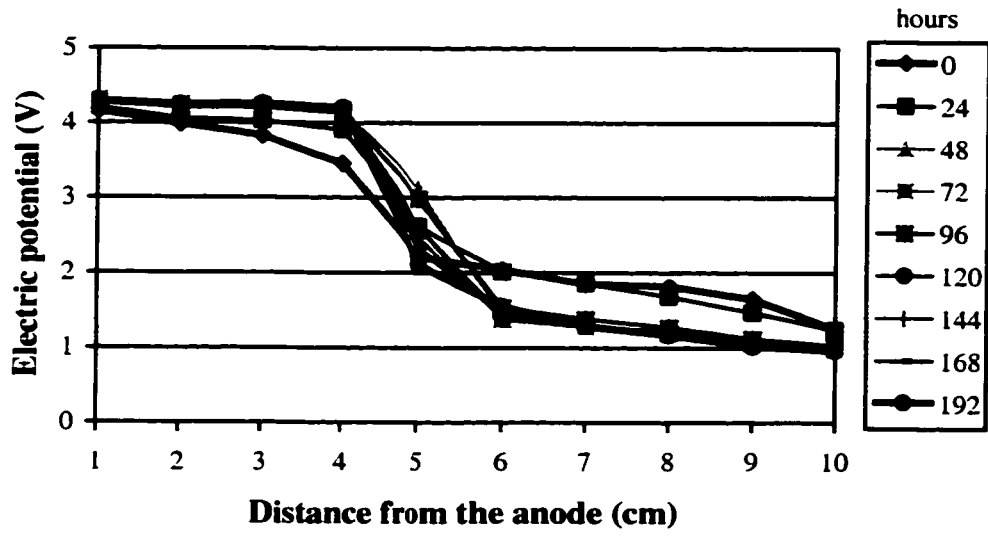


Figure 8.12 Electrical potential distribution in cell T4C3 after daily introduction of biosurfactants with a concentration of 166 mg/l

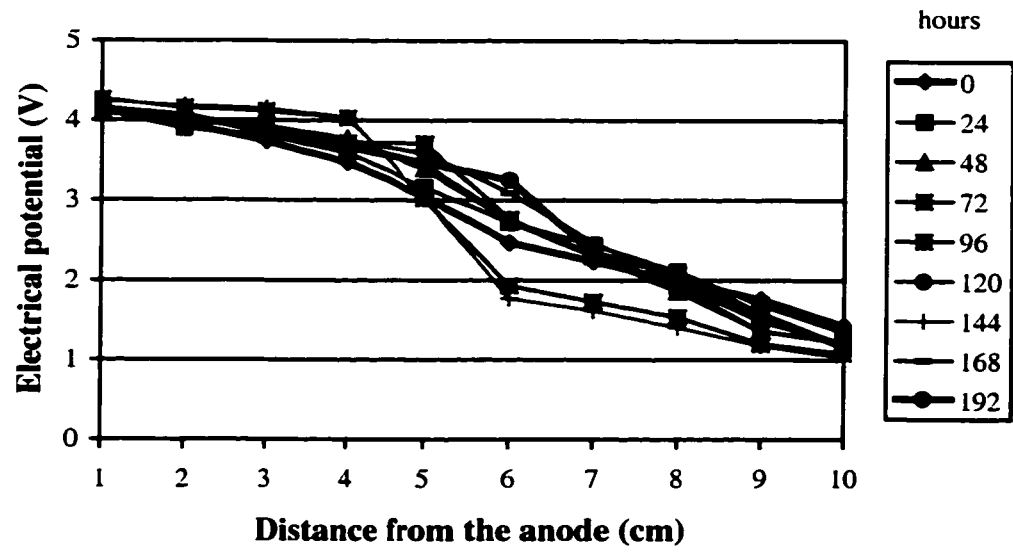


Figure 8.12 Electrical potential distribution in cell T3C4 after daily introduction of biosurfactants with a concentration of 166 mg/l



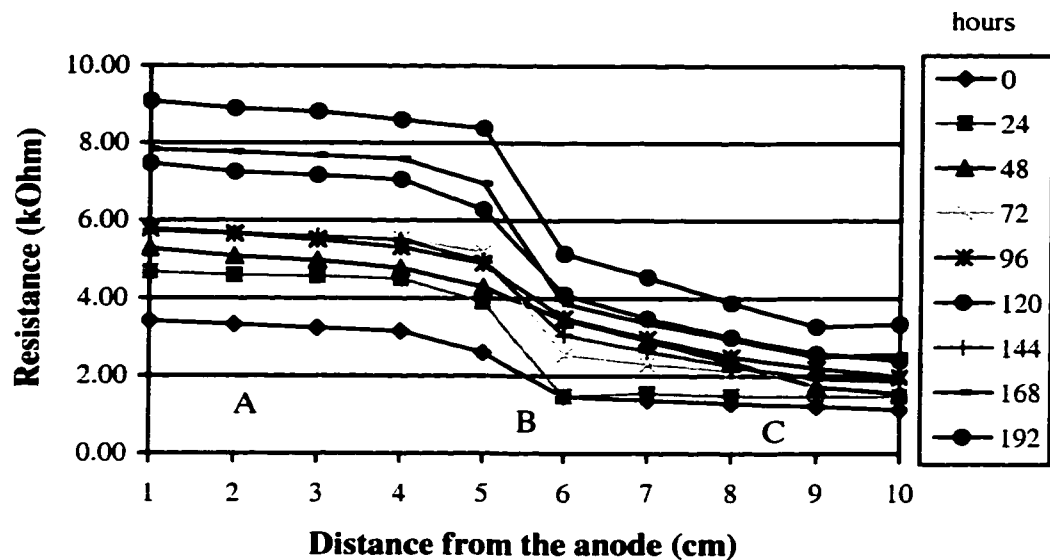


Figure 8.13 Resistance distribution in cell T3C3 before daily introduction of biosurfactants

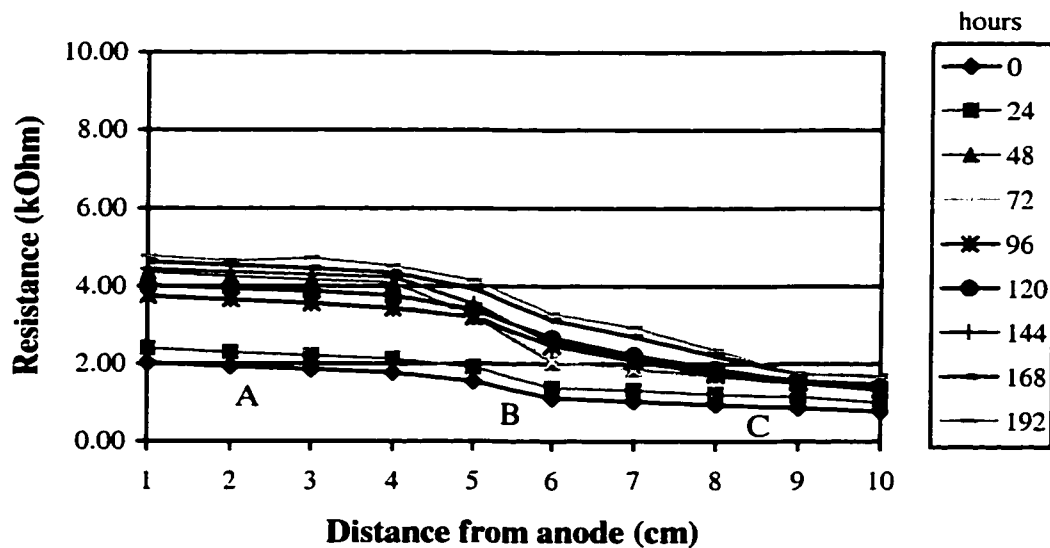


Figure 8.14 Resistance distribution in cell T3C3 after daily introduction of biosurfactants with a concentration of 166 mg/l

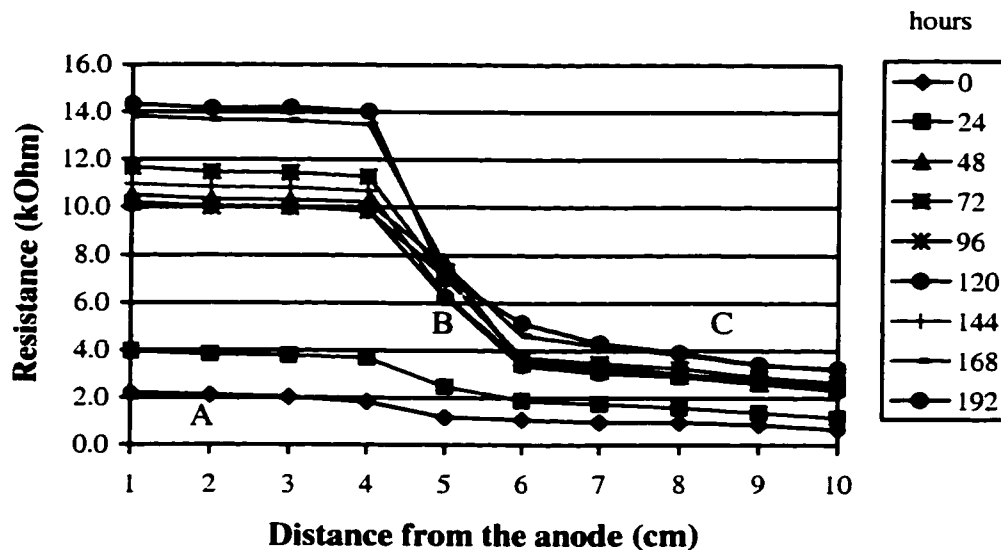


Figure 8.15 Resistance distribution in cell T3C4 before daily introduction of biosurfactants

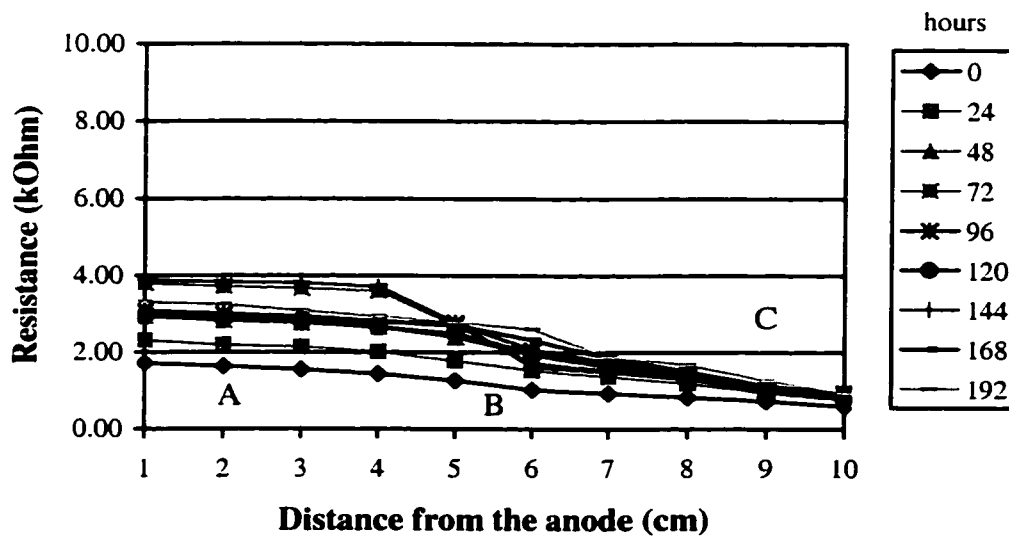


Figure 8.16 Resistance distribution in cell T3C4 after daily introduction of biosurfactants with a concentration of 166 mg/l

In summary, the introduction of biosurfactants and a supply zone had an impact on the resistance distribution. Regarding the comparison of daily introduction of biosurfactants, the electric gradient did not have a significant change before and after introduction. A similar pattern was obtained for both cells. It was observed that the resistance decreased in both cells after the introduction of biosurfactants. Comparing the response of the contaminated soil, cells T3C2 and T3C4 containing contaminated soil had a lower resistance difference than cells T3C1 and T3C3 free of phenanthrene. It is speculated that the presence of phenanthrene on the surface of clay, when the introduction of high biosurfactants took place, the emulsification of phenanthrene into the bio-micelles promoted higher conductance and correspondingly decreased the resistance of the electrical cell.

### **8.3 pH distribution in the electrokinetic cells**

After the termination of the experiment, soil was sampled and analyzed, in order to display the pattern of pH across the electrokinetic cells. The final pH profiles along the electrokinetic cell are presented in Figure 8.17 for cells T3C1 and T3C2 with a low concentration of biosurfactants applied. Figure 8.18 shows pH distribution in cells T3C3 and T3C4 with a high concentration of biosurfactants applied. In the first case, it is clearly shown that pH was 7.4 close to anode and increased up to 8.5 just after the supply zone (Figure 8.17). The two cells showed a similar pattern of pH distribution along the cell. Slight decrease of pH to 6.2 at the anode areas was observed and an increase up to 10.5 at the cathode area. It demonstrates that water electrolytic reactions were taking place as expected. The difference at the anode area was associated with the oxidation

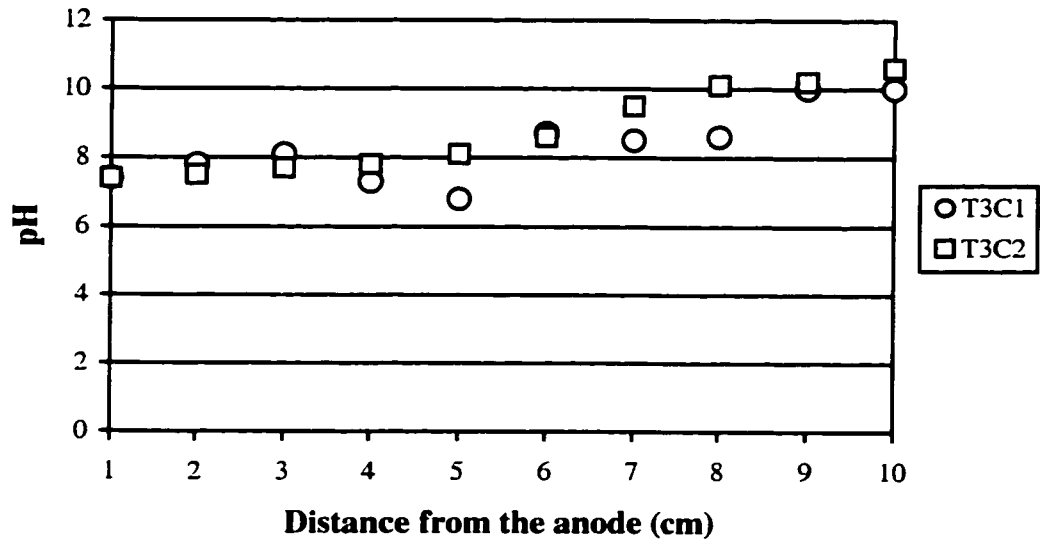


Figure 8.17 Final average pH value of soil in cells T3C1 and T3C2

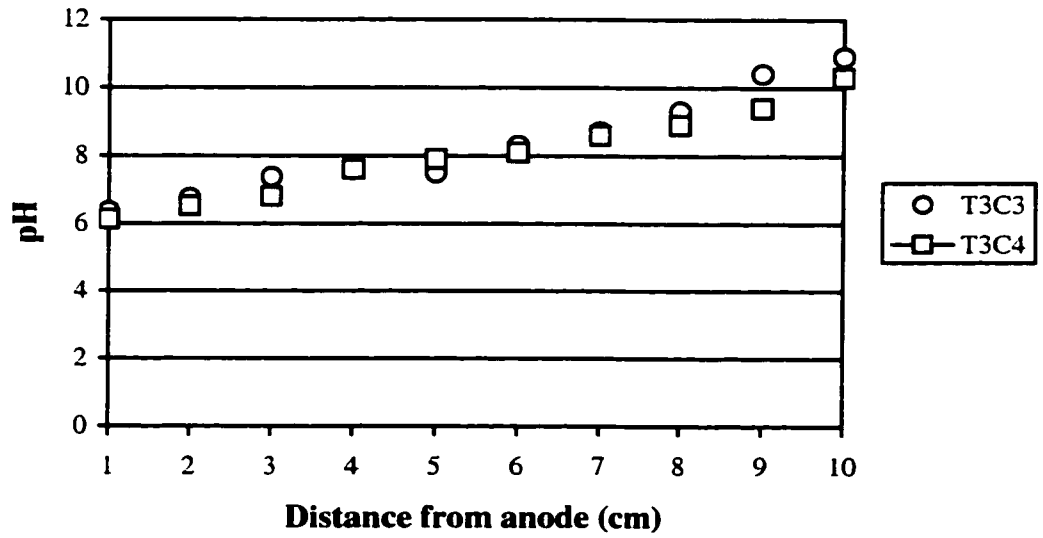


Figure 8.18 Final average pH value of soil in cells T3C3 and T3C4

process in the presence of biosurfactants having different concentrations. Near the cathode, the reduction results were similar for both cases indicating that the concentration of biosurfactants did not influence pH distribution in this area. The non-contaminated soil and contaminated soil showed a similar pattern.

#### **8.4 Moisture distribution in the electrokinetic cells**

The profile of the final soil moisture content was shown in Figure 8.19 for cells T3C1 and T3C2 and Figure 8.20 for cells T3C3 and T3C4. Moisture contents of 49% to 48% for cell T3C1 and 26% to 50 % for cell T3C2 were obtained across the specimens at the end of testing. It was mainly caused by water transport due to electroosmosis. Higher moisture contents were observed near the anode area due to direct contact with the water supply system. A higher moisture content in T3C4 was observed as a result of the change of the affinity between water and clayey soil due to the partitioning of phenanthrene into the bio-micelles. The moisture content in cells T3C3 and T3C4 followed the same trend as cell T3C1 and T3C2 (Figure 8.20). The average moisture content in cell T3C1 was 39% and 46% in cells T3C2. Similarly, the average moisture content was 39% in cell T3C3 and 48% in cell T3C4, respectively. As observed, electroosmosis is a significant process in electrokinetic soil processing. Lockhart (1983) and Gray and Mitchell (1967) showed that increasing electrolyte concentration in the pore fluid would minimize the electroosmotic flow. However, in this research, it was found that the introduction of biosurfactants enhanced the electroosmosis flow.

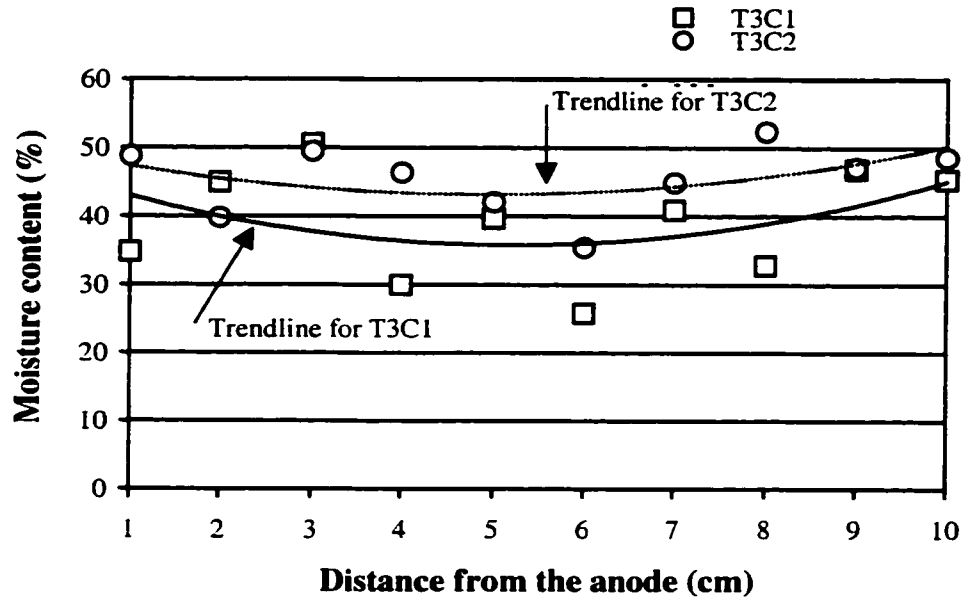


Figure 8.19 Final average moisture content of soil in cells T3C1 and T3C2

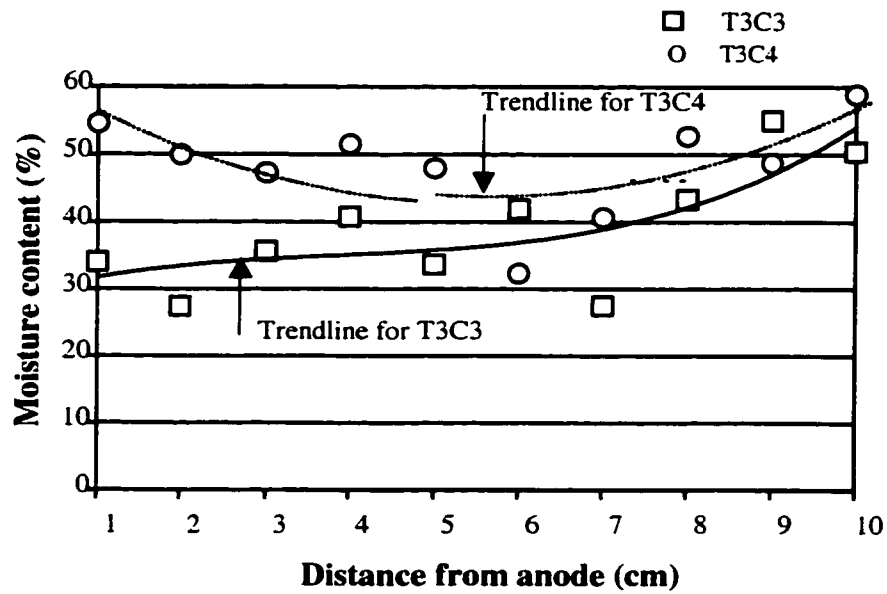


Figure 8.20 Final average moisture content of soil in cells T3C3 and T3C4

In summary, it is evident that the higher moisture content present in soil corresponding to the high concentration of introduced biosurfactants, especially in phenanthrene contaminated soil. This phenomenon is most probably associated with the formation of bio-micelles, where the affinity of water to clay materials changed in the presence of bio-micelles.

### **8.5 Rhamnolipids concentration in the electrokinetic cells**

It is hypothesized that the negatively charged biosurfactant molecules will form negatively charged micelles with phenanthrene, and migrate to the anode, resulting in an increase of the removal efficiency. The introduction of biosurfactants at concentrations of 20 mg/l and 166 mg/l into the contaminated soil was designed to investigate the transport of biosurfactants under the electric field and finally to achieve the objective of enhancing electrokinetic remediation.

As shown in Figure 8.21 and Figure 8.22, the distribution of a low concentrations of biosurfactants was approximately uniform at the end of the experiment. With regards to a higher concentration, the biosurfactants tended to be uniformly distributed in the non-contaminated soil (cell T3C3) and accumulate near the cathode area in the contaminated soil (cell T3C4), contrary to the above-mentioned hypothesis. Due to the anionic property of biosurfactants, they should be transported to the anode area by electromigration and electrophoresis, and should not be expected to be present in the cathode area. However, as shown in Figure 8.21 and 8.22, there was a substantial level of biosurfactants which were transported to the cathode.

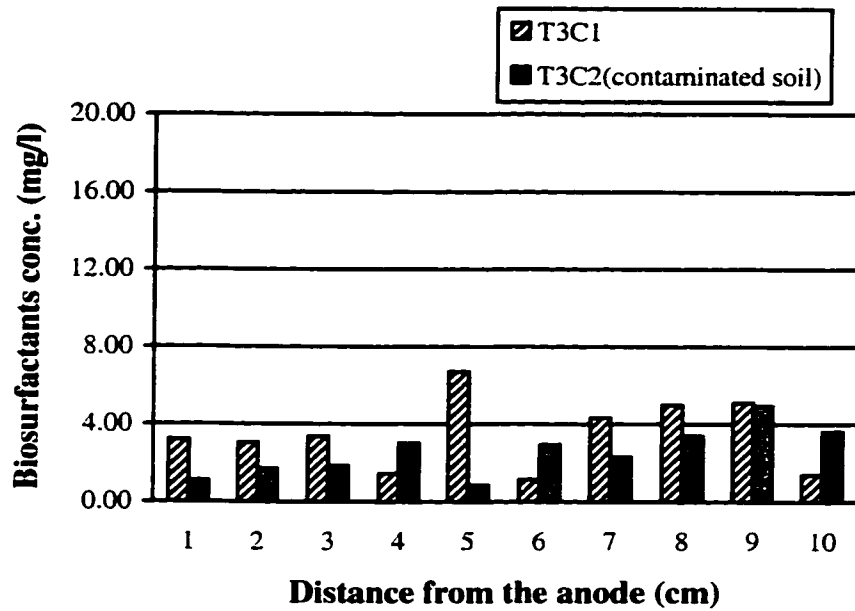


Figure 8.21 Final average biosurfactants distribution in cells T3C1 and T3C2 (the introduced concentration of biosurfactants: 20 mg/l)

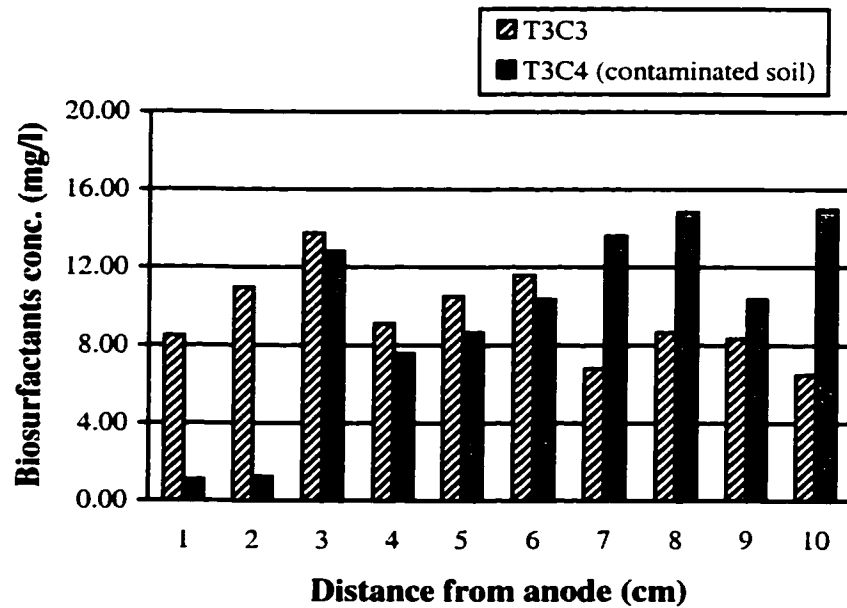


Figure 8.22 Final average biosurfactants distribution in cells T3C3 and T3C4 (the introduced concentration of biosurfactants: 166 mg/l)



The comparison between the non-contaminated soil and contaminated soil cells, shows that the biosurfactants were equally transported to the anode and the cathode areas in cells contained soil free of phenanthrene (cell T3C1 and cell T3C3). In cells containing contaminated soil (cell T3C2 and cell T3C4), the amount of biosurfactants tended to accumulate in the cathode area. The insignificant levels were observed in cell T3C4 close to anode. It can be concluded that the formation of bio-micelles plays an important role in transport, since soil with and without phenanthrene showed different patterns.

The transport of biosurfactants in the electrokinetic cell is mainly a result of electrophoretic and electroosmotic flow. Electrophoresis played a predominate role and seems to be related to the lower concentration of introduced biosurfactants. In case of introducing a higher concentration of biosurfactants, it indicated that the electroosmotic flow has a greater impact than electrophoresis. The final answer probably can be obtained after the accurate analysis of the kinetic formation of bio-micelles under the electric field (discussed in Chapter 10).

## **8.6 Phenanthrene concentration in the electrokinetic cells**

This section deals with the results and discussion of the phenanthrene concentration in the soil and its spatial distribution. The ratio of final concentration of phenanthrene in soil after testing to the initial concentration of phenanthrene across the soil specimens is presented in Figure 8.23 for cell T3C2 and in Figure 8.24 for cell T3C4. In the case of the introduction of a lower concentration of biosurfactants, the highest ratio of phenanthrene concentration in cell T3C2 was 0.91 near the anode region (Figure 8.23). It is also shown that the average concentration ratio of phenanthrene in an entire

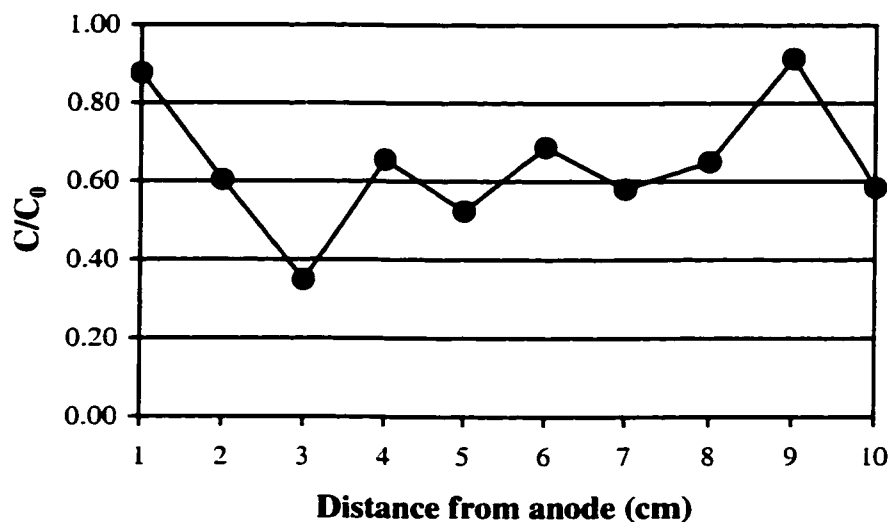


Figure 8.23 Average remaining phenanthrene distribution in cell T3C2 (the introduced concentration of biosurfactants: 20 mg/l)

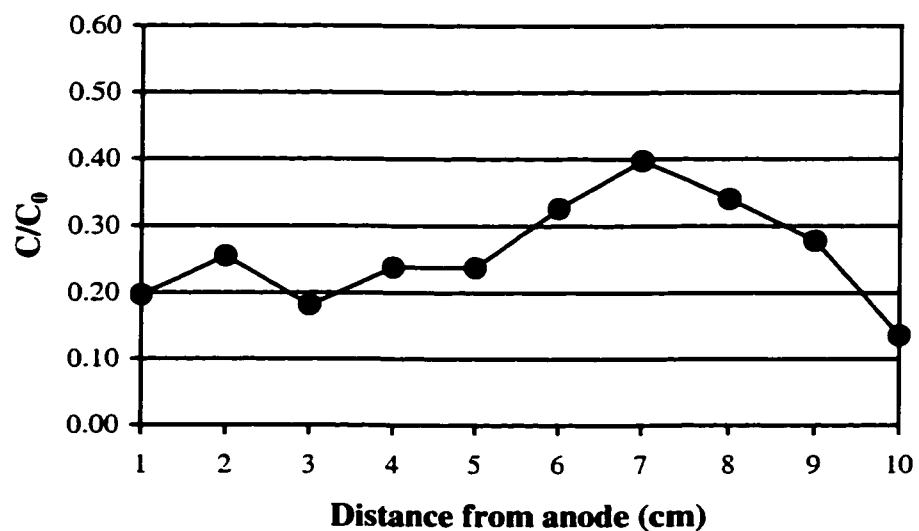


Figure 8.24 Average remaining phenanthrene distribution in cell T3C4 (the introduced concentration of biosurfactants: 166 mg/l)

specimen was 0.64. This means that the average removal of phenanthrene in the soil specimen was 36% after 8 days of testing. The experimental results clearly demonstrated that the addition of biosurfactants at a low concentration did not cause a significant phenanthrene removal. It can be speculated that due to the concentration of biosurfactant which were lower than the CMC and its partial sorption on soil particles, an insufficient amount of biosurfactants was involved in the micelle formation. Consequently, it affected the solubilization of phenanthrene and its mobility and removal by means of electrokinetics.

Regarding the introduction of a higher concentration of biosurfactants, cell T3C4 was characterized by relatively lower phenanthrene concentration in the entire soil compared to T3C2 (Figure 8.24). The highest ratio of phenanthrene concentration in cell T3C4 was 0.40, at 7 cm away from the anode. The average concentration ratio of phenanthrene in an entire specimen was 0.26. This means that the average removal of phenanthrene in the soil specimen was 74% after 8 days of testing. The experimental results clearly demonstrate that significant phenanthrene removal was obtained in the case of the introduction of a higher biosurfactant concentration.

Electrokinetic processes are primarily utilized for the removal of toxic ionic contaminants. The available data indicated substantial removal of charged contaminants including heavy metals, radionuclides, and selected organics. Although removal of free phase nonpolar organics is questionable, Pamukcu et al. (1995) states that this would be possible if they were presented as small bubbles (emulsions) that could be swept along with water movement by electroosmosis. It is hypothesized that the biosurfactants can readily form soluble micelles with phenanthrene, reducing the quantity of phenanthrene

retained by soil particles, thereby increasing phenanthrene mobility, and easily removing phenanthrene bound by soils.

The general occurrence of phenomena in cell T3C2 with the introduction of a low concentration of biosurfactants and cell T3C4 with the addition of a high concentration of biosurfactants to contaminated soil are as follows:

- I. The removal of phenanthrene took place in both cells. The introduced concentration of biosurfactants at 3 times higher than the CMC obtained a twice higher removal efficiency than that biosurfactant at a concentration of 2.5 times lower than the CMC.
- II. The adsorbed phenanthrene partitioning into the aqueous phase and advancing across the soil specimens into the removal areas in response to the presence of biosurfactants, resulted in an abundance of bio-micelles within the system.
- III. Electroosmosis, which was prevalent as compared to electrophoresis, was the primary driving force in the transport of micelles in the soil pore fluid under the electric field.

These results showed the effectiveness of biosurfactants as an agent for enhancing solubility and mobility of phenanthrene during electrokinetic treatment. In the experiments with low currents and short times, phenanthrene was partially removed near the cathode section. The time factor plays a very important role in the removal of phenanthrene. When the remediation process was operated for a relatively short period, phenanthrene was mostly removed from the section near the cathode, but accumulated to some extent near the anode. Therefore, when the remediation process was executed for a longer period, phenanthrene could be eventually removed at a higher extent from the soil specimens.

## **CHAPTER 9 RESULTS AND DISCUSSION FOR TEST SERIES 4: Investigation on bio-micelles formation under the electric field**

In order to determine the mechanism of phenanthrene removal during enhancement by biosurfactants and electrokinetics, and to investigate the transformation phenomena of bio-micelles (micelle created by biosurfactants and phenanthrene), test series 4 were performed. The tests, conducted in identical cells, demonstrated the fundamental formation process of bio-micelles under an electric field as a function of time and in the presence of clayey soil. It may identify and quantify the governing processes involved in coupled transport of PAHs and biosurfactants in the pores of contaminated clayey soil, under an applied electric field.

### **9.1 Results from test series 4**

In order to investigate the formation of micelles and aggregation processes under the electric field, experiments were conducted, and were designated as T4C1, T4C2 and T4C3 (described in Chapter 4.5.4). In order to verify whether the formation of bio-micelles is a function of time, under the influence of electric field, studies of a variety of samples, representing different systems at different time intervals, were conducted.

To obtain the required data, the analysis of relative optical density of samples using FTIR were applied. The value of the relative optical density was calculated as the ratio of absorbance values of two typical bands. One represents a typical band for the component, using spectra in Chapter 5.2 as a reference, and the other represents the band at approximately  $3280\text{ cm}^{-1}$ . This band is attributed to OH stretching vibration without soil, while the band at  $1150\text{ cm}^{-1}$  is attributable to Si-O vibration with soil in the studying

system. The physical structure of bio-micelles was shown on topographies produced by Atomic Force Microscopy (AFM).

In the phenanthrene-water-biosurfactant system (cell T4C1), Figure 9.1 clearly shows the three distinctive phases for the distribution of biosurfactants in the middle of electrokinetic cell. The first phase, from 0-11 hours, presents a slightly decreasing pattern for the three layers. The corresponding regression analysis was shown in Figure 9.2. The plot remains linear with decreases proportional to the amount of biosurfactant present. The second phase, appearing between 14 and 48 hours, shows that the value dramatically increased four times at the 14<sup>th</sup> hour, reaching a maximum for the entire test (Figure 9.3). The distribution of the second phase can be represented by the linear equation. The value at the 48<sup>th</sup> hour decreased to the initial value. In the third phase, the system tended to be stable as shown in Figure 9.4.

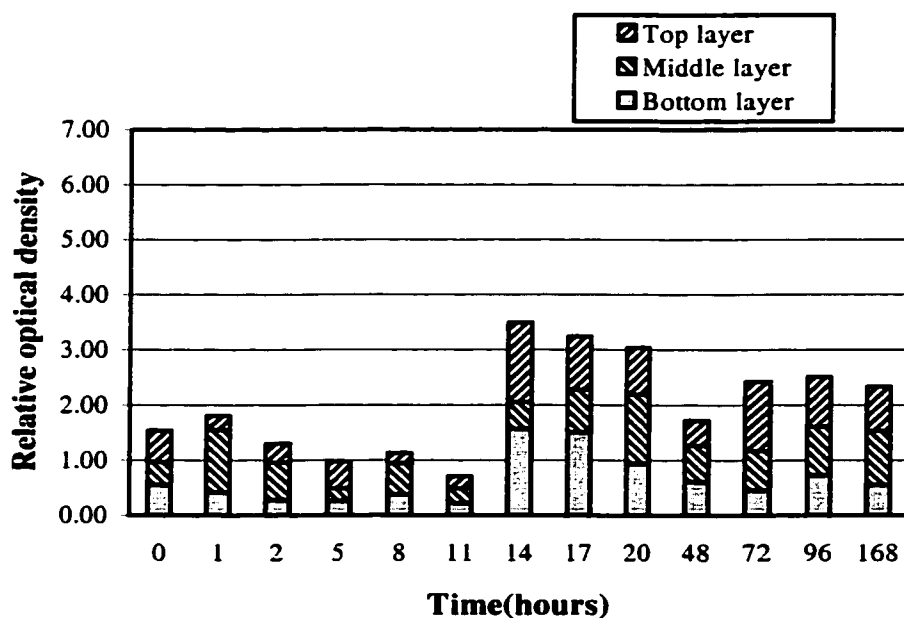


Figure 9.1 Biosurfactant profile in different layers during the test in the phenanthrene-water-biosurfactant system (cell T4C1)

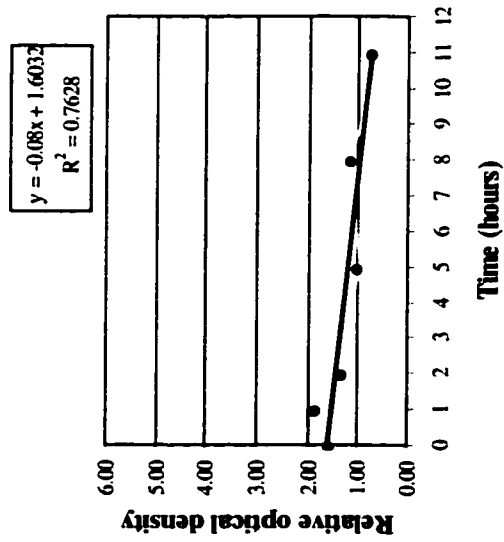


Figure 9.2 Biosurfactants profile during first 11 hours test in the phenanthrene-water-biosurfactant system (cell T4C1)

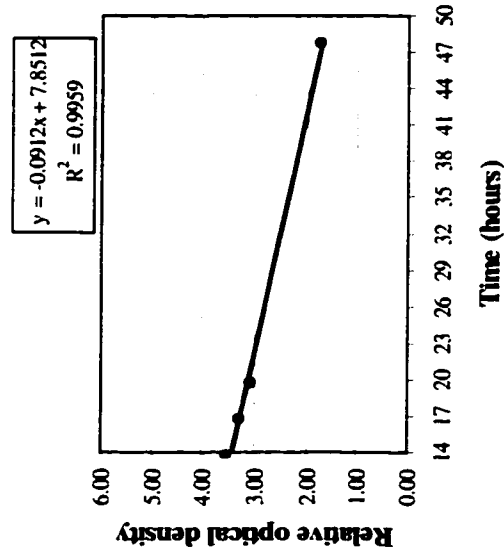


Figure 9.3 Biosurfactants profile from 14 hours to 48 hours test in the phenanthrene-water-biosurfactant system (cell T4C1)

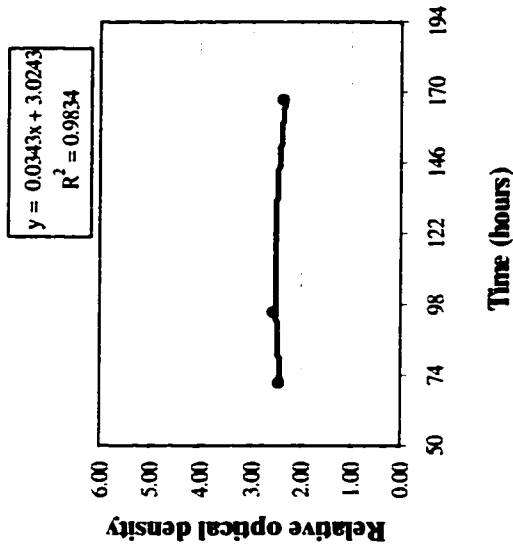


Figure 9.4 Biosurfactants profile during last 120 hours test in the phenanthrene-water-biosurfactant system (cell T4C1)

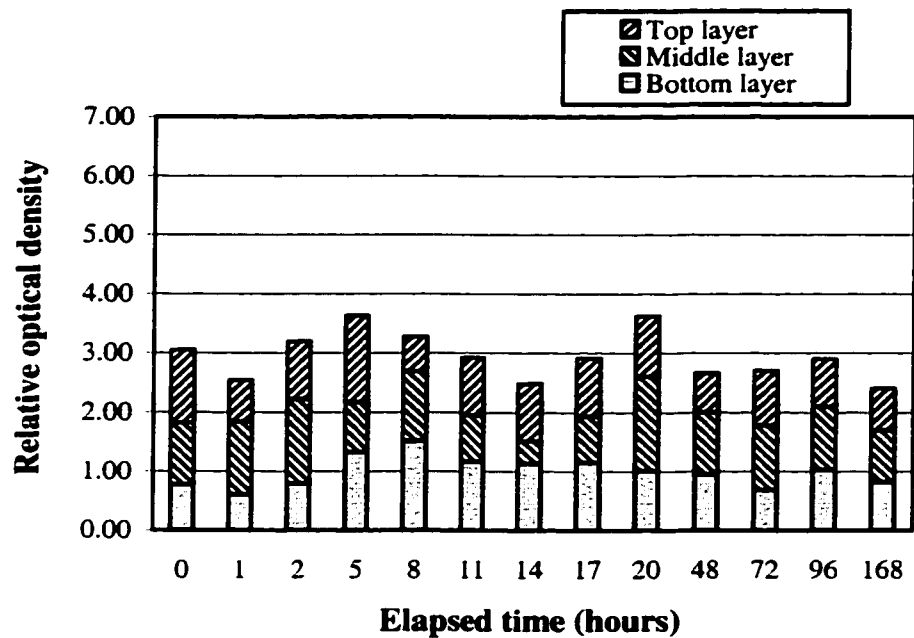


Figure 9.5 Phenanthrene profile in the different layers during the test in the phenanthrene-water-biosurfactant system (cell T4C1)

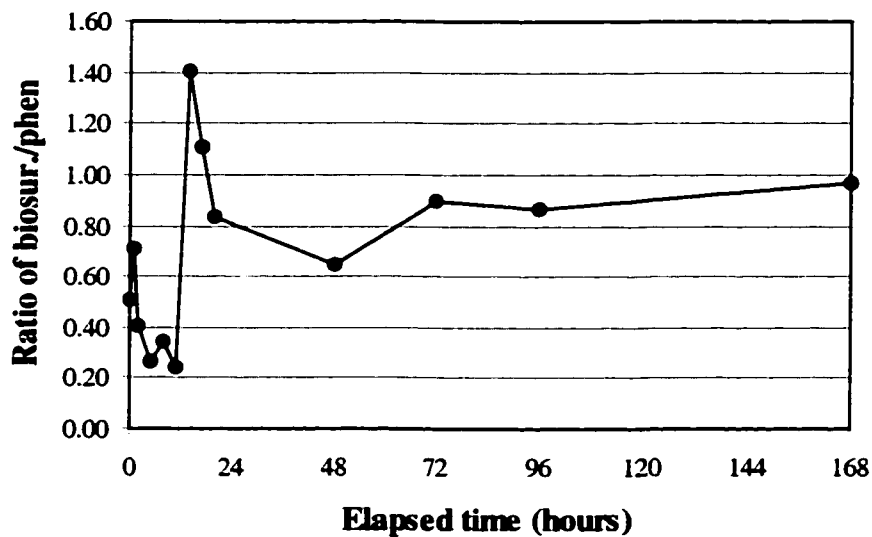


Figure 9.6 Ratio of bio-micelles to phenanthrene during the test in the phenanthrene-water-biosurfactant system (cell T4C1)



Figure 9.5 shows phenanthrene present in the three layers, indicating the incorporation of phenanthrene into the bio-micelles. In order to describe the change in bio-micelle structure with time, the ratio between the relative optical density of biosurfactant and phenanthrene were calculated (Figure 9.6). This analysis showed a decrease of the ratio in the first phase. After that, the ratio increased instantaneously 5.8 times, reaching the critical point at the 14<sup>th</sup> hour of second phase. The ratio subsequently dropped to 0.81 and tended to be asymptotically stable. It was concluded that the prevalent density of biosurfactant over phenanthrene showed evident changes in the bio-micelle structure, building up maybe several layers of biosurfactant micelles. Variation of the ratio with time shows a time dependence of micelle formation under the electric field.

When comparing the soil-phenanthrene-water-biosurfactant system (cell T4C2) to the system without soil (cell T4C1), the different patterns were observed with respect to the biosurfactant profile. Two distinctive phases were observed in Figure 9.7. The first

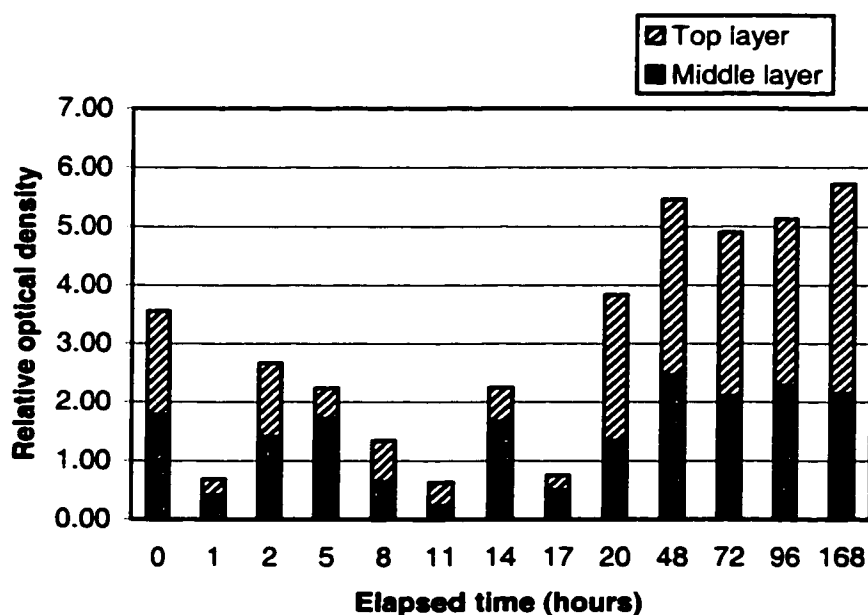


Figure 9.7 Biosurfactant profile during the test in the soil-phenanthrene-water-biosurfactant system (cell T4C2)

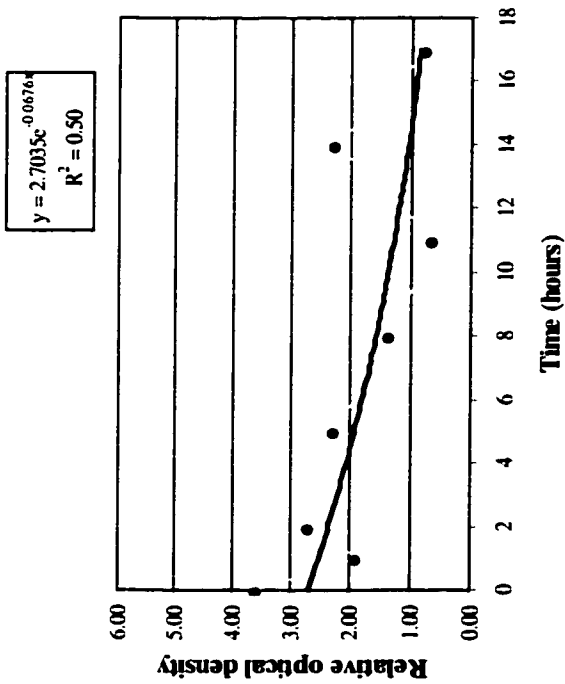


Figure 9.8 Biosurfactants profile during first 17 hours test in the soil-phenanthrene-water-biosurfactant system (cell T4C2)

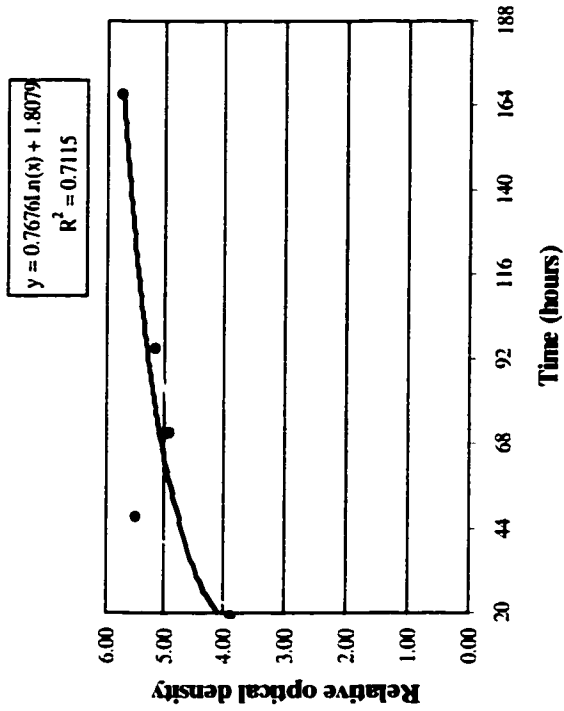


Figure 9.9 Biosurfactants profile during last 147 hours test in the soil-phenanthrene-water-biosurfactant system (cell T4C2)

phase (up to 17 hours) showed a decreasing pattern for the three layers. As shown in the corresponding regression curve, in Figure 9.8, an exponential decrease was observed. Dispersed data show an unstable stage. The second phase formed around the 20<sup>th</sup> hour showed the value increased four times and increased continuously, following a logarithmic equation until the end of the test (Figure 9.9).

As compared to the soil profile in this system (Figure 9.10), it is clearly shown that a significant level of soil was present in the top and middle layers within the first 5 hours. After 6 hours, the soil was only detected in the bottom layer. This indicates that the interaction of bio-micelles with clay materials occurred at the beginning of the test, and then the settling of clay particle was accelerated. Eventually most of the particles settled at the bottom of electrokinetic cell.

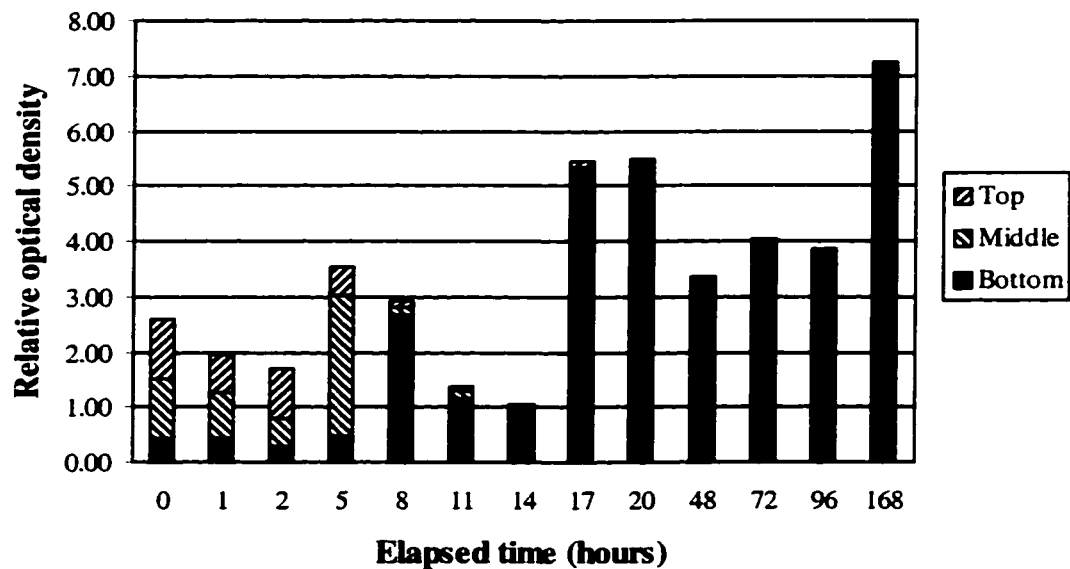


Figure 9.10 Soil profile during the test in the soil-phenanthrene-water-biosurfactant system (cell T4C2)

To examine whether phenanthrene can be desorbed from the soil surface into the aqueous phase due to the presence of biosurfactants, the comparison of phenanthrene spectra in T4C2 and T4C3 is presented in Figure 9.11. Cell T4C3 was not connected to an electric field as a control cell. In this cell, the relative optical density of phenanthrene in the top and middle layer was below the FTIR detection. The general pattern of phenanthrene in the different layers of cell T4C2 followed the biosurfactant distribution. It showed that phenanthrene in the bottom layer of cell T4C2 is much lower than those in the bottom layer of cell T4C3. The value of phenanthrene in the top and middle layers was much higher in cell T4C2 than in cell T4C3. It indicates that phenanthrene is desorbed from the soil surface due to the formation of bio-micelles. Due to the involvement of biosurfactants and the electric field, phenanthrene can be detached from the clayey particles and transported into the aqueous phase. In order to investigate the bio-micelles formation in the presence of clayey soil particles, the ratio of relatively optical density of biosurfactants and phenanthrene was calculated. The Figure 9.12 shows the average ratio was 1.24, but the lowest value in the 8<sup>th</sup> hour was 0.92. After that, the ratio increased approximately 4 times to reach the critical point in the 20<sup>th</sup> hour. The ratio then dropped to 0.76 and slowly increased to the end of test. The observed changes in the ratio indicate as follows:

- I. The formation of bio-micelles is a kinetic process, especially in the first 2 days of experiment;
- II. Bio-micelles do not keep the same shape under the electric field;
- III. The pattern of bio-micelle formation changed and was deferred comparing to the system without soil;

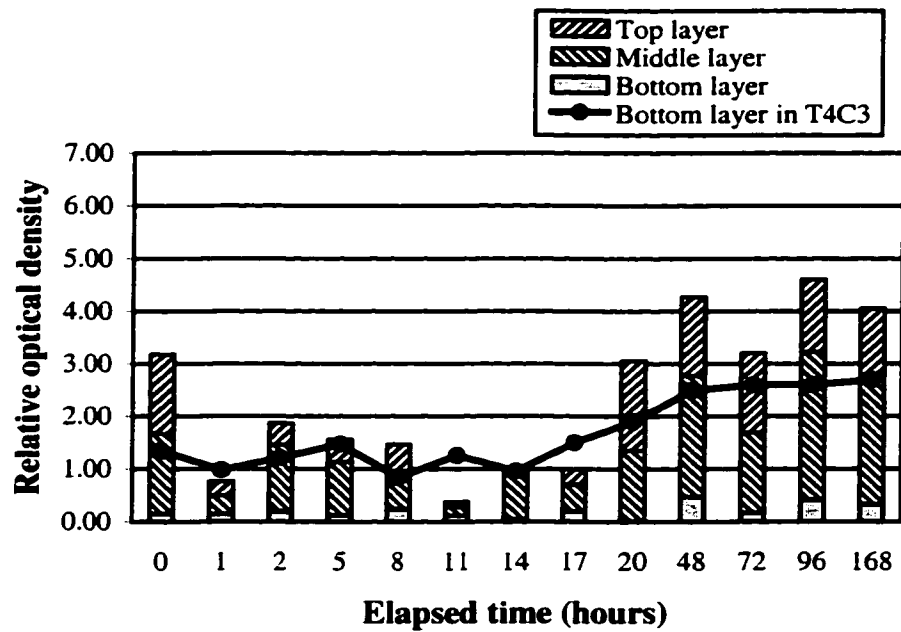


Figure 9.11 Phenanthrene profile of different layers during the test in the soil-phenanthrene-water-biosurfactant system (cell T4C2)

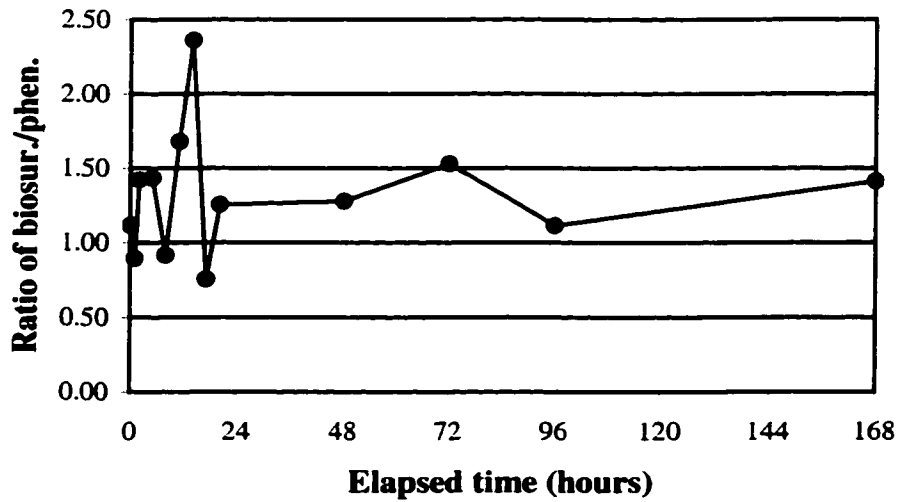


Figure 9.12 Ratio of bio-micelles to phenanthrene during the test in the soil-phenanthrene-water-biosurfactant system (cell T4C2)

- IV. An exponential decrease was observed in the phase 1, instead of linear changes. Phase 2 existing in the phenanthrene-water-biosurfactant system almost disappeared in this system. However, it was replaced with the increased pattern of logarithmic curve.
- V. The critical point of bio-micelle growth probably due to coalescence was also observed to the same extent.
- VI. Generally all changes in bio-micelle formation appear to be slower than those in the system without soil. Clay particles seem to attenuate bio-micelle formation process.

From the above-mentioned facts, the form of bio-micelles is not only spherical. Therefore, further research must be performed on the type of bio-micelles, and the factors that affect the kinetics of bio-micelle formation.

## **9.2 Mechanism of phenanthrene removal**

Based on the properties of phenanthrene such as non-polarity and low solubility in water, it is difficult to promote its mobility by means of standard electrokinetic phenomena. With the application of biosurfactants, transport can be enhanced since solubilization of phenanthrene increases due to the micellization process. Since rhamnolipids are anionic biosurfactants, ionic micelles may also be transported by electrophoresis under the electric field, in addition to electroosmosis.

The hypothesized process of phenanthrene removal from clayey soil, enhanced by biosurfactants under the electric field is as follows: 1) Biosurfactants form micelles after an equilibrium process is reached, known as micellization; 2) Phenanthrene is

incorporated into bio-micelles, so called solubilization; 3) Desorption of phenanthrene from soil surface takes place; 4) Aggregation/de-aggregation of bio-micelles occurs.

It can be assumed that upon the influence of the electric field, the thermodynamical stability of the multiphase system will be disturbed and the equilibrium in the transfer processes between the phases will be shifted. During the electrokinetic processes, the charged particles such as fine soil particles, biosurfactants, and phenanthrene in the core of micelles can be transported. In addition, electrokinetic processes cause an excess of hydroxyl ions in the cathode and protons in the anode areas. In these conditions, Rosen (1989) pointed out that the changes in the charge and in specific density of many colloid particles occur, and the reactions of flocculation and emulsification start or accelerate.

Results of test series 4 showed that the changes in properties of systems upon the action of electric field were visible from above-mentioned facts. Assuming all studied electrokinetic cells are thermodynamically stable systems before and after the acting of the electrokinetic processes, the influence of electric field on the behaviour of the components and their transfer between different phases of the system could be proposed.

### **9.2.1 Factors effecting the fate of bio-micelles**

In the soil-water-phenanthrene-biosurfactant system, upon the application of an external electric field, the electrokinetic forces are imposed on the suspended solids carrying electric charges and transporting the particles to the opposite charged electrode. In aqueous solutions, the phenomenon of sedimentation of fine clay particles also occurs. The sedimentation of clay is governed by the combined action of gravitational force,

Brownian force, inter-particle electrical forces, van der Waals force, and Stokesian viscous force (Russel et al. 1989).

A balance between hydrocarbon chain attraction and ionic repulsion controls the formation of biosurfactants micelles. Hence, formed micelles are aggregates composed of a compressive core surrounded by a less compressive surface structure (Bloor et al. 1995). From a biological standpoint, biosurfactants have also been shown to form a variety of microstructures such as spherical micelles, cylindrical micelles, vesicular and lamellar sheets (Figure 9.13) (Vinson et al. 1989). The aggregation of sheets can be generally called bilayers.

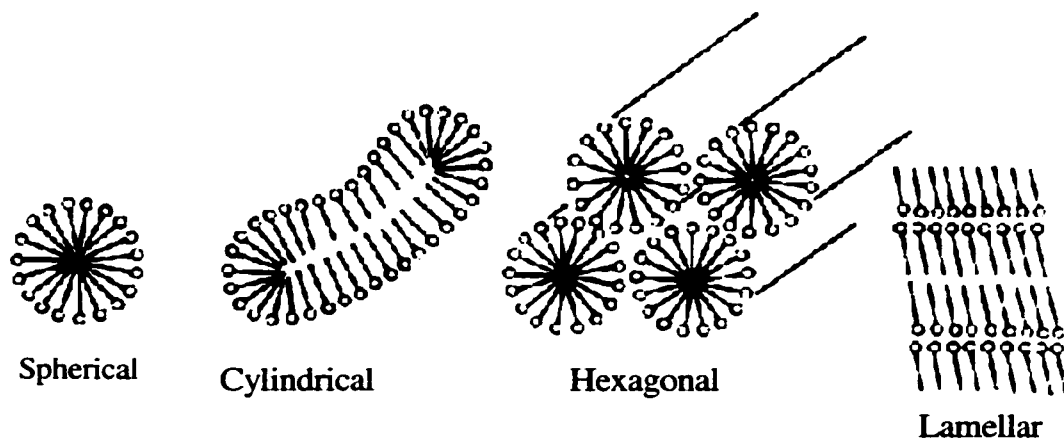


Figure 9.13 Morphology of biosurfactants (adapted from Vinson et al., 1989)

The results from test series 4 showed that under the electric field, the behaviour of bio-micelles seems to be related to the kinetics of bio-micelles formation and transformation. The recognition of this behaviour highlights understanding the fate of bio-micelles during the soil bio-electrokinetic remediation. The factors that can influence the formation of bio-micelles are discussed as follow:



I. Intermolecular forces controlling micelle formation: The forces that hold surfactants in micelles and bilayers are not strong covalent or ionic bonds due to the same surface charged headgroups. However, it can be caused by weaker van der Waals attraction, hydrophobic interaction, hydration forces, and electrostatic repulsion (Marsh and Phil, 1990). The attractive pressure ( $P_A$ ) between the bilayer surfaces is expressed by:

$$P_A = (H / 6\pi) \left( 1/d_w^3 - 2/(d_w + d_l)^3 + 1/(d_w + 2d_l)^3 \right) \quad 9.1$$

where:

H: effective London-Hamaker coefficient  
 $d_w$ : the separation distance of the two surfaces  
 $d_l$ : the bilayer thickness

Therefore, the bilayer thickness increases, which could cause a dramatic decrease of attractive force. However, the van der Waals force between bilayers is fairly weak and has an effective range of at most 15 nm. The attractive hydrophobic interaction between hydrocarbon molecules in water is prevalent over a long range and is much stronger than van der Waals attraction.

Repulsive hydration forces arise with the range of 1-3 nm whenever water molecules bind strongly to hydrophilic surface groups. The hydration forces can be given by the repulsive pressure ( $P_H$ ):

$$P_H = P_o \exp(-d_w / \xi) \quad 9.2$$

Here,  $\xi$  is correlation length, which is in the short range, approximately 0.2 to 0.3 nm. This value in soil could be even smaller. In the case of charged bilayers, the electrostatic repulsive pressure ( $P_e$ ) in an ion-free medium is expressed by:

$$P_c = [2kT / (A_c d_w)] [e^2 / (4\epsilon\epsilon_0 kT)] [d_w / A_c]$$

9.3

where,  $A_c$  is the area per charge,  $\epsilon$  is the dielectric constant of the medium. In solution, these forces work together to effect the formation of the bilayers. They are very sensitive to the distance of bilayers, and change of environmental factors, such as electrolyte in the system, pH and surface charge density.

- II. Energy requirement: Addition of phenanthrene into the bulk of surfactants, hydrophobic energy can transfer it from water into micelles. For an alkane chain of radius 0.2 nm and an interfacial energy with water of 50 mJ/m<sup>2</sup>, the hydrophobic energy per unit length will be  $6 \times 10^{-11}$  J/m. Since the CH<sub>2</sub>-CH<sub>2</sub> distance along a chain is 0.126 nm, hydrophobic energy corresponds to  $8 \times 10^{-21}$  J per CH<sub>2</sub> group added to the chain (Jacob, 1992). In this research, where rhamnolipids were used, the total hydrophobic energy therefore is  $1.28 \times 10^{-19}$  J.

When there are strong repulsive forces between the initially small spherical micelles, with increasing biosurfactant concentration, the micelles are forced to come closer together, which is energetically unfavourable. However, if the biosurfactants rearrange to form an ordered array of cylinders and a stack of bilayers, their surfaces can be spread. Therefore, the formation of cylinder and lamellar micelles are energetically favourable.

- III. pH value in the environment: The morphology of bio-micelles can be significantly impacted by pH. Champion et al. (1995) stated that the morphology of rhamnolipid was a function of pH, changing from lamellar, to vesicular, and afterwards to micellar as pH increased from 5.5 to 8.0 monitored by cryo-transmission electron microscopy. The data showed that large lamellar sheets

predominated at pH 5.5. The reported  $pK_a$  for rhamnolipid is 5.6 (Ishigami, 1987). Thus, as the pH increase from 5.5 to 8.0, the negative charge of the polar head of the rhamnolipid increases. As the headgroup becomes more charged, the repulsive forces between adjacent polar head will effectively create a large head diameter, causing the observed progression in morphology from bilayer sheets to vesicles and subsequently to spherical micelles (Champion et al., 1995).

Previous work (Elektorowicz et al., 1995a), performed in electrokinetic cells, showed that at the first 48 hours, the measured value of pH in the anode is was between 3.0-5.0, around 7.3 in the middle, and close to 8.5 in the cathode, where the ratio of soil to water was 1:10. After 48 hours, the values of pH measured in the middle were practically 7.5 and stable. It could be assumed that the formation of micelles in the middle site of cell should have the favourable structure of bilayers at the beginning of testing. The redox reaction causes the change of pH in the electrode areas. The negatively charged micelles would be formed as bilayers at the anode area and transported by electroosmosis to the middle point. On the other hand, the bilayers would be de-fused by the increase of pH near the cathode area. Consequently, the formation of spherical micelles could occur.

IV. Biosurfactant concentration: The biosurfactant concentration also affects the transformation of micelles. When the lower concentration changes to higher concentration, the spherical micelles can form cylindrical and laminar micelles (Mitchell and Ninham, 1981). In this research, due to the transport of the bio-

micelles by electroosmotic flow and electrophoresis, a change occurs in the shape via the enhanced aggregation and coalescence process.

- V. Temperature: There are no consistent conclusions regarding temperature affecting the formation of micelles. An increased temperature causes disruption of the structured water environment, which disfavours micellization. On the other hand, an increase in temperature decreases hydration of the hydrophilic head group, increasing the ability of micellization. Rosen (1978) pointed out that the micelle formation was found to be an exothermic process, favoured by a decrease in temperature. In addition, CMC seemed to reach a minimum for ionic surfactants at about 25 °C. In the described experiment, the temperature was 25 °C and stable.
- VI. Chemical structure: Biosurfactants (rhamnolipids), which cannot form into compact spherical micellar structures, generally could form vesicles and extended lamellar bilayers due to their chemical structure. In order to assemble into spherical micelles, molecular optimal surface area  $A_0$  must be sufficiently large and their hydrocarbon volume  $V$  small enough so that the radius of the micelle  $R$  will not exceed the critical chain length  $L_c$ . Suppose the biosurfactant molecule is depicted in Figure 9.14.

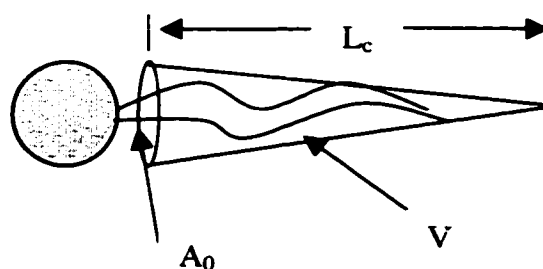


Figure 9.14 Schematic representation of biosurfactant molecule (adapted from Jacob, 1992)

In the case of the rhamnolipids, used in this research, with two 8-carbon chains, the number of molecules in one micelle  $M$  found experimentally is 50. Using Jacob's equations 9.1 to 9.4(1992), placing  $n=8$ , gives the hydrocarbon volume  $V \approx 0.24 \text{ nm}^3$ . Therefore, the optimal micelle radius is  $R = 1.43 \text{ nm}$ , and  $L_c \approx 1.12 \text{ nm}$ , which is  $0.31 \text{ nm}$  shorter than the optimal radius.

$$L_c \leq L_{\max} \approx (0.154 + 0.1265n) \quad 9.1$$

$$V \approx (27.4 + 26.9n) \times 10^{-3} \quad 9.2$$

$$M = 4\pi R^2 / a_0 = 4\pi R^3 / 3V \quad 9.3$$

hence,

$$\frac{V}{A_0 L_c} > \frac{1}{3} \quad 9.4$$

For rhamnolipids, used in the experiment,  $V/A_0 L_c \approx 0.41$ . Mitchell and Ninham (1981) have found that for spherical micelles  $V/A_0 L_c$  is less than  $1/3$ , for cylindrical micelles  $1/3 < V/A_0 L_c < 1/2$ , for lamella or vesicles  $1/2 < V/A_0 L_c < 1$ . It means that rhamnolipids just cannot pack into spherical micelles, and therefore must be in the shape of cylindrical or bilayer micelles. This is confirmed by Champion et al. (1995), who stated that the most likely form for rhamnolipid aggregates are cylindrical micelles or vesicles. Typically, a vesicle has a diameter between 30-100 nm.

On the other hand, the bilayer-forming surfactant increases the lifetime of the molecules within aggregates. Wennerstrom and Lindman (1979) had found that typical lifetime for surfactants in micelles is  $10^{-4}$ s, and in bilayers is  $10^{+4}$ s,

which is 8 orders of magnitude higher. Concerning the stability of the bilayer structure with time, the vesicles fuse, form clusters, and finally coagulate (Ghosh et al, 1998). In the case of no-stressed bilayers, the hydrophilic headgroups “shadow” the hydrocarbon groups from the aqueous phase into the core of micelles. In this experiment, when bilayers are stressed by means of electric field across them, they expand laterally, and this increases the hydrophobic area exposed to the aqueous phase. This may be the primary cause of bilayer fusion, which is also confirmed by Jacob (1992). These bilayers are dynamic structures in which the component can move around relatively freely.

In summary, all above-mentioned factors have to be considered in order to describe the formation process of bio-micelles under the electric field. The favorable form of rhamnolipids is bilayers (including cylindrical, lamellar, and vesicle). The change of pH can cause the transformation of bio-micelles. When bilayers are stressed by applying electric field across them, they tend to form bilayers and fuse together. Since these bilayers move around freely, the electroosmotic flow and electrophoresis can transport them, resulting in the change of the concentration of rhamnolipids, which eventually affect on the formation of bio-micelles.

Image analysis by using AFM provided the solid confirmation of the above discovered bio-micelles formation. At pH of 7.5, the image of aggregation of bio-micelles (phenanthrene/biosurfactants) is shown in Figure 9.15. The diameter of vesicular type of biosurfactants obtained from the image was approximately 200 nm with a height of height of 50 nm. Figure 9.16 shows aggregation of vesicles to form the bilayers with a

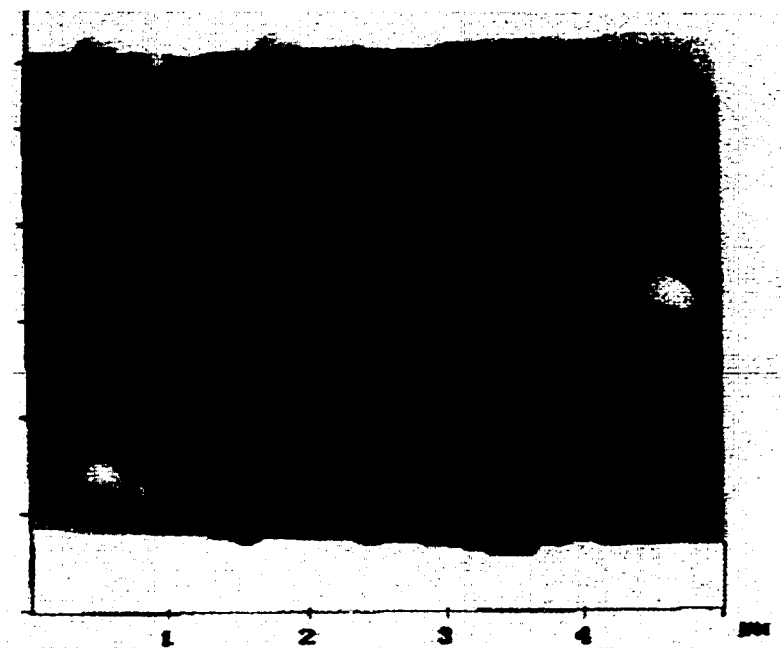


Figure 9.15 Image of vesicular micelles by AFM with scan rate of 1.001 Hz, scan size of 5.00  $\mu\text{m}$  and data scale of 50.00 nm

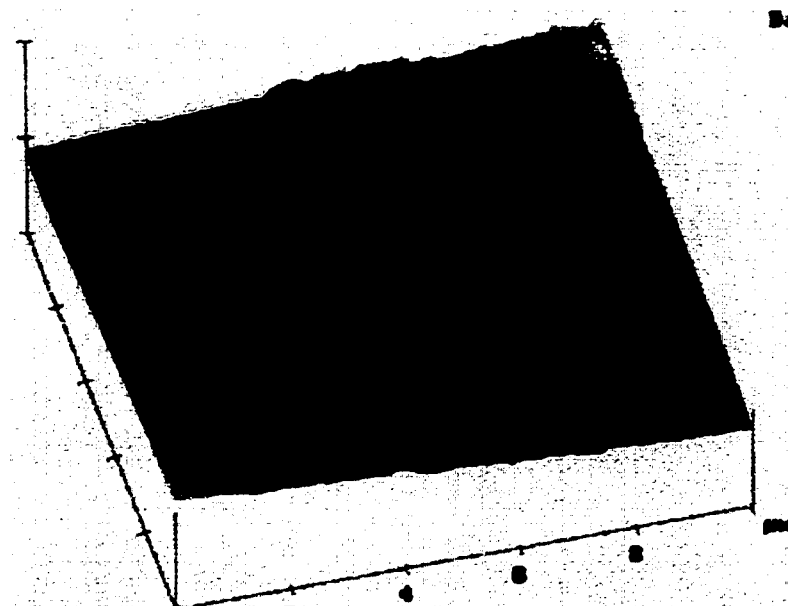


Figure 9.16 Image of bilayer micelles by AFM with scan rate of 1.001 Hz, scan size of 10.00  $\mu\text{m}$  and data scale of 200.0 nm



Figure 9.17 Image of clayey soil by AFM with scan rate of 1.001 Hz, scan size of 5.00  $\mu\text{m}$  and date scale of 2.00  $\mu\text{m}$

height of 200 nm. The Figure 9.17 presents the image of clayey soil used for this research. The image analysis allows to measure the size of various particles and the porosity of specimen. The distribution of bio-micelles on the clay particles is also visible.

### **9.2.2 Kinetic approach to the fate of bio-micelles**

Following the above-mentioned discussion, the process of formation of bio-micelles, desorption of phenanthrene from soil, and transport of phenanthrene must be seen as a kinetic process. Phenanthrene in such a system is hypothesized to be distributed among three separate physical phases: the soil, the micellar pseudophase, and the aqueous pseudophase. Phenanthrene in the soil phase is sorbed, and the micellar pseudophase are



solubilized in the hydrophobic interiors of the anionic bio-micelles, while in the aqueous pseudophase they are freely dissolved.

It is hypothesized that there are six general processes in the soil-water-phenanthrene-biosurfactant system under an applied electric field: 1) Phenanthrene sorption on soil; 2) Partial biosurfactant sorption onto the soil; 3) Bilayer-micelle or spherical micelle formation; 4) Partition of phenanthrene into micelles; 5) Transport of phenanthrene into the aqueous phase; 6) Transport of bio-micelles with phenanthrene via electroosmotic processes. The kinetics of partitioning of phenanthrene into the micelles at cathode, between electrodes, and at anode areas are proposed in Figure 9.18, Figure 9.19 and Figure 9.20, respectively.

Having the same charge as clayey soil, repulsion makes the sorption between biosurfactant and clayey soil difficult. However, the sorption of phenanthrene and biosurfactants can be caused by the presence of 2.3% organic matter in the soil sample. Aliphatic side chains and lignin groups in humic substances (one of main components of organic matter) are highly hydrophobic (Senesi and Chen, 1989). Therefore, phenanthrene may be adsorbed through hydrophobic interaction with the soil organic matter. When the biosurfactant is added into the bulk of the soil, its hydrophobic portion will have a tendency to sorb onto soil organic matter. Alternatively, the hydrophilic portion of biosurfactant can line up on the surface of wetted clayey mineral. Generally, when the concentration of biosurfactants exceeds above the CMC, biosurfactant molecules may also interact with other biosurfactant molecules to form bio-micelles

Due to the high values of  $K_{ow}$ , phenanthrene has an affinity for the hydrophobic portion of biosurfactants, and prefers to be retained in the interior of the bio-micelles,

which contain the hydrophobic portion of the biosurfactants inside the core. In this manner, it can prevent phenanthrene from re-adsorbing onto the soil. From the analysis of FTIR spectra in test series 4, the phenanthrene content in the bottom layers of cell T4C2 was much lower than the bottom layers of cell T4C3, as the experiment progressed. The amount of phenanthrene increased in the aqueous phase (Figure 9.11). It clearly shows that the increase of phenanthrene in the aqueous phase is mainly a result of incorporation with different forms of micelles according to pH conditions and electrokinetic transport.

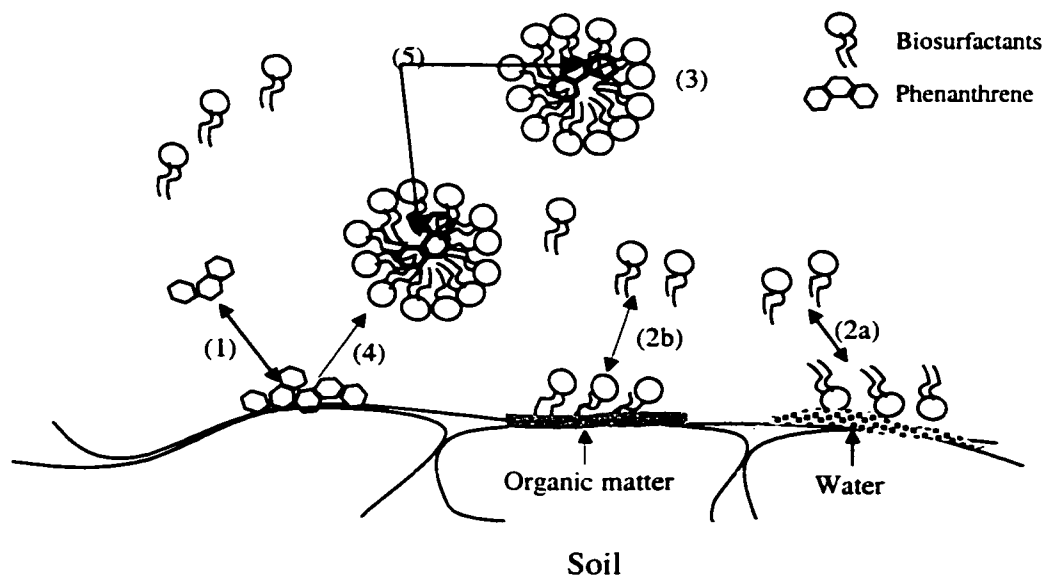
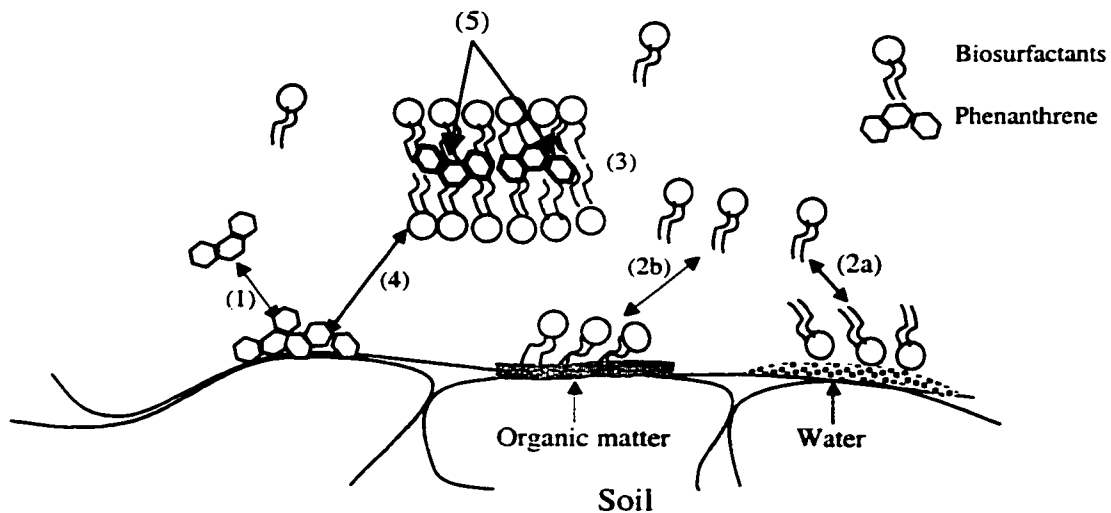


Figure 9.18 Conceptual representation of the process related to the partitioning of phenanthrene and biosurfactants at the cathode region (at pH of 8.0)

- (1) Phenanthrene sorption on soil
- (2) Biosurfactant sorption on wetted mineral (2a) and organic matter (2b)
- (3) Spherical micelles formation
- (4) Phenanthrene partition into micelles
- (5) Phenanthrene transport into aqueous phase



**Figure 9.19** Conceptual representation of the process related to the partitioning of phenanthrene and biosurfactants in the middle of electrokinetic cell (at pH of 7.5)

- (1) Phenanthrene sorption on soil
- (2) Biosurfactant sorption on wetted mineral (2a) and organic matter (2b)
- (3) Cylindrical or bilayer-micelles formation
- (4) Phenanthrene partition into micelles
- (5) Phenanthrene transport into aqueous phase

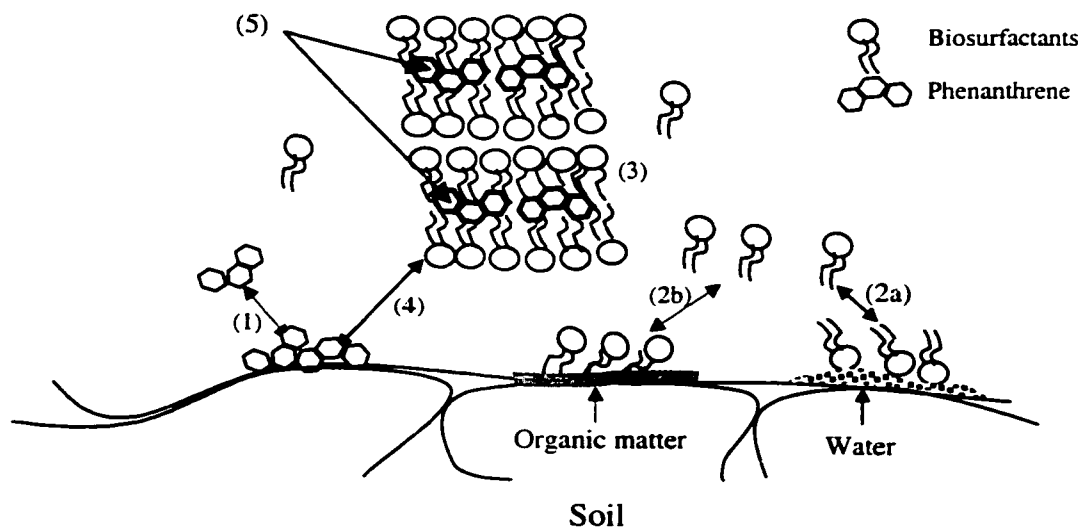


**Figure 9.20** Conceptual representation of the process related to the partitioning of phenanthrene and biosurfactants at the anode area (at pH of 5.0)

- (1) Phenanthrene sorption in soil
- (2) Biosurfactant sorption on wetted mineral (2a) and organic matter (2b)
- (3) Bilayer-micelles formation
- (4) Phenanthrene partition into micelles
- (5) Phenanthrene transport into aqueous phase

Under the electric field, the partitioning of phenanthrene into the micelles should take different conditions into consideration. As discussed above, the change of pH has a very important impact on the transformation of biosurfactant morphology. Due to the redox reaction at the electrode area, the low value of pH at the anode is favorable to the formation of lamellar micelles, and the high value of pH at the cathode is favorable to form spherical micelles. In the middle of the electrokinetic cell, biosurfactants likely formed bilayers in the aqueous system.

Consequently, the favourable bilayer structure was formed spontaneously during the first phase (Figure 9.2), due to the special morphology of rhamnolipids, as described in Chapter 9.2.1. This was also seen on the AFM micrograph (Figure 9.15). It showed relatively higher values of relative optical density. After that, the formation of micelles decreased slightly with time. It could be due to the change of pH environment in the system, created by redox reactions at the electrode area or weakening certain forces (Chapter 9.2.1). Due to the negatively charged properties of bio-micelles, they can be transported via electrokinetic processes. The negatively charged micelles will be formed as bilayers at the anode area. On the other hand, the bilayers will be de-fused by an increase in pH, and transported towards the anode area (electrophoresis). It was observed that the value dramatically increased four times (Figure 9.3 and Figure 9.6) after 11 hours of experiment. At the 14<sup>th</sup> hour, the amount of micelles achieved the maximum. This is the critical point for the aggregation of spherical and vesicular micelles to bilayers. It represents the presence of largest multi-lamellar bilayers due to coalescence (seen Figure 9.16). Passing this point, the bilayer micelles began to form the stable and favorable

structures. In the final stage, the bio-micelles became stable flocs in the system (Figure 9.4 and Figure 9.6).

Due to the presence of clayey particles in cell T4C2, the pattern of formation of bio-micelles was different. At the first 17 hours, since the clayey particles are negatively charged, they would be transported towards the anode due to electrophoresis under the electric field. Settling of clayey particles occurred simultaneously. Therefore, the initial phase is destabilized by the presence of the clayey particles. The mobility of headgroups of rhamnolipids, which tend to form the micelles, decrease due to interactions with the clayey particles (Figure 9.8). The biggest transition occurred between 17 and 20 hours (Figure 9.9). It indicated that the transformation of micelles to bilayers was attenuated and deferred by the involvement of clayey particles and required a longer time to aggregate the multi-lamellar bilayers. At the last stage, shown in Figure 9.9 and Figure 9.12, the formation of bilayers tends to stability.

In summary, due to the influence of the electric field, the transformation of bio-micelles changed with time. The time and type of clayey mineral should be taken into consideration in order to understand the process of bio-micelle formation. The electric field clearly is another important factor, which can have a profound impact on the formation of bio-micelles. The formation of different types of bio-micelles plays a crucial role in the biosurfactant-enhanced electrokinetic remediation technique.

## **CHAPTER 10 CONCLUSIONS AND RECOMMENDATIONS**

This thesis focuses on the enhancement of standard electrokinetic methodology through the use of biosurfactants, for the remediation of natural clayey soils contaminated with phenanthrene. A four test series and application of new techniques of FTIR, AFM, and SFE analysis were performed. The conclusions from the experiments are presented below.

### **10.1 Conclusions**

Electrokinetic test series 1 showed that clay materials provide an adequate habitat for bacterial survival under an electric field. The average moisture content in soil was controlled and reached approximately 40%, which provided the required moisture condition for the bacterial survival. The pH value in the phenanthrene-contaminated soil had 7.1 almost across the entire soil, suitable for bacterial growth. It is postulated that the oxidation process was modified by the presence of the contaminant. Near the cathode area, the pH was as high as 10.0. In this region, the number of bacteria dropped to around 1.5 log CFU/soil dry wt. in the non-contaminated soil and was undetectable in the contaminated soil. This low number could be associated with a potential transport of bacteria towards the anode area. This experiment demonstrated that when a low electric current is applied into phenanthrene contaminated clayey soil, bacteria could multiply in an amount sufficient (up to 7.6 log CFU/g soil dry wt.) to incite the process of secretion of extracellular substances (biosurfactants). This allows bacteria to uptake phenanthrene as a sole carbon source.

Electrokinetic test series 2 confirmed the hypothesis from test series 1. It was shown that *in-situ* production of biosurfactants by bacteria under the electric field was feasible. In both cells (containing contaminated soil and soil free of phenanthrene), the electrical gradient was uniformly distributed. The highest resistance was presented near the anode area. The moisture content in the soil after the test ranged between 46% (for the soil free of phenanthrene) and 51% (for the contaminated soil). This level provides a good condition for bacterial growth. At the end of experiment, the pH value near the anode area in the contaminated soil was 6.2, which was twice higher than that in the soil free of phenanthrene. This condition allowed for normal metabolism with an amount of 6.8 log CFU/g soil dry wt. bacteria in contaminated soil. The pH near the cathode was 10.0 in both cells. The measured number of bacteria found, in this region, was approximately 2.0 log CFU/g soil dry wt. The highest amount of rhamnolipids production occurred in the central area of the electrokinetic cells. The production of rhamnolipids was enhanced in the presence of phenanthrene. Due to the produced rhamnolipids, the 85% removal efficiency was achieved near the cathode area during the 14-day test. Production of biosurfactants *in-situ* demonstrated the feasibility of a new hybrid method: bio-electrokinetics.

The augmentation of the biosurfactant content in the electrokinetic cells performed by test series 3, presented the feasibility of biosurfactant transport in clay materials using a DC electric field. The existing electrical gradient in all testing cells showed the possibility of the species transport via electroosmosis and electrophoresis. These phenomena caused the uniform distribution of biosurfactants. The introduction of biosurfactants decreased the resistance of the soil specimens. It could cause a higher

electroosmotic flow to the cathode area. The average moisture content in this series test ranged between 39 % and 48 %. The distribution of a low concentration biosurfactant (2.5 lower than the CMC) was uniform. The development of a biosurfactant profile was due to the involvement of electroosmotic and electrophoretic phenomena. In the case of a high concentration biosurfactant (3 times higher than the CMC), the amount of biosurfactants in the contaminated soil near the cathode area was approximately 7 times higher than that near the anode area. The accumulation of biosurfactants close to the cathode can be as a result of electroosmotic flow being dominant over electrophoresis. Removal of phenanthrene was twice higher (74%) in the case of a high concentration of biosurfactants after 8 days of testing.

Research showed that the efficiency of phenanthrene removal from clayey soil is associated with the formation of bio-micelles. The transformation of bio-micelles under the electric field has been investigated in the association with influential factors, such as inter molecular forces, pH, and chemical structure, etc. The results of test series 4 confirmed that the favorable structure of rhamnolipids was bilayers. Under the electric field, the transformation from cylindrical to lamellar, and subsequently to spherical micelles, occurred as pH changed from anode to cathode area. Transformation of biosurfactants also varied with time, due to electroosmotic and electrophoretic phenomena. At the beginning, the favorable structure of bilayer micelles was formed. Under the influence of the electric field, the second phase showed the spontaneous formation of multi-lamellar layers due to coalescence. Finally, a stable and favorable structure of bio-micelles was formed. In the case of the presence of clayey particles, this kinetic process was attenuated and deferred, but the transformation process of bio-



micelles was still observed. The understanding of the kinetic bio-micelle formation process is very important to the accurate application of biosurfactants for electrokinetic remediation of PAH contaminated clayey soil.

To date, biological surfactants remain untested for their ability to mobilize contaminants in a multiphase soil environment. The enhancement of electrokinetics for application to contaminated clayey soil, as presented by the author, represents a first and unique achievement. The achieved objective of this study permitted the development of a new methodology called bio-electrokinetics, which is expected to make the remediation of contaminated clayey soil *in situ* possible.

## **10.2 Recommendations**

Some recommendations for future research derived from this thesis are:

- Soils with a higher concentration of phenanthrene (in the range of 1,000 to 200,000 mg/kg soil) and other PAHs' candidates should be tested in order to evaluate the limit of biosurfactant application by means of bio-electrokinetics.
- The control of the pH conditions at both electrode areas, especially at the cathode area should be further investigated in order to improve the metabolism of bacteria under the electric field.
- The enhancement of phenanthrene production *in-situ* need to be tested further in order to enhance the efficiency of biosurfactants up to 99% under the electric field. The techniques such as washing system and electrokinetic introduction of nutrients could be combined.

- Different concentrations of rhamnolipids or other types of biosurfactants, such as sophorolipids and trehalose dimycolates, should be tested for their applicability into the electrokinetic process.
- The biodegradation rate of phenanthrene may be studied to obtain a true understanding of the overall remediation process.

## REFERENCES

- Abdul, A. S., Gibson, T. L., Ang, C. C., Smith, J. C. and Sobczynski, R. E. (1992) *In situ* surfactant washing of polychlorinated biphenyls and oils from a contaminated site. *Ground Water*, **30**:219-231.
- Abdul, A. S. and Ang, C. (1994) *In situ* surfactant washing of polychlorinated biphenyls and oils from a contaminated field site: phase II pilot study. *Groundwater*, Vol. **32**, No.5.
- Abu-Ruwaida, A. S., Banat, I. M., Haditirto, S. and Khamis, A. (1991) Nutritional requirements and growth characteristics of a biosurfactant producing *Rhodococcus* bacterium. *World Journal of Microbiological biotechnology*. **7**:53-61.
- Abu-Ruwaida, A. S., Banat, I. M., Haditirto, S., Salem, S. and Kadri, M. (1991) Isolation of biosurfactant producing bacteria-product characterization and evaluation. *Acta Biotechnology*, **11**: 315-324.
- Acar, Y. B., Li, H. and Gale, R. J. (1992) Phenol removal from kaolinite by electrokinetics. *Journal of geotechnology engineering*, ASCE, **118**(11):1837-1852.
- Acar, Y. B. and Alshawabkeh, A. N. (1993) Principles of electrokinetic remediation. *Environmental Science and Technology*, **27**:2638-2647.
- Acar, Y. B., Alshawabkeh, A. N. and Gale, R. J. (1993) Fundamental aspects of extracting species from soils by electrokinetics. *Waste management*, **12**:1410-1421.
- Acar, Y. B., Hamed, J. T., Alshawabkeh, A. N. and Gale, R. J. (1994) Removal of cadmium (II) from saturated kaolinite by the application of electric current. *Geotechnique*, **44**:239-254.

- Acar, Y. B. and Alshawabkeh, A. N. (1995) Electrokinetic remediation – multicomponent species transport in soils under an electric field. *Electrochemical society proceedings*, **12**:219-223.
- Acar, Y. B., Gale, R. J., Alshawabkeh, A. N., Marks, R. F., Puppala, S., Bricka, M. and Parker, R. (1995) Electrokinetic remediation: basics and technology status. *Journal of Hazardous Materials*, **40**:117-137.
- Acar, Y. B. and Alshawabkeh, A. N. (1996) Electrokinetic remediation. I: Pilot-scale tests with lead-spiked kaolinite. *Journal of Geotechnical Engineering - ASCE*, **122**:173-185.
- Al-Awadhi, N., Williamson, K. J. and Isok, J. D. (1994) Remediation of Kuwait's oil-contaminated soils. In: *Hydrocarbon Contaminated Soils and Groundwater*, KostECKI, P. T., Calabrese, E. J., Eds., Michigan, USA: Lewis Publisher, **3**:9-21.
- Alshawabkeh, A.N. and Acar, Y. B. (1996) Electrokinetic Remediation. II: Theoretical Model. *Journal of Geotechnical Engineering - American Society of Civil Engineers*, **122**(3): 186-197.
- Appelo, C. A. J. and Postma, D. (1993) *Geochemistry, groundwater and pollution*. Balkema, Rotterdam, Netherlands.
- Aronstein, B. N. and Alexander, M. (1993) Effect of a non-ionic surfactant added to the soil surface on the biodegradation of aromatic hydrocarbons within the soil. *Applied Microbiology and Biotechnology*, **39**(3):386-390.
- Aronstein, B. N., Calvillo, Y. M. and Alexander, M. (1993) Effect of surfactants at low concentrations on the desorption and biodegradation of sorbed aromatic compounds in soil. *Environmental Science & Technology*, **25**(10):1728-1731.

- Ashok, B. T. and Saxena, S. (1995) Biodegradation of polycyclic aromatic hydrocarbon – A review. *Journal of scientific & industrial research*, **54**:443-451.
- Bai, G., Brusseau, M. L. and Miller, R. M. (1997) Biosurfactant-enhanced removal of residual hydrocarbon from soil. *Journal of Contaminant hydrology*, **25**:157-170.
- Banat, I. M. (1995a) Characterization of biosurfactants and their use in pollution removal -- state of the art (review). *Acta Biotechnologica*, **15** (3):251-267.
- Banat, I. M. (1995b) Biosurfactants production and possible uses in microbial enhanced oil recovery and oil pollution. *Bioresource Technology*, **51**(1):1-12.
- Bruell, C. J., Segall, B. A. and Walsh, M. T. (1992) Electroosmotic removal of gasoline hydrocarbons and TCE from clay. *Journal of Environmental Engineering, ASCE*, **118**:68-83.
- Burger, M. M., Glaser, L. and Burton, R. M. (1963) Enzymatic synthesis of a rhamnose-containing glycolipid by extracts of *Pseudomonas aeruginosa*. *Journal of Biological chemistry*, **238** (8): 2595-2602.
- Casagrande, L. (1949) Electroosmosis in soil. *Geotechnique*, **1**(3):159.
- CCME (1991) Canada Council of Ministers of the Environment: Interim Canadian environmental quality criteria for contaminated sites. Report CCME EPC-CS3, Winnipeg, Manitoba, Canada.
- Cerniglia, C. E. and Yang, S. K. (1984) Stereoselective metabolism of anthracene and phenanthrene by the fungus *Cunninghamella elegans*. *Applied and Environmental Microbiology*, **47**:119-124.
- Cerniglia, C. E. (1984) Microbial metabolism of polycyclic aromatic hydrocarbon. *Advances in applied microbiology*, **30**:31-71.

- Cerniglia, C. E. and Heitkamp, M. A. (1989) Microbial degradation of polycyclic aromatic hydrocarbons in the aquatic environment. In: *Metabolism of polycyclic aromatic hydrocarbons in the aquatic environment*, Varanasi, U. Ed., CRC Press, Boca Raton, FL, U. S. A., p 41-68.
- Cerniglia, C. E. (1992) Biodegradation of polycyclic aromatic hydrocarbons. *Biodegradation*. **3**: 351-368.
- Champion, J. T., Gilkey, J. C., Lamparski, H., Retterer, J. and Miller, R. M. (1995) Electron microscopy of rhamnolipid (biosurfactant) morphology: effects of pH, cadmium, and octadecane. *Journal of colloid and interface science*, **170**:569-574.
- Chandrasekaran, E. V. and Bemiller, J. N. (1980) Constituent analyses of glycosaminoglycans, In: *Methods in carbohydrate chemistry*, Whistler, R. L. Ed., Academic Press, Inc., New York, p 89-96.
- Characklis, W. G. (1984) Biofilm development: a process analysis. In: *Microbial adhesion and aggregation*, Marshall, K. C. Ed., Dahlem Konferenzen, Springer-Verlag, p 137-157.
- Cheng, K. J., Ingram, J. D. and Costerton, J. W. (1970) Release of alkaline phosphatase from cells of *Pseudomonas aeruginosa* by manipulation of cation concentration and of pH. *Journal of Bacteriology*, **104**:748-753.
- Cookson, J. T. (1995) *Bioremediation engineering: design and application*. McGraw-Hill, Inc. U. S. A.
- Choudhury, A. and Elektorowicz, M. (1997) Enhanced electrokinetic methods for lead and nickel removal from natural clayey soil. *32<sup>nd</sup> Central symposium on water pollution research*, Burlington, ON.

- Das, B. M. (1994) Principles of geotechnical engineering. 2<sup>nd</sup> edition, PWS publishing company, Boston.
- DeFlaun, M. F. and Condee, C. W. (1997) Electrokinetic transport of bacteria. *Journal of Hazardous Materials*, **55**:263-277.
- Deziel, E., Paquette, G., Villemur, R., Leqine, F. and Bisailon, J. (1996) Biosurfactant production by a soil Pseudomonas strain grown on polycyclic aromatic hydrocarbons. *Applied and Environmental Microbiology*, **62**:1908-1912.
- Dibble, J. T. and Bartha, R. (1979) Effect of environmental parameters on the biodegradation of oil sludge. *Applied and Environmental Microbiology*, **37**: 729-739.
- Edwards, D. A., Luthy, R. G. and Liu, I. (1991) Solubilization of polycyclic aromatic hydrocarbons in micellar nonionic surfactant solutions. *Environmental Science & Technology*, **25**(1): 127-142.
- Elektorowicz, M., Chifrina, R. and Konyukhov, B. (1995a) Enhanced removal of diesel fuel from soil by electrokinetic method. *30<sup>th</sup> Central Canadian Symposium on Water Pollution Research*, Burlington ON.
- Elektorowicz, M. (1995b) Bio-electrokinetic removal of petroleum products from the soil in northern territories. *Joint US/Canada Military and Civilian Workshop On Techniques and Technologies for Hydrocarbon Remediation in Cold and Arctic Climates*, Kingston.
- Elektorowicz, M. and Boeva, V. (1996) Electrokinetic supply of nutrients in soil bioremediation. *Environmental Technology*, **17**:1339-1349.

- Elektorowicz, M. and Hatem, G. (1999) Design of the electrokinetic system to supply surfactants in pilot-scale conditions. In: 2<sup>nd</sup> symposium on Heavy metals in the environment and electromigration applied to soil remediation, Denmark.
- Elektorowicz, M., Jahanbakhshi, P., Chifrian R., Hatim J. and Lombardi, G. (1996) Phenol removal from groundwater using electrokinetics. *International Conference on Municipal and Rural Water supply and Water Quality*, Poznan, Poland, 2: 105-116.
- Elektorowicz, M. and Ju L. (1997) Accuracy of PAHs' extraction from sensitive clays using the SFE ISCO system. CSCE-ASCE, *Environmental Engineering Conference*, Edmonton, Alberta, Canada, p531-541.
- Elektorowicz M., Ju L., Smaragiewicz, W. and Dube, L. (1999) Behavior of biosurfactant-producing bacteria upon the application of electrokinetics. 27<sup>th</sup> Annual CSCE-ASCE Environmental Engineering Conference, Regina, Saskatchewan, Canada.
- Elektorowicz, M., Ju, L. and Oleszkiewicz, J.A., (1999) Bioavailability of xenobiotic organic compounds to remediate soil containing clay fractions-Limits of engineering solutions. In: Bioavailability of organic xenobiotics in the environment and practical consequences for bioremediation, edited by Block, J.C., Baveye, P., Goncharuk, V. V., Kluwer Scientific publishers, U.S.A, p349-376.
- Ellis, W. D., Payre, J. R. and McNabb, G. D. (1985) Treatment of contaminated soils with aqueous surfactants. EPA/600/2-85/129.
- El-Nawawy A. S., El-bagouri, I. H., Abdal, M. and Khalafawi, M. S. (1992), *World Journal of Microbial Biotechnology*, 8:618.



- Evangelou, V. P. (1998) Environmental soil and water chemistry: principles and applications. John Wiley & Sons, Inc., U. S. A.
- Farmer, V. C. and Russel, J. D. (1967) Infrared absorption spectrometry in clay studies.
- Fietcher, A. (1992) Biosurfactants: moving towards industrial application. *Trends Biotechnology*, **10**:208-217.
- Fountain, J. C., Klimek, A. and Middleton, T. M. (1991) The use of surfactant for in-situ extraction of organic pollutants from a contaminated aquifer. *Journal of Hazardous Materials*, **28**:295-311.
- Francy, D. S., Thomas, J. M., Raymond, R. L. and Ward, C. H. (1991) Emulsification of hydrocarbons by subsurface bacteria. *Journal of Industrial Microbiology*, **8**:237-246.
- Galameau, A., Renzo, F. D., Fajula, F., Mollo, L., Fubini, B. and Ottaviani, M. F. (1998) Kinetics of formation of micelle-templated silica mesophases monitored by electron paramagnetic resonance. *Journal of colloid and interface science*, **201**:105-117.
- Ghisalba, O. (1983) Microbial degradation of chemical waste, an alternative to physical methods of waste disposal. *Experientia*, **39**:1247-1257.
- Ghosh, P., Sengupta, S. and Bharadwaj, P. K. (1998) Synthesis and characterization of a new generation of cryptand-based triple-tailed amphiphiles: spontaneous formation of vesicles and x-ray crystallographic studies. *Langmuir*, **14**:5712-5718.
- Grosser, R. J., Warshawsky, D. and Kinkle, B. K. (1994) The effects of fulvic acids extracted from soils on the mineralization of pyrene by an isolated *Mycobacterium*

- spp.* Proceeding 9<sup>th</sup> annual conference of hazardous waste remediation. Erickson, L. E. Ed., p309-321.
- Guerra-Santos, L., Kappeli, O. and Fiechter, A. (1986) Dependence of *Pseudomonas aeruginosa* continuous culture biosurfactant production on nutritional and environmental factors. *Applied Microbiology and Biotechnology*, **24**:443-448.
  - Guha, S. and Jaffe, P. R. (1996) Biodegradation kinetics of phenanthrene partitioned into the micellar phase of nonionic surfactants. *Environmental Science & Technology*, **30**(2): 605-611.
  - Hamed, J., Acar, Y. B. and Gale, R. J. (1991) Pb (II) removal from kaolinite using electrokinetics. *Journal of Geotechnology Engineering, ASCE*, **112**:241-271.
  - Hamed, J. and Bhadra, A. (1997) Influence of current density and pH on electrokinetics. *Journal of Hazardous Materials*, **55**:279-294.
  - Harvey, S., I., Eiashvili, J. J., Valdes, D., Kamely, A. and Chakrabarty, M. (1990) Enhanced removal of Exxon Valdez spilled oil from Alaskan gravel by a microbial surfactant. *Biotechnology/Technology*. **8**:228-230.
  - Hassett J. J., Means J. C., Banwart, W. L. and Wood S. G., Report 1980, EPA-600/3-80-041. Order No. PB 80-189-574, 150.
  - Herman, D. C., Artiola, J. F. and Miller, R. M. (1995) Removal of cadmium, lead, and zinc from soil by a rhamnolipid biosurfactant. *Environmental Science and Technology*, **29**:2280-2285.
  - Hunt, W. P., Robinson, K. G. and Ghosh, M. M. (1994) The role of biosurfactants in biotic degradation of hydrophobic organic compounds. In: Hydrocarbon

bioremediation. Hinchee, R. E., Alleman, B. C., Hoeppe, R. E., Miller, R. N., Eds., Lewis Publishers.

- Hunter, R. J. (1981) Zeta potential in colloid science: principles and applications. Academic Press, London.
- Ishigami, Y., Gama, Y., Nagahora, H., Yamaguchi, M., Nakahara, H. and Kamata, T. (1987) *Chemistry Letter*, p763.
- Keedwell, M. J. (1984) Rheology and soil mechanics. Elsevier Applied Science, U.S.A.
- Keith, L. H. and Telliard, W. A. (1979) Priority pollutants: a perspective view. *Environmental Science & Technology*, **13**: 416-423.
- Keller, R. J. (1986) The sigma library of FT-IR spectra. Sigma Chemical. Company, St. Louis, MO.
- Keuth, S. and Rehm, H. J. (1991) Biodegradation of phenanthrene by *Arthrobacter polycharomogenes* isolated from a contaminated soil. *Applied Microbiology and Biotechnology*, **34**:804-808.
- Kim, S. and Corapciogla, M. Y. (1997) The role of biofilm growth in bacteria-facilitated contaminant transport in porous media. *Transport in porous media*, **26**:161-181.
- Klekner, V. and Kosaric, N. (1993) Biosurfactants for cosmetics, p 329-372. In: Biosurfactants: production, properties, applications. Kosaric, N., Ed., Marcel Dekker, Inc., New York.
- Knox, R. C., Sabatini, D. A. and Canter, L. W. (1993) Subsurface transport and fate processes. Lewis Publishers, Boca Raton, FL.

- Koch, A. K., Kappeli, O., Fiechter, A. and Reiser, J. (1991) Hydrocarbon assimilation and biosurfactant production in *Pseudomonas aeruginosa* mutants. *Journal of bacteriology*, **173**: 4212-4219.
- Kosaric, N., (1993) Biosurfactants-production, properties, applications. Vol. 48, Madison Dekker, Inc., New York.
- Jacob, N. I. (1992) Intermolecular and surface forces. 2<sup>nd</sup> edition, Academic press.
- Jain, D. K., Lee, H. and Trevors, J. T. (1992) Effect of addition of *Pseudomonas aeruginosa* UG2 inocular of biosurfactants on biodegradation of selected hydrocarbons in soil. *Journal of Industrial Microbiology*, **10**:87-93.
- Jarvis, F.G. and Johnson, M. J. (1949) A glyco-lipid produced by *Pseudomonas aeruginosa*. *Journal of the American Chemical Society*, **71**:4124-4126.
- Jenkins, M. B. and Lion, L. W. (1993) Mobile bacteria and transport of polynuclear aromatic hydrocarbons in porous media. *Applied and Environmental Microbiology*, **59**(10):3306-3313.
- Ju, L. and Elektorowicz, M. (1999) Potential production of biosurfactants under electric field supplied to clayey soil. Proceeding of ASCE-CSCE national conference on environmental engineering, Norfolk, Virginia, p612-620.
- Lageman, R. (1989) Theory and practice of electro-reclamation. NATA/CCMS pilot study: Demonstration of Removal Action Technologies for Contaminated Land and Groundwater, Copenhagen, Denmark, May 9, p18.
- Little, L. H., Kiselev, A. V. and Lygin, V. I. (1966) Infrared spectra of adsorbed species. Academic press inc., New York.

- Mahro, B., Eschenbach, A., Kaestner, M. and Schaefer, G. (1994) Investigation of possibilities for targeted stimulation of biogenic mineralization and humification of PAH in soils. *Biological abwasserreinig.* **4**:55-68.
- Manilal, V. B. and Alexander M. (1991) Factors affecting the microbial degradation of phenanthrene in soil. *Applied Microbiology and Biotechnology*, **35**:401-405.
- Marshall, C. E. (1964) The physical chemistry and mineralogy of soils. Vol. 1: Soil materials, John Wiley & Sons, Inc. U. S. A.
- Marsh, D. and Phil, M. A. (1990) CRC handbook of lipid bilayers. CRC Press, Inc. U.S.A.
- Means J. C., Ward, S. G., Hassett, J. J. and Banwart, W. L.(1980), Sorption of polynuclear aromatic hydrocarbons by sediments and soils. *Environmental Science & Technology*, **14**:1524-1528.
- Mihelcic, J. R., Lueking, D. R., Mitzell, R. J., and Stapleton, J. M., (1993) Bioavailability of sorbed- and separate-phase chemicals. *Biodegradation*, **4**(3):141-155.
- Miller, R. M. (1995) Biosurfactant-facilitated remediation of metal-contaminated soils. *Environmental Health Perspectives*, **103**:59-62.
- Mitchell, D. J. and Ninham, B. W. (1981) Micelles, vesicles and microemulsions. *Chem. Soc. Faraday Trans.* **77**:601-629.
- Mitchell, J. K. (1976) Fundamentals of soil behavior. In: Series in soil engineering, Lambe, T. W. and Whitman, R. V. Ed., Berkeley, California.
- Moroi, Y. (1992) Micelles-theoretical and applied aspects. Plenum Press, Inc., U.S.A.

- Mulligan, C. N. and Gibbs, B. F. (1989) Correlation of nitrogen metabolism with biosurfactant production by *Pseudomonas aeruginosa*. *Applied and Environmental Microbiology*, **55**:3016-3019.
- Mulligan, C. N., Yong, R. N., Gibbs, B. F., James, S. and Bennett, H. P. J. (1999) Metal removal from contaminated soil and sediments by the biosurfactant surfactin. *Environmental Science & Technology*, **33**: 3812-3820.
- Myers, D. (1992) Surfactant science and technology. 2<sup>nd</sup> edition. VCH Publishers, Inc. U. S. A.
- Nakanishi, K. (1977) Infrared absorption spectroscopy. 2<sup>nd</sup> edition.
- Nash, J. H. (1987) Field studies of in situ soil washing. EPA/600/2-87/110.
- Nyer, E. K. (1992) Treatment for organic contaminants, physical/chemical methods, In: Bioremediation, the state of practice in hazardous waste remediation operations, Seminar sponsored by Air and Waste Management Association and HWAC.
- Oberbremer, A. R., Muller-Hurtig and Wagner, F. (1990) Effect of the addition of microbial surfactants on hydrocarbon degradation in a soil population in a stirred reactor. *Applied Microbiology and Biotechnology*, **32**:485-489.
- Ochsner, U. A., Hembach, T. and Fiechter, A. (1995) Production of rhamnolipid biosurfactants. *Advances in Biochemical Engineering/Biotechnology*, **53**: 89-118.
- Pamukcu, S. and Wittle, J. K. (1992) *Environmental progress*, AIChE, **11**(3):241-250.
- Pamukcu, S. and Wittle, J. K. (1993) Electrokinetically enhanced *in-situ* soil decontamination. In: Remediation of hazardous waste contaminated soils, Wise and Trantolo, Eds., Marcell Dekker, Inc., NY. p245-298.

- Pamukcu, S., Filipova, I. and Wittle, J. K. (1995) The role of electro-osmosis in transporting PAH compounds in contaminated soils. *Electrochemical Society Proceedings*, **12**:252-263.
- Probst, R. F. and Hicks, R. E. (1993) Removal of contaminants from soils by electric fields. *Science*, **260**:498-504.
- Providenti, M. A., Flemming, C. A., Lee, H. and Trevors, J. T. (1995) Effect of addition of rhamnolipid biosurfactants or rhamnolipid-producing *Pseudomonas aeruginosa* on phenanthrene mineralization in soil slurries. *FEMS Microbiology Ecology*, **17**:15-26.
- Puppala, S. K., Alshawabkeh, A. N., Acar, Y. B., Gale, R. J. and Bricka, M. (1997) Enhanced electrokinetic remediation of high sorption capacity soil. *Journal of Hazardous Materials*, **55**:203-220.
- Ramana, K. V. and Karanth, N. G. (1989) Factors affecting biosurfactants production using *Pseudomonas aeruginosa* CFTR-6 under submerged conditions. *Journal of Chemical Technology and Biotechnology*, **45**:249-257.
- Reed, B. E., Berg, M. T., Thompson, J. C. and Hatfield, J. H. (1995) Chemical conditioning of electrode reservoirs during electrokinetic soil flushing of Pb-contaminated silt loam. *Journal of environmental Engineering*, **121**(11):805-815.
- Reena, M. P. and Desai, A. J. (1997) Surface-active properties of rhamnolipids from *Pseudomonas aeruginosa* GS3. *Journal of Basic Microbiology*, **37**(4):281-286.
- Reiling, H. E., Wyass, U. T., Guerra-Santos, L. H., Hirt, R., Happeli, O. and Fiechter A. (1986) Pilot plant production of rhamnolipid biosurfactant by *Pseudomonas aeruginosa*. *Applied and Environmental Microbiology*, **51**:985-989.

- Robert, M., Mercade, M. E., Bosch, M. P., Parra, J. L., Espuny, M. J., Manresa, M. A. and Guinca, J. (1989) Effect of the carbon source on biosurfactant production by *Pseudomonas aeruginosa* 44T1. *Biotechnology letter*, **11**:871-874.
- Robertson, R. P. and Wilson, D. J. (1995) Soil cleanup by in-situ surfactant flushing IX. Electrical effects in micelle formation. *Separation science and technology*, **30**(14):2821-2848.
- Rosen, M. (1978) Surfactants and Interfacial phenomena. John Wiley & Sons, New York.
- Runnels, D. D. and Wahli, C. (1993) *In situ* electromigration as a method for removing sulfate, metals, and other contaminants from groundwater. *Groundwater Monitoring Review*, p 121-129.
- Russel, W. B., Saville, D. A. and Schowalter, W. R. (1989) Colloidal dispersions. Cambridge University Press, Cambridge, U. K.
- Sale, A. J. and Hamilton, W. A. (1967) Effects of high electric fields on microorganisms: Killing of bacteria and yeasts. *Biochimica et Biophysica Acta*, **148**:781-788.
- Scheibenbogen, K., Zytner, R. G., Lee, H. and Trevors, J. T. (1994) Enhanced removal of selected hydrocarbons from soil by *Pseudomonas aeruginosa* UG2 biosurfactants and some chemical surfactants. *Journal of Chemical Technology and Biotechnology*, **59**:53-59.
- Schnitzer, M. (1986) Binding of humic substances by soil mineral colloids. In: Interactions of soil minerals with natural organics and microbes, Huang, M. and



Schnitzer, M. Ed. Special Publication No. 17, Soil Science Society of America  
Madison, WI. p77-101.

- Senesi, N. and Chen, Y. (1989) Interactions of toxic organic chemicals with humic substances. In: Toxic organic chemicals in porous media. Gerstl et al. Eds., Springer-Verlag, New York, p37-90.
- Shiau, B., Sabatini, D. A. and Harwell, J. H. (1994) Solubilization and microemulsification of chlorinated solvents using direct food additive (edible). *Surfactants, Groundwater*, **32** (4): 561-570.
- Shapiro, A. P. and Probstein, R. F. (1993) Removal of contaminants from saturated clay by electroosmosis. *Environmental Science & Technology*, **27**:283-291.
- Sims, R. C. and Overcash, M. R. (1983) Fate of polynuclear aromatic compounds (PNAs) in soil-plant systems. *Residue reviews*, **88**:1-68.
- Sims, R. C., Doucette, W. J., Mclean, J. E., Grenney, W. J. and Dupont, R. R. (1988) Treatment potential for 56 EPA-listed hazardous chemicals in soil. EPA/600/6-88/001. Robert Kerr Environmental Research Laboratory, Ada, OK.
- Sreekala, T. and Shreve, G. S. (1994) Effect of anionic biosurfactant on hexadecane partitioning in multiphase systems. *Environmental Science & Technology*, **28**(12):1993-2001.
- Stenstrom, T. A. (1989) Bacterial hydrophobicity: an overall parameter for the measurement of adhesion potential to soil particles. *Applied and Environmental Microbiology*, **55**:142-147.

- Sun, S. and Boyol, S. A. (1993) Sorption of Nonionic-organic compounds in soil-water systems containing petroleum sulfonate-oil surfactants. *Environmental Science & Technology*, **27**:1340-1346.
- Syldatk, C., Lang, S., Matulovic, U. and Wagner F. Z. (1985) Production of four interfacial active rhamnolipids from n-alkanes or glycerol by resting cells of *Pseudomonas sp.* DSM 2874. *Z. Naturforsch.* **40C**:51-60.
- Syldatk, C. and Wagner F. Z. (1986) Production of biosurfactants. p 89-120. In: *Biosurfactants and biotechnology*, Kosaric, N., Cairns, W. L., Gray, N. C. C. Eds. Marcel Dekker, Inc., New York.
- U. S. Agency for toxic substance and disease Registry (1990) Public health statement: polycyclic aromatic hydrocarbons (PAHs). Atlanta, Georgia, U.S.A.
- U. S. EPA (1993) Bioremediation using the land treatment concept. EPA 600/R-93/164.
- U. S. EPA (1994) *In situ* remediation technology status report: cosolvent. Engineering Bulletin, EPA/542/K-94/006.
- U. S. EPA (1995a) Remediation case studies: soil vapor extraction. By member agencies of the federal remediation technologies roundtable, EPA-542-R-95-004.
- U. S. EPA (1995b) Emergency technology bulletin: electrokinetic soil processing. Electrokinetics, Inc., EPA/540/F-95/504.
- U. S. EPA (1995c) Member Agencies of the Federal Remediation Technologies Roundtable: Remediation Case Studies: Bioremediation, EPA/542/R-95/002.
- Van Dyke, M. I., Couture, P., Brauer, M., Lee, H. and Trevors, J. T. (1993) *Pseudomonas aeruginosa* UG2 rhamnolipid biosurfactants: structural characterization

and their use in removing hydrophobic compounds from soil. *Canadian Journal of Microbiology*, **39**:1071-1078.

- Van Loosdrecht, M. C. M., Lyklema, J., Norde, W., Schraa, G. and Zehnder, A. J. B. (1987) Electrophoretic mobility and hydrophobicity as a measure to predict the initial step of bacterial adhesion. *Applied and Environmental Microbiology*, **53**:1898-1901.
- Van Olphen, H. and Fripiat, J. J. (1979) Data handbook for clay materials and other non-metallic minerals. 1<sup>st</sup> edition, Pergamon Press, U. S. A.
- Velikonja, J. and Kosaric, N. (1993) Biosurfactant in food applications. In: Biosurfactants: production, properties, applications, Kosaric, N. Ed., Marcell Dekker Inc., New York, p419-446.
- Verschueren, K. (1983) Handbook of environmental data on organic chemicals. 2<sup>nd</sup> Ed. Van Nostrand, p11-91.
- Vinson, P. K., Talmon, Y. and Walter, A. (1989) *Journal of biophysics*, **56**: 669.
- Volkering, F., Breure, A. M., Vanandel, J. G. and Rulkens, W. H. (1995) Influence of nonionic surfactants on bioavailability and biodegradation of polycyclic aromatic-hydrocarbons. *Applied and Environmental Microbiology*, **61**:1699-1705.
- Warren, A. J., Ellis, A. F. and Campbell, J. J. R. (1960) Endogenous respiration of *Pseudomonas aeruginosa*. *Journal of bacteriology*, **79**:875-880.
- Weissenfels, W. D., Beyer, M. and Klein, J. (1990) Degradation of phenanthrene, fluorene and fluoranthene by pure bacterial cultures. *Applied Microbiology and Biotechnology*, **32**: 479-484.
- Wennerstrom, H. and Lindman, B. (1979) *Phys. Rep.*, **52**:1-86.

- West, C. C. and Harwell, J. H. (1992) Surfactants and subsurface remediation. *Environmental Science & Technology*, **26**:2324-2330.
- West, L. J., Stewart, D. I., Binley, A. M. and Shaw, B. (1999) Resistivity imaging of soil during electrokinetic transport. *Engineering Geology*, **53**:205-215.
- White, K. L. (1986) An overview of immunotoxicology and carcinogenic polycyclic aromatic hydrocarbons. *Environmental Carcinogen Review*, **C4**:163-202.
- Wiesel, I., Wuebker, S. M. and Rehm, H. J. (1993) Degradation of polycyclic aromatic hydrocarbons by an immobilized mixed bacterial culture, *Applied Microbiology and Biotechnology*, **39**: 110-116.
- Wilson, S. C. and Jones, K. C. (1993) Bioremediation of soil contaminated with polynuclear aromatic hydrocarbons (PAHs): a review. *Environmental pollution*, **81**:229-249.
- Wilun Z. and Starzewski K. (1972) Soil mechanics in foundation engineering. In: Properties of soils and site investigations, Surrey University Press, London. Vol. 1.
- Wittle J. K and Pamukcu, S. (1993) Electrokinetic treatment of contaminated soils, sludges and lagoons. DOE/CH-9206, No. 02112406, US Department of Energy, Argonne National Laboratories, Argonne.
- Wodzinski, R. S. and Johnson, M. J. (1968) Yields of bacterial cells from hydrocarbons. *Applied microbiology*, **16**:1886-1891.
- Yong, R. N. and Warkentin, B. P. (1966) Introduction to soil behavior. Macmillan Company, U. S. A.

- Yong, R. N. and Rao, S. M. (1991) Mechanistic evaluation of mitigation of petroleum hydrocarbon contamination by soil medium. *Journal of Canadian Geotechnology*, **28**(1): 84-91.
- Yong, R. N., Tousignant, L. P., Leduc, R. and Chan, E. C. S. (1991) Disappearance of PAHs in a contaminated soil from Mascouche, Quebec. In: *In situ Bioremediation. Applications and Investigations for hydrocarbon and contaminated site remediation.* Hincsee, R. E., Olfenbittel, R. F., Eds. Butterworth-Heinemann, Stoneham, MA, p 377-395.
- Yong, R. N., Mohamed, A. M. O. and Warkentin B. P. (1992) Principles of contaminants transport in soils. Elsevier Science Publishers B. V., Netherlands.
- Zhang, Y. and Miller R. M. (1992) Enhanced octadecane dispersion and biodegradation by a *Pseudomonas rhamnolipid* surfactant (biosurfactant). *Applied and Environmental Microbiology*, **58**:3276-3282.
- Zhang, Y. and Miller, R. M. (1994) Effect of a *Pseudomonas rhamnolipid* biosurfactant on cell hydrophobicity and biodegradation of octadecane. *Applied and Environmental Microbiology*, **60**:2101-2106.
- Zhang, Y. and Miller, R. M. (1995) Effect of rhamnolipid (biosurfactant) structure on solubilization and biodegradation of n-alkanes. *Applied and Environmental Microbiology*, **61**:2247-2251.